University of Pannonia

Doctoral School of Chemical Engineering and Material Sciences

Submitted for the degree of
Doctor of Philosophy
of the University of Pannonia, Hungary

Author: Dong Sun
Supervisor: Dr. habil. Gusztáv Fekete

Dissertation Title: Gait analysis and musculoskeletal modeling used in athletes recovery from Achilles tendon rupture

DOI:10.18136/PE.2020.742

Veszprém
2020

GAIT ANALYSIS AND MUSCULOSKELETAL MODELING USED IN ATHLETES RECOVERY FROM ACHILLES TENDON RUPTURE

Thesis for obtaining a PhD degree in the Doctoral School of Chemical Engineering and Material Sciences of the University of Pannonia

in the branch of Material Sciences and Technologies

Written by Dong Sun

Supervisor: Dr. habil. Gusztáv Fekete

propose acceptance (yes / no)

……..……..……
Dr. habil. Gusztáv Fekete
supervisor

As reviewer, I propose acceptance of the thesis:

Name of Reviewer: Dr. habil. Krisztián Andor yes / no

……..……..……
Dr. habil. Krisztián Andor
1st reviewer

Name of Reviewer: Dr. Gábor Katona yes / no

……..……..……
Dr. Gábor Katona
2nd reviewer

The PhD-candidate has achieved ….....% at the public discussion.
Veszprém,

……..……..……
Prof. Dr. László Gubicza
Chairman of the Committee

The grade of the PhD Diploma …..... (…….. %)
Veszprém,

……..……..……
Prof. Dr. Katalin Bélafiné Bakó
Chair of the UDHC

Submitted with 113 pages and 176 references

The Dissertation contains 34 Figures, and 5 Tables

Supervision

Dr. habil. Gusztáv Fekete	*Supervisor*	PhD supervisor, Doctoral School of Chemical Engineering and Material Sciences, University of Pannonia. Associate Professor at Savaria Institute of Technology, Faculty of Informatics, Eötvös Loránd University

Acknowledgements

Firstly, I would like to express my sincere gratitude to my supervisor Dr. habil. Gusztáv Fekete and Prof. Dr. Yaodong Gu for the continuous support of my PhD dissertation and related research, for your patience, motivation, and immense knowledge. I am glad to have the opportunity to be your student and have the benefit of all your knowledge. Your guidance helped me in all the time of research and writing of this thesis. I could not have imagined having a better advisor and mentor for my PhD dissertation.

Many other academic, secretarial and technical members of staff have facilitated the realization of this thesis and I express them all my gratitude. I acknowledge the Faculty of Engineering, University of Pannonia (PE), Savaria Institute of Technology, Eötvös Loránd University (ELTE) and Faculty of Sports Science, Research Academy of Grand Health, Ningbo University (NBU) for the facilities and support provided.

I'm very fortunate to work in a group full of talented people who have not only helped me in conducting my experiments, but also given me invaluable advices and support. Special thanks to all the professors and colleagues, Prof. Jianshe Li, Prof. Dr. László Kollár, Dr. Endre Jánosi, Dr. Tej Singh, Dr. Qichang Mei, Dr. Shirui Shao, Dr. Yan Zhang, Dr. Gongju Liu, Dr. Meizi Wang, Dr. Yang Song, Dr. Liangliang Xiang and all PhD students for their helpful assistance, comments, and suggestions during my research work and sharing the experience of being a postgraduate student. Thanks to everyone who took part in the studies of this dissertation, your time was much appreciated. This dissertation could not completed without you. Many thanks to Prof. Dr. Katalin Bélafiné Bakó, Dr. Varga Tamás, Ms. Madléna Albert, Ms. Judit Szirmay, Ms. Tajnai Anita for managing many administrative processes and excellent help for managing administrative letters and various affairs during my PhD dissertation.

I would like to thanks my family and particularly my father, Mr. Youqiang Sun, my mother, Mrs. Jing Dong, and my beloved girlfriend, Ms. Yanping Zhang, thank you for supporting me to pursue what I loved, and thank you for your endless motivation and your unconditional love.

Finally, the financial support from Stipendium Hungaricum Programme, Tempus Public Foundation and China Scholarship Council (CSC) is gratefully acknowledged.

Content

Acknowledgements **7**
Abstract **11**
Abbreviations **15**
List of Figures **17**
List of Tables **19**
1. Introduction **21**
1.1 Achilles tendon (AT) and human movement 21
1.2 Human gait analysis 26
1.3 Musculoskeletal modeling based on OpenSim software 30
1.4 Achilles tendon rupture mechanism 40
1.5 Aims and objectives 46
2 Materials and methods **49**
2.1 Introduction to the experimental and computational workflow 49
2.2 Experiments 51
2.3 Musculoskeletal modeling 58
2.4 Model validation 61
2.5 Data analysis 62
3 Results **63**
3.1 AT anthropometric 63
3.2 Gait abnormality and asymmetry 63
3.3 Musculoskeletal modeling estimation 71
4 Discussion **79**
4.1 Gait abnormality and asymmetry 79
4.2 Musculoskeletal modeling and estimation 82
5 Conclusions and future work **87**
5.1 Conclusions 87
5.2 Recommendations for future works 88
Thesis points **91**
List of publications **95**
References **100**

Abstract

Achilles tendon rupture (ATR) is common and life-altering injury. A patient who sustains an ATR should expect recovery in years with extensive rehabilitation. In general, the incidence of acute ATR has been 53/100.000 persons/year. Incidence of ATR highly increased over the last years, which can alter tissue composition while having non-wanted effects on long-term tendon mechanics and lower limb functions during daily movement.

The first research question of this thesis: It has been revealed in the literature study, that in case of musculoskeletal modeling, no authors have considered to alter two important musculotendon related parameters, namely: tendon slack length l_s^t and optimal fiber length l_o^m. Without considering these parameters, the musculotendon forces will be very likely overestimated in the pathological side for ATR patients. By changing these parameters, it is possible to alter the Achilles tendon to behave like if it was ruptured and therefore, we could obtain realistic muscle forces for the triceps surae and the joint reaction forces.

The first objective of this thesis: To create a new musculoskeletal model, combined with experimental techniques (involving motion capture, ground reaction force measurement and medical imaging) which can realistically calculate the musculotendon forces and joint reaction forces in case of simulated Achilles tendon rupture. As a novel augmentation, the tendon slack length l_s^t and optimal fiber length l_o^m are determined by medical imaging, and they are integrated into the model. Therefore, it is possible to quantify the percentile difference between the musculotendon forces with or without Achilles tendon rupture.

The second research question of this thesis: It has been not discussed whether the Achilles tendon rupture has any critical effect on the knee joint and its area. However, it is assumed that it does and this effect is very likely resulted in higher knee adduction moment and joint forces during walking, which should be quantified.

The second objective of this thesis: By creating the new musculoskeletal model, the effect of Achilles tendon rupture on the knee kinetics will be quantified. The aim of this part is to compare the magnitude of the knee adduction moments in frontal plane and estimate knee joint reaction forces between the injured side (with ATR) and the uninjured side (without ATR) during walking, jogging and running. On one hand, by knowing the realistic joint loading in the injured side, a safer physical activity guideline during ATR rehabilitation process can be proposed to avoid the risk of knee pain and knee osteoarthritis in case of overloading. On the other hand, it should be evaluated if the Achilles tendon can increase the chance of knee osteoarthritis or it is an irrelevant factor.

The third research question of this thesis: In the previous studies, reduced ankle plantarflexion moments, plantarflexion joint power (moment multiply by angular velocity) were found during walking in the injured side of unilateral ATR patients. However, little is known regarding ankle joint mechanics during high demand sporting tasks such as jogging and running after an ATR.

It is also unclear in what way is the ankle-knee relationship effected by the ATR and whether it can cause negative long-term effect on the joints?

The third objective of this thesis: To reveal how the kinematics (trajectory of the center of pressure) and the kinetics (joint moments, gastrocnemius medialis, gastrocnemius lateralis, soleus and ankle joint reaction forces) of the ankle joint can be realistically estimated during walking and especially high demand sporting tasks consists of jogging and running. In addition, long-term physical effects are also addressed and explained in this part.

It is supposed that side to side gait variable differences, found between lower limbs, may be related to the AT elongation of surgical repaired side. The previous part revealed that gait asymmetry, in a higher degree, exist after surgical repair in case of patients with unilateral ATR history. However, few information was reported about the muscular contribution with ATR in case of normal daily activities like walking, jogging and running. Therefore, this part aimed to reveal how gastrocnemius and soleus muscles contribute to walking/jogging/running tasks, and investigate the inter-limb (injured and non-injured side) joint loading characteristics via subject-specific musculoskeletal modeling. The modelling process has been carried out in several steps, as follows:

- First, the evaluation of bilateral AT lengths by ultrasound imaging and magnetic resonance imaging (MRI). By this method, I could reconstruct the geometry of the AT to serve as an input for the subject-specific model in the OpenSim software.
- Second, data were collected from the experimental part of the thesis to serve as input, for the subject-specific modell in the OpenSim software. These data are: three-dimensional marker trajectories, ground reaction forces (GRF) and surface electromyography (sEMG).
- Third, subject-specific musculoskeletal models were created to compute joint kinematics, joint moments, muscle forces and joint reaction forces in the OpenSim software.
- Forth, based on the simulation results, one-dimensional statistical parametric mapping (SPM1d) with a two-sample t-test was conducted to assess differences over a stance phase on the variables of interest between the injured and uninjured sides.

It has been concluded that AT lengths were significantly (cca. 10%) longer in the injured side. The side-to-side triceps surae muscle-strength deficits were combined with decreased plantarflexion angles and moments in the injured leg during walking, jogging and running. However, the increased knee-extensor femur muscle forces were associated with greater knee extension degrees and moments in the injured limb during all tasks. Greater knee joint moments and joint reaction forces versus decreased ankle joint moments and joint reaction forces in the injured side indicate elevated knee joint loads compared with reduced ankle joint loads that are present during normal activities after an ATR. In the frontal plane, increased subtalar inversion angles and eversion moments in the injured side were demonstrated only during jogging and running, which were regarded as an indicator for greater medial knee joint loading. After an

ATR, the elongated AT accompanied by decreased ankle plantarflexion degrees and calf muscle strength deficits indicate ankle joint function impairment in the injured leg. Practically, this means that the force-transmission efficiency of the injured side is heavily. In addition, increased knee extensor muscle strength and knee joint loads may be a possible compensation mechanism for decreased ankle function. These data suggest that patients after an ATR may suffer from increased injury risk due to knee overuse.

The results, obtained from the experiments and the simulation, will provide implications on designing optimal rehabilitation movements. This workflow will show the most significant factors that contribute to rehabilitation and how these factors can be changed by alteration in external load, position and execution of the exercises. The individual tendon properties and computational workflow can be used to investigate which rehabilitation exercise will provide an optimal loading stimulus for athletes or simple patients.

In summary, this dissertation innovates a multidisciplinary approach combining biomechanics, sports medicine, rehabilitation sciences and medical imaging. A combined experimental and computational workflow was created to model inter-limb asymmetry, muscular contribution and joint loading to reveal the mechanism and effect of ATR during normal activities.

Abbreviations

AT: Achilles tendon
ATR: Achilles tendon rupture
ATRs: Achilles tendon ruptures
ATRS: Achilles tendon rupture score
TB: tibia
HF: hindfoot
FF: forefoot
HX: hallux
GRF: ground reaction force
DF: dorsiflexion
PF: plantarflexion
SP: supination
PR: pronation
ADD: adduction
ABD: abduction
IV: inversion
EV: eversion
COM: center of mass
IC: initial contact
TO: toe-off
OFM: Oxford foot model
PIG: plug-in-gait
ROM: range of motion
BMI: body mass index
HC: heel contact
RMS: root mean square
SH: shod
HO: heel-off
TC: toe contact
sEMG: surface electromyography
SPM1d: one-dimensional statistical parametric mapping
ICC: intraclass correlation efficient
MVIC: maximal voluntary isometric contraction
ATL: Achilles tendon length
IS: injured side
US: uninjured side
MG: gastrocnemius medialis
LG: gastrocnemius lateralis
SL: soleus
IK: inverse kinematics
ID: inverse dynamics
RRA: residual reduction algorithm
SO: static optimization

List of Figures

Figure 1 (a) Anatomy of the AT; (b) The poor blood supply region of Achilles tendon (Egger and Berkowitz, 2017, used by permission) *21*
Figure 2 Stress-strain curve of AT and a schematic view of the surgical technique used (Karlsson et al., 2019, used by permission). *24*
Figure 3 Functional divisions of the gait cycle (Perry and Burnfield, 2010, used by permission). *28*
Figure 4 Steps for generating a muscle-driven simulation of a subject's motion with SimTrack (Delp et al., 2007), used by permission. *30*
Figure 5 Hill-type model of muscle used to estimate tendon and muscle force (Rajagopal et al., 2016). used by permission. *31*
Figure 6 (A) Musculoskeletal model used to generate three-dimensional simulations of walking for eight subjects, each walking at four speeds (very slow, slow, free, and fast) (Liu et al., 2008); (B) Snapshots from a simulation of the running gait cycle (Hamner et al., 2010), used by permission. *33*
Figure 7 Illustration of OpenSim musculoskeletal model with different jumping and landing patterns; (A) Counter movement jump; (B) Single-leg jump landing; (C) Standing long jump. (Morgan et al., 2014) (Palmieri, Callegari, & Fioretti, 2015). Used by permission. *36*
Figure 8 Graphical (A) and schematic (B) depictions of the medial/lateral compartment joint structures in the musculoskeletal model; (C) Medial (top) and lateral (bottom) compartment tibiofemoral contact forces during stance (Lerner, DeMers, Delp, & Browning, 2015), used by permission. *37*
Figure 9 (A) MRI-based patient-specific foot-ankle model; (B, C) to define motion axis and muscle tendon insertion points; (D) for the comparative analysis of ankle joint reaction force. (Prinold et al., 2016), used by permission. *39*
Figure 10 Data processing flow chart, from experimental testing to OpenSim simulation. Note. GRF: ground reaction force; sEMG: surface electromyography. *49*
Figure 11 Experimental and computational process flowchart. *50*
Figure 12 The human informed consent form and institutional review board procedures. *51*
Figure 13 Experimental set-up (not on scale). *52*
Figure 14 Ultrasonography images in the sagittal (longitudinal) plane of the (A) AT injured side and (B) AT uninjured side. *53*
Figure 15 Ultrasonography images in the transverse plane of the (C) AT injured side and (D) AT uninjured side. *53*
Figure 16 Magnetic resonance imaging for the participants. *54*
Figure 17 Three dimensional motion capture for the lower extremities. *55*
Figure 18 The illustration of cut-off points (I-V) for stance phase division. Note. I: first foot contact (FFC); II: first metatarsal contact (FMC); III: forefoot flat (FFF); IV: heel off (HO); V: toe off (TO). *56*
Figure 19 The Delsys surface electromyography devices (https://www.delsys.com/). *56*
Figure 20 The placement of the EMG electrodes on the lower limbs. *57*

Figure 21 The scaling flowchart (left) and the operating principle (right). Experimental marker positions are measured with motion capture equipment (dark blue). Virtual markers are placed on a model in anatomical correspondence (https://simtkconfluence.stanford.edu/display/OpenSim/How+Scaling+Works). 58
Figure 22 Schematic depiction of the subject-specific musculoskeletal modeling used in this dissertation. a) The generic musculoskeletal model is scaled for each subject using experimental markers placed on anatomical landmarks. b) The slack AT length of the injured side was measured with an ultrasound of each subject to obtain subject-specific parameters. c) Graphic depiction of modifying gas_med, gas_lat and soleus musculo-tendon parameters. Note. Gas Med: gastrocnemius medialis, Gas Lat: gastrocnemius lateralis.....59
Figure 23 Comparison of muscle activations from static optimization estimated (blue line) and filtered electromyography (EMG) signals measured from the subjects during the same trial of normal walking, jogging and running. Note. EMG and activations were normalized from zero to one for each subject based upon the minimum and maximum values over the stance phase. 61
Figure 24 The knee joint adduction moments and joint reaction forces between injured and uninjured limbs during walking, jogging and running. 67
Figure 25 The comparison of plantar pressure during walking between injured and uninjured side.....68
Figure 26 The comparison of plantar pressure during running between injured and uninjured side.....69
Figure 27 In the first line (center of pressure trajectories),"a" and "b" represent COP trajectory between Uninjured and injured leg during walking, "c" and "d" represent COP trajectory between Uninjured and injured leg during running; In the second line, higher ankle inversion moments were found in the injured side during walking and running. 70
Figure 28 Mean and standard deviation lower extremity joint angle waveforms over stance phase (100%) for the uninjured side (yellow) and injured side (blue) during self-selected speed walking, jogging and running. Grey shaded regions on graphs indicate a significant difference between the two sides ($p<0.05$) from SPM1d analyses.....72
Figure 29 Mean and standard deviation of lower extremity joint moment waveforms over stance for the uninjured side (yellow) and injured side (blue) during self-selected speed walking, jogging and running. Grey shaded regions on graphs indicate a significant difference between the two sides ($p<0.05$) from SPM1d analyses.....73
Figure 30 Mean and standard deviation of estimated vas_med (vastus medialis), vas_lat (vastus lateralis), vas_inter (vastus intermedius) and rectus femoris musculo-tendon forces waveforms over stance between uninjured side (yellow) and injured side (blue) during walking, jogging and running. Grey shaded regions on graphs indicate a significant difference between the two sides ($p<0.05$) from SPM1d analyses.....75
Figure 31 Mean and standard deviation of estimated gas_med (gastrocnemius medialis), gas_lat (gastrocnemius lateralis) and soleus musculo-tendon forces waveforms over

stance between uninjured side (yellow) and injured side (blue) during walking, jogging and running. Grey shaded regions on graphs indicate a significant difference between the two sides (p<0.05) from SPM1d analyses.....76
Figure 32 The compared estimated triceps surae muscle forces between patient-specific from this dissertation and study from Modenese et al., 2018, used by permission...77
Figure 33 Mean and standard deviation of estimated joint reaction forces waveforms over stance at the hip, knee and ankle joints for uninjured side (yellow) and injured side (blue) during walking, jogging and running. Grey shaded regions on graphs indicate a significant difference between the two sides (p<0.05) from SPM1d analyses.....78
Figure 34 The center of pressure (COP) trajectories in the injured and uninjured sides 92

List of Tables

Table 1 Subject AT length details (n=6). The gastrocnemii and soleus AT lengths (ATL) of each subject were measured for both the injured and uninjured sides. 63
Table 2 Comparisons of kinematic variables between injured side and un-injured side during walking and running.....64
Table 3 Comparison of Angular velocity variables between injured side and uninjured side during walking and running. 65
Table 4 Comparison of kinetic variables between injured limb and uninjured limb during walking and running. 66
Table 5 Differences of selected biomechanical variables in symmetry angles (SA) between walking and running. 71

1. Introduction

1.1 Achilles tendon (AT) and human movement

1.1.1 The anatomy of the Achilles tendon

The AT is the largest and thickest tendon structure in the body, consisting of the calf triceps tendon (which includes the medial- and lateral gastrocnemius and the soleus muscle). However, the AT of some people are composed only of calf triceps tendon, accounting for 6% to 8% of the total population. The AT has a unique behavior since it rotates 90° during its distal travel and ends at the posterior calcaneus. Unlike other parts of the tendon, the AT does not have a true synovial sheath. The AT is composed of para-orbital tissues, which are divided into visceral and parietal layers, and they are called as adventitia and intima (Doral et al., 2010). The artery is worn in front of the capsule and penetrates the anterior capsule to nourish the AT. The inner surface of the film has a plurality of lubricating structures composed of a thin layer of mucopolysaccharide. This facilitates the sliding of the AT in the film where the maximum relative sliding distance is about 15 mm. The tendon sheath is composed of connective tissues, rich in blood vessels, as it is seen on Figure 1(a) (Egger & Berkowitz, 2017).

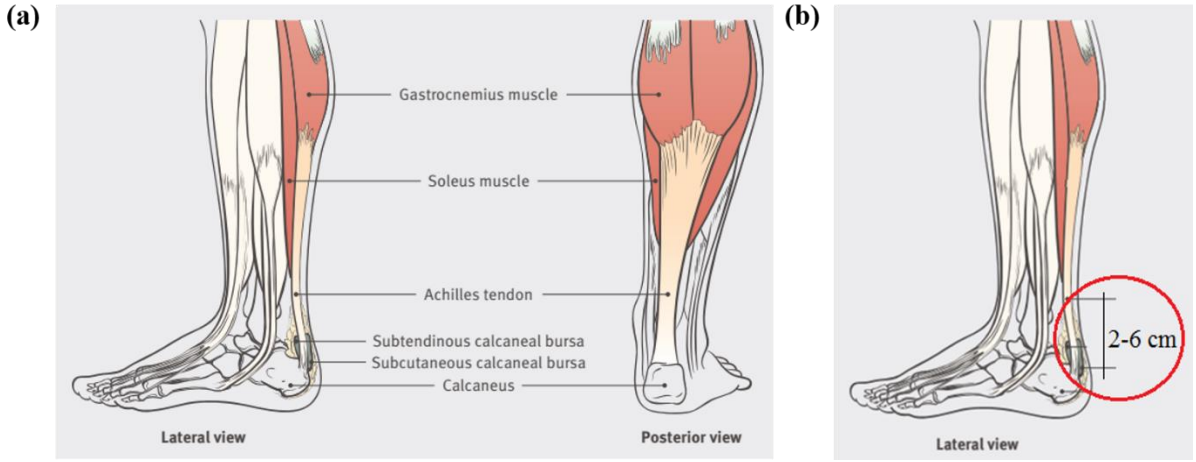

Figure 1 (a) Anatomy of the AT; (b) The poor blood supply region of Achilles tendon (Egger and Berkowitz, 2017, used by permission)

A clear understanding of the Achilles blood supply is crucially important to the surgeon. The posterior tibial artery recirculates through the abdomen and the abdomen junction to nourish the proximal part of the AT. The anterior tibial artery and the osteogenesis branch include a number of perforating arteries behind the humerus to nourish the distal part of the AT. It must be noted, that nuclear medicine research has shown that AT has the worst blood supply in the following range: if calcaneus is taken as an origin, the AT has a poor blood supply in its length between 2 to 6 cm, horizontally measured, as shown in Figure 1 (b). Further research has shown that as age increases, the number of blood vessels in the AT will be further reduced. This may be the reason why the risk of AT injury increases with age (O'Brien, 2005).

Many AT diseases are closely related to their surrounding structural lesions. For example, patients with Haglund malformations (abnormal protrusions behind the lateral wall of the calcaneus) are more prone to have post-calcaneal bursitis and mechanical irritations of the AT. It must be noted that AT is mainly composed of collagen, elastin, mucopolysaccharide, and glycoprotein (Ganestam, Barfod, Klit, & Troelsen, 2013). Type I and type III collagen are produced by mature fibroblasts in the AT. 95% of the normal AT is composed of type I collagen. After the ATR, the proportion of type III collagen in the AT increases, which may eventually lead to a decrease in the strength of the AT. As the age increases, the density of fibroblasts, the diameter of collagen fibers, and the density of collagen fibers in the AT decrease, causing a decrease in the strength of AT fibers (Hansen et al., 2013). That is the reason for higher injury risk to AT in elder athletes.

1.1.2 The biomechanical function of Achilles tendon

The AT is a key structure in the lower limb since it transmits force upward through the joint chain and further consumes energy through the bone and soft tissues (Müller, Siebert, & Blickhan, 2012). This process takes place as follows: the AT stores energy in the early stage of ground contact and releases energy in the push-off of the stance phase. Farris et al. found that the contribution of the AT to the ankle joint during running was more than 50% (Farris, Trewartha, & Polly McGuigan, 2011). Therefore, AT is related to the improvement of running economy. Larger AT stiffness can significantly reduce oxygen consumption, while longer AT arms can improve running economy by reducing the required muscle activity (Kubo, Tabata, Ikebukuro, Igarashi, & Tsunoda, 2010; Fletcher, Esau, & MacIntosh, 2010; Kunimasa et al., 2014).

With regard to the stiffness of the AT, studies have shown that the load that AT could withstand is the largest in the body. At full speed run, the peak load of the AT is about 12.5 times the bodyweight (about 9000N) while during jumping or shuttle run, the peak load of the AT can reach 1000~4000N (Lorimer & Hume, 2014). AT is highly sensitive to mechanical stimuli, therefore regular exercise can increase the diameter of the AT, while less activity results in a decrease in the diameter (Bramble & Lieberman, 2004; Lorimer & Hume, 2016). By controlling the amount of exercise, it is possible to effectively increase the collagen content, increase the diameter of the collagen fibers, and thereby improve the quality of the AT (O'Neill, Watson, & Barry, 2016).

With respect to the biomechanical characterization of the aforementioned tendon, we must note that recent biomechanical studies have mainly used ultrasound systems to study the functions and characteristics of the AT, including AT length and cross-sectional area. Ueno et al. compared the AT cross-sectional area of numerous athletes under three different speeds and the AT length at three different positions (the calcaneal tubercle to the medial head of the gastrocnemius/the lateral head of the gastrocnemius/the point of junction of soleus and AT) (Ueno et al., 2018).

They concluded that AT connected to the medial head of gastrocnemius had showed a reduction in energy consumption, while the cross-sectional area of AT was not significantly related to running economy (Ueno et al., 2018). These results suggest that a longer AT connected to the medial head of the gastrocnemius may be more beneficial for middle and long-distance runners to achieve superior running performance (Hunter et al., 2011). This is consistent with the results of previous studies. The improvement of the mechanical properties of the AT after training is not mainly achieved by hypertrophy. This may be because fewer blood vessels are distributed in the AT accompanied with a slower metabolism and recovery process. The increase in elastic modulus and stiffness after training indicates that the AT will undergo adaptive changes after training to withstand higher stress. Since AT cannot do work alone, it is intrinsically linked to the movement of the triceps and the ankle joints of the calf, while it is indirectly related to the proximal muscles and their joint movements. Compared with healthy runners, the runners with AT diseases are in a more inverted posture when they touch the ground, and the heel joints show a more everted posture after the heel touches the ground. It has been also proven that muscle activation decreases during the load-bearing period (Baur et al., 2011). Achilles tendinopathy does not seem to affect neuromuscular control but may affect the output of the lower limb mechanical power during the stance period, thereby affecting joint stability. Consequently, when discussing complex AT injuries, it is not possible to consider only the mechanical properties and functions of the AT itself.

At the end, with regard to its physiology, the latest epidemiological survey shows that Achilles tendinopathy is the most common and most difficult injury to cure among the medium and long-distance runners and its incidence can reach 8% to 15% (Arampatzis, Peper, Bierbaum, & Albracht, 2010). It is well known in sport science, that AT injury seriously reduces the athletic performance of professional athletes, ultimately leading to ATR or early termination of athlete career (Munteanu & Barton, 2011). Here it must be mentioned, that the incomplete recovery of the Achilles tendinopathy after a long period of abnormal force are the primary causes of ATR (Khan, Cook, Kannus, Maffulli, & Bonar, 2002).

1.1.3 Achilles tendon pathology and ruptures

The incidence of ATR continues to grow, due to the fact that there are fewer daily activities and more "weekend warriors" (people who participate in sports only on weekends). Facts about the ATR are as follows: the age of high incidence is between 30 to 40, the ratio of male to female gradually changes from 2:1 to 19:1, the incidence on the left side is higher than on the right side while 75% of acute ATR is associated with exercise. Incidences regarded to the right side may be due to the fact that the right leg is more often used to pushing the weight to the left leg (Egger & Berkowitz, 2017). It is worth noting that 80% of the ATR occurs in the range of 2 to 6 cm above the AT. High-risk factors for ATR include a sedentary lifestyle, corticosteroid injection (leading to local collagen necrosis), use of anabolic steroids (resulting in abnormal collagen hyperplasia to reduce AT strength), hyperthyroidism, incomplete renal function, gout,

atherosclerosis, and the use of fluoroquinolones. In addition, cardiovascular issues can also lead to the risk of ATR (Magnan, Bondi, Pierantoni, & Samaila, 2014). Naturally, acute ATR usually occurs when mechanical overload acts on the gradual degeneration of the AT. Sedentary can lead to a decrease in local blood vessels in the AT, which makes it difficult to repair the micro-injury; such damage gradually accumulates and eventually leads to macroscopic fracture (as shown in Figure 2). This theory is supported by the fact that 15% of patients have local symptoms before having an ATR. These typical manifestations or symptoms of acute ATR include pain in the posterior malleolus, difficulty in lifting, weakness in the knee, and a sound of fracture when injured (Hess, 2010).

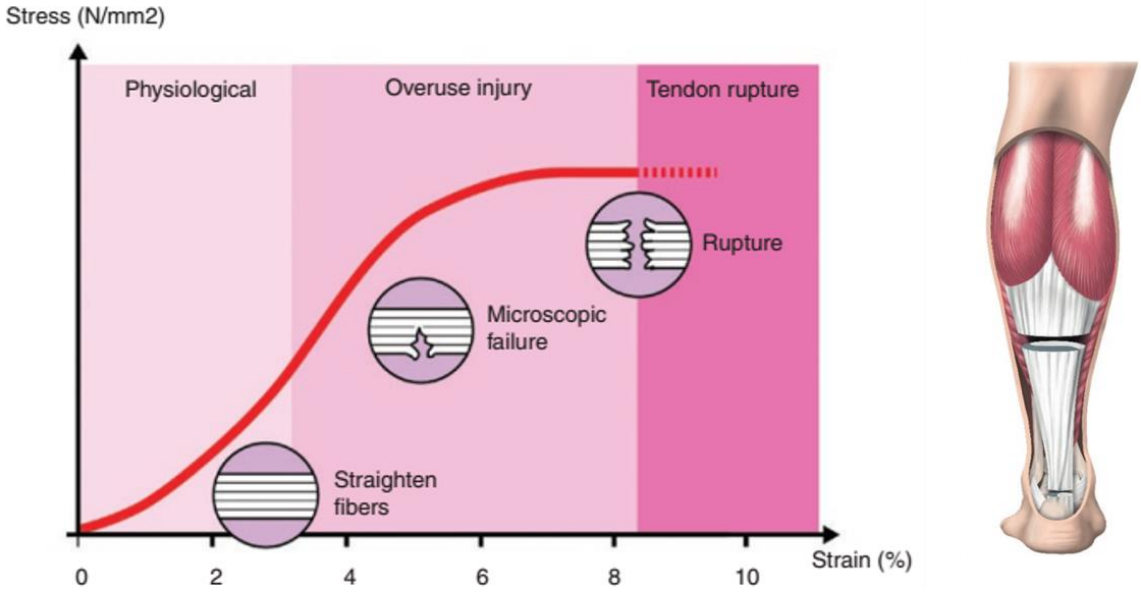

Figure 2 Stress-strain curve of AT and a schematic view of the surgical technique used (Karlsson et al., 2019, used by permission).

The mechanism of injury can be related to rapid plantarflexion movements in the ankle joint when the soleus muscle contracts. This can be explained as follows: when stepping on the edge of the sidewalk, the knee is in full extension while at the same time the ankle joint is in complete plantarflexion. In this moment a huge ankle dorsiflexion force is exerted on the foot likewise as an athlete jumps or falls from a height. This dorsiflexion force can rupture the AT suddenly. As a results, local swelling and ecchymosis can be seen during a physical examination, and obvious tender points and AT defects can be reached (Hess, 2010). Compared with the contralateral limbs, the passive lateral extension of the affected side increases and the plantar flexion is weakened. The bilateral contrast Thompson test is often used to assess the patient's active plantar flexion function and to effectively remove the false-negative test results caused by long flexor tendon assisted plantar flexion. It is also important to assess the resting position of the injured side of the AT. The patient should remain in a prone position during the examination (Lorimer & Hume, 2014). An increase in the resting position of the AT may indicate an increase in the ATR.

Since the trauma is mainly diagnosed based on typical medical history and physical examination results, further imaging examination is required only when the medical history and physical examination results are not clear.

The “Kager Triangle” in the X-ray film, the high translucent area at the AT, and the avulsion fracture of the calcaneus are typical imaging findings. If the ultrasound shows low echo zone at the AT, that means the density is lower compared to normal tissues, which is a clear diagnosis for rupture. (N. Maffulli, Regine, Angelillo, Capasso, & Filice, 1987).

Chan’s dynamic ultrasound study showed no significant difference in the incidence of ATR after non-surgical or surgical treatment in patients with a hernia stump separation of less than 5 mm (Chan et al., 2011). Although ultrasonography can measure the distance separating the AT, its reliability is closely related to operator proficiency; in this respect, its reliability is not as good as MRI. Although MRI is more expensive and time-consuming, it has an advantage in assessing the degree of ATR and surrounding tissue damage. MRI will reflect the interruption signal of the ATR on the Tl and T2 phases (Khan et al., 2003). Postoperative rehabilitation includes a short intertemporal brake and early functional exercise. Athletes can achieve satisfactory functions through rehabilitation training with increasing postoperative strength, including joint activity training starting 72 hours after surgery, bed-away training with 2 weeks postoperatively, and complete weight-bearing training after 6 weeks.

Through this training, 93% of athletes can rejoin the competition about 6 months after surgery. Only 2% to 3% of patients will feel the loss of plantar flexion force (Nilsson-Helander et al., 2010). In addition, the use of gypsum brakes after surgery is better than traditional plaster fixation, which can reduce the incidence of postoperative adhesions, paresthesia, scar hypertrophy, infection, and other complications (Gwynne-Jones & Sims, 2011).

1.2 Human gait analysis

1.2.1 The state-of-the-art of human gait analysis

The generalized definition of gait is a pattern in which the limbs of animals move on a solid surface. The gait patterns vary greatly between different species due to the anatomical structure. The same species can select a variety of different gait patterns according to different moving speed, ground conditions and functional requirements (Shapiro, Zernicke, Gregor, & Diestel, 1981). Bipedalism walking is one of the characteristics that distinguish human beings from other animal species (McGrath et al., 2019). Humans only use the lower limbs to carry out walking. It is the result of the long-term evolution of species in the gravitational environment. One study found that this walking mode only consumes a quarter of four feet of energy (Bennett et al., 2009). Clinical gait analysis refers specifically to the behavior and manner of human physical activity. Walking is the basic movement during human daily life, which is the ability acquired and continuously practiced in the process of growth and development. Through repeated learning and adjustment, human beings gradually form walking pattern suitable for themselves. This process is the result of the establishment of neural pathways and the coordinated development of muscles. It reflects the ability of central nervous system to control peripheral and skeletal muscles (Stolwijk et al., 2014).

Gait analysis can be used for the examination and evaluation of individual activities by different ways. The most commonly used is the assessment of walking on the ground, followed by running, jumping, up and downstairs (Simon, 1993). Quantitative gait analysis is an important clinical tool for distinguishing normal and abnormal gait pattern. Early gait analysis was performed by taking continuous photos, however it was soon disregarded due to the limited technology, poor accuracy and the fact that only general description could be made (Davis, Õunpuu, Tyburski, & Gage, 1991).

With the development of motion capture technology, a variety of methods and tools for gait analysis have been developed. One early but still useful technique for quick field testing among athletes is the electronic protractor. This device can be used to measure the instantaneous three-dimensional rotation angle of the lower limb joints, and the accelerometer has been used as an indirect measurement tool for the angular displacement of the limb. The sagittal displacements can be calculated by performing intermittent optical photography with a reflective markers attached to important anatomical landmarks (Whittle, 2007). The photographic images can also be converted into three-dimensional movement patterns. In the past decade, two-three dimensional (2D/3D) motion capture technology has been developed and utilized to meet the need of more precise kinematic analysis. These techniques use a simple perspective image and a pre-stored 3D model to match the marker position and silhouette contours in the perspective (Wren, Gorton, Õunpuu, & Tucker, 2011). By doing this, the position of the model can be reconstructed, and if a series of image processing is completed, the relative motion of the joints can be calculated.

Currently, it is only used for scientific research purposes, especially artificial joint prosthesis and wear analysis, and it is unlikely to be carried out on a large scale (Muro-de-la-Herran, García-Zapirain, & Méndez-Zorrilla, 2014).

The commonly used three-dimensional gait analysis system usually consists of three parts: a motion capture system for capturing three-dimensional motion trajectories of reflective markers; a force measuring platform for collecting ground reaction forces; and a surface electromyography (sEMG) device. The motion capture system is generally composed of more than six high-resolution infrared cameras. According to the special spatial position arrangement, the infrared reflective marker ball is attached to each anatomical landmark of the human body during data acquisition (Carse, Meadows, Bowers, & Rowe, 2013). The camera can capture the three-dimensional coordinate positions of the marker set in the space and by the use of inverse kinematics algorithm, the joint motions can be calculated (Ceseracciu, Sawacha, & Cobelli, 2014). The force platform is generally installed in the ground, while the force and its direction can be recorded when the subject walks over the force plate (Ismadi Ismail, 2018). The surface EMG system is attached to the skin surface through the electrode slices, while the main muscle EMG signals at different time steps, during walking, are being recorded. The collected data include the relative position and direction of various parts of the body, the force between the foot and the ground, the time-space relationship, and the activity of the lower limb muscles (Bovi, Rabuffetti, Mazzoleni, & Ferrarin, 2011).

The three systems are integrated via a computer software to maintain consistency in data collection during motion capture. The human gait is biphasic, and the gait cycle can be divided into two parts according to the position of the limb in the gait cycle: the stance phase and the swing phase (Figure 3). The stance phase accounts for around 60% of the entire gait cycle. In the stance phase, one side of the lower limb carries most of the body weight. The swing phase accounts for around 40% of the entire gait cycle, and in the swing phase, the bodyweight is carried by the contralateral side (Mummolo, Mangialardi, & Kim, 2013). The stance phase could be further divided into heel strikes, mid-stance and push-off phases. These phases are named according to the position of the ipsilateral foot. The swing phase is further divided into an acceleration phase, an intermediate phase, and a deceleration phase (Figure 3). The lower limbs swing forward in the acceleration phase, catching up and surpassing the torso. While the lower limbs swinging in the deceleration phase prepare the heel to strike the ground and begin the next stance phase. However, the actual human walking gait is much more complicated than this division. The above-mentioned gait cycle detection is only a general simplification of the human walking gait. However, this division creates a convenient and widely-accepted protocol to analyze the muscle contraction changes of the lower limb joints during the gait cycle (Kharb, Saini, Jain, & Dhiman, 2011).

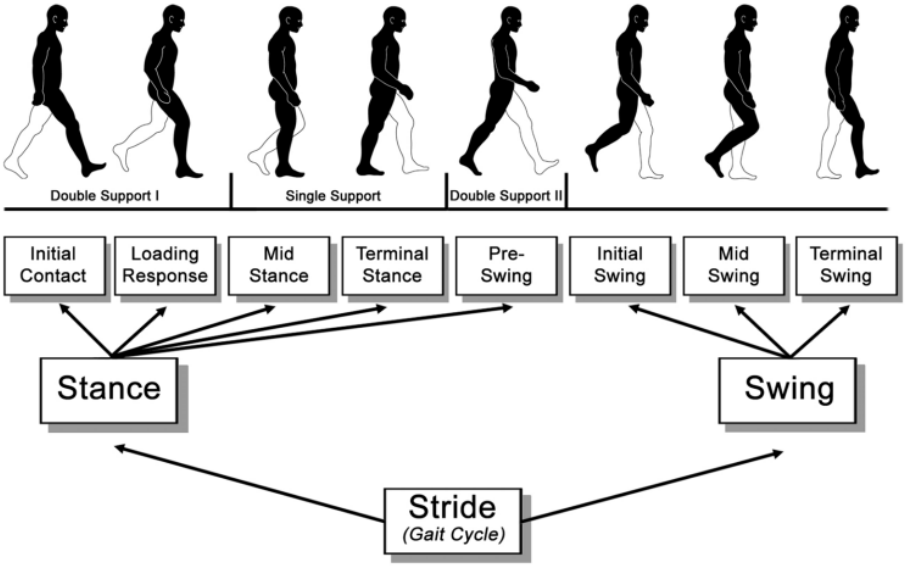

Figure 3 Functional divisions of the gait cycle (Perry and Burnfield, 2010, used by permission).

Gait consists of a series of gait cycles. In each gait cycle, a series of gait events are produced that mark changes in the gait phase. The gait phase includes the swing phase and the stance phase, and each phase is divided into early, middle, and late phases, and there is a pre-swing phase for the swing phase. The gait phase is distinguished by a gait event that includes the heel strike, the plantar contact, the heel push-off, and the toe-off the ground (Pistacchi et al., 2017). One side of the heel strikes the ground to toe-off the ground as a stance phase of the side foot. Gait analysis refers to the measurement and description of the skeletal muscle function of the human body during exercise and quantitative assessment during rehabilitation assessment and physical therapy through biomechanical methods (Esquenazi, 2014). Objectively and quantitatively reveals the walking function and comprehensively reflects the patients' rehabilitation. Gait analysis often contributes to clinical diagnosis and efficacy evaluation. Through gait analysis, we can calculate the spatial-temporal, kinematic, kinetic parameters, etc., and make some guidance for the clinical intervention (Fukuchi, Fukuchi, & Duarte, 2018).

1.2.2 Gait analysis used in functional assessment and rehabilitation

Rehabilitation refers to the patient's ability to regain and adapt to normal life. The purpose of rehabilitation is to comprehensively and coordinately use various methods such as medicine, education, occupation, society, and engineering to reduce the physical and mental dysfunction of the disabled and to exert their highest potential to help them return society and improve the quality of life (Cimolin & Galli, 2014). Rehabilitation mainly includes assessment and treatment. Assessment is physiological check-up on the functional progress of the patient.

Treatment refers to planning and designing therapeutic programs using various methods after a clear understanding of the location and extent of the obstacles (Ornetti et al., 2010; Montero-Odasso, Verghese, Beauchet, & Hausdorff, 2012).

In the evaluation of rehabilitation effects, the general methods and contents of sports evaluation include: muscle tension, muscle strength, measurement of joint range of motion, assessment of balance and coordination function and finally gait evaluation.

Since muscle tension, muscle strength, joint range of motion, and balance are ultimately reflected in walking, so gait is the most intuitive response to exercise ability (Lienhard, Schneider, & Maffiuletti, 2013). Therefore, gait functional evaluation is based on gait analysis. The purpose is to evaluate the gait of the person and obtain the rehabilitation or disease status by comparing the gait parameters (Leardini et al., 2014). It must be mentioned that the motion control mechanism is highly complicated, including the central command, body balance, and coordinated control, involving the joint operation of the lower limbs muscles (Nadeau, Betschart, & Bethoux, 2013). Any of the problems associated with the reproduction of normal gait or the interconnection of various links may affect the gait performance, resulting in abnormal gait pattern. The main causes of abnormal gait can be divided into two categories: neurological diseases, and non-neurological diseases (Axer, Axer, Sauer, Witte, & Hagemann, 2010). Neurological diseases mainly include stroke, brain trauma, spinal cord injury, cerebral palsy, Parkinson's disease whilst non-neurological diseases are mainly caused by sports injuries, bone, and joint diseases, congenital malformations, amputations, and surgery (Kainz et al., 2017).

The rehabilitation process of ATR patients is divided into four stages: inflammation, hyperplasia, plasticization, and maturity. In the first 6 weeks of healing (inflammation and proliferative phase), AT is the most vulnerable, and the intensity increases slowly over the next 6 weeks to 12 months (molding and mature). Patient rehabilitation is a standard functional recovery process (Matt L. Costa, 2005). At present, gait analysis is applied to sports injury rehabilitation. The following problems exist:

1. Generally, research and clinical practice set the focus on the evaluation of rehabilitation on the large joints such as the hip, knee, and ankle (Oda, Sano, Kunimasa, Komi, & Ishikawa, 2017) based on the comparison of the population with and without lower limb injury history. This evaluation was carried out to investigate the correlation between the gait parameters and the amplitude of the parameter curve (Mezzarobba et al., 2013). However, the application of foot inter-segmental joint motion characteristics and gait parameters in the rehabilitation of athlete's foot-related injuries are still quite limited (Dubbeldam et al., 2010; Sun, Fekete, Mei, & Gu, 2019).
2. Lack of gait comprehensive evaluation indicators. At present, gait evaluation method mainly finds the problem by comparing the individual with the normal range and lacks an intuitive score, which is difficult to be directly applied to any population for precise diagnosis (Sun, Fekete, Baker, & Gu, 2019).

3. Treatment and rehabilitation evaluation are not synchronized. Few studies combine them to do the real-time treatment and evaluation system. The real-time synchronization technology of rehabilitation treatment and evaluation can provide timely feedback to therapists and patients, which could help patients to adjust their rehabilitation strategies and to accelerate their recovery (Van Den Bogert, Geijtenbeek, Even-Zohar, Steenbrink, & Hardin, 2013).

1.3 Musculoskeletal modeling based on OpenSim software

1.3.1 Introduction of OpenSim software

At present, experts and scholars in the field of sports biomechanics often use VICON Motion System and other infrared capture systems based on optical principles, high-speed camera, photography and other equipment to record the movement of the human body. Then input the data into Visual 3D, VICON Nexus and other motion analysis software to analyze the human motion and the movement characteristics of each joint. However, the traditional motion analysis method has several deficits in detecting of human motion characteristics e.g. is difficult to measure dynamically large amount of important information, like muscle forces intensity, in the laboratory.

OpenSim is an open source software based on C++ and JAVA for musculoskeletal model building, simulation, and analysis (website: https://simtk.org/). The OpenSim software dynamically simulates human motion to study muscle geometry, muscle-tendon properties, muscle forces and joint reaction forces generated by muscles (Delp et al., 2007). OpenSim includes a computing tool (SimTrack) and related algorithms for users to study and analyze static model optimization and dynamic visualization of human musculoskeletal models. In OpenSim software, the musculoskeletal model consists of bones that are connected by joints and muscle-tendon units that span the joints and generate forces to drive various human motion. In addition, the software is designed to provide collaborative tools and platforms for biomechanics researchers to develop, share and extend the simulation of musculoskeletal models (E. M. Arnold, Ward, Lieber, & Delp, 2010; Pandy & Andriacchi, 2010; Rajagopal et al., 2016), as shown in Figure 4.

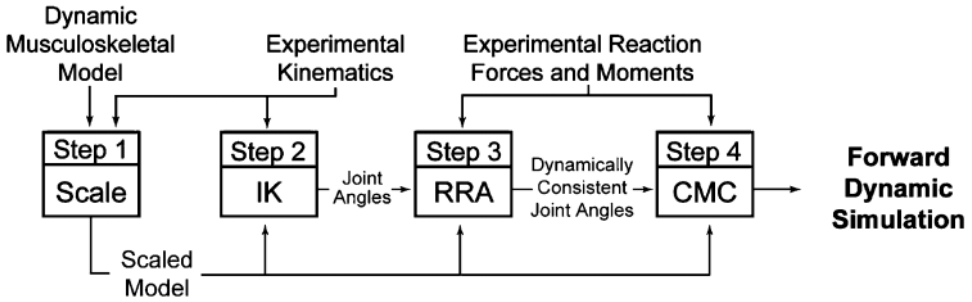

Figure 4 Steps for generating a muscle-driven simulation of a subject's motion with SimTrack (Delp et al., 2007), used by permission.

The operation steps of the SimTrack tool include four steps:

- Step 1: Input the subject's relevant anthropometric data and static model experimental data to scale and calibrate the dynamic musculoskeletal model;
- Step 2: Input experimental kinematics data combined with the scaled musculoskeletal model using Inverse Kinematics (IK) tool to calculate and obtain joint kinematics;
- Step 3: Input the experimentally measured ground reaction force data combined with joint kinematics, using Inverse Dynamics (ID) and Residual Reduction Algorithm (RRA) to reduce the error between simulated and experimental data;
- Step 4: Initiate the Computed Muscle Control Algorithm (CMC), which is used to obtain the muscle activation, muscle force, muscle-tendon length changes and other parameters (Figure 4) (Delp et al., 2007). The muscle-tendon units in OpenSim are composed of muscles and tendons. The muscles generate force through the tendon to drive the musculoskeletal system and produce different patterns of human movements. The total muscle-tendon length (L^{MT}) can be determined by muscle fiber length (L^{M}), tendon length (L^{T}), muscle pennation angle (α), muscle strength (F^{M}), and tendon-generated force (F^{T}) (Figure 5) (Rajagopal et al., 2016).

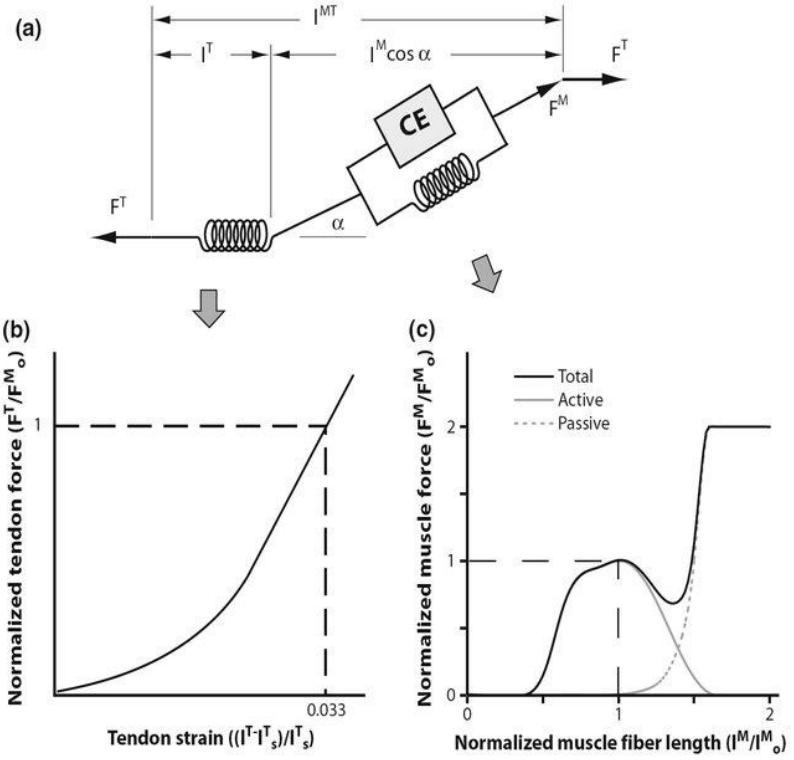

Figure 5 Hill-type model of muscle used to estimate tendon and muscle force (Rajagopal et al., 2016). used by permission.

OpenSim simulation analysis can establish and clarify the quantification and causal relationship between neuromuscular activation patterns, muscle strength, and geometric changes, external reaction forces and motion patterns obtained from laboratory tests.

The aim is to explore the changes in the above-mentioned principle mechanism during abnormal movement by revealing the functional principle of muscle coordination control and to predict potential rehabilitation treatment plans. The program can enable us to acquire functional characteristics on special groups such as people with obesity, diabetes, hemiplegia, as well as knee- or other sort of arthritis (Pandy & Andriacchi, 2010).

1.3.2 OpenSim lower extremity modeling in human basic movements

WALKING

At different walking speeds, the spatial-temporal parameters, joint angle, joint moment and plantar pressure distribution show different characteristics, so the level of muscle activity that provides the power also shows a certain difference (Sun, Fekete, Mei, & Gu, 2018). Arnold et al found that with the increase of walking speed, the knee joint flexion angular velocity increased at the end of the stance phase, and knee joint extension angular velocity increased immediately after push-off (A. S. Arnold, Schwartz, Thelen, & Delp, 2007). This mechanism works as follows: the knee joint accelerates knee flexion at the end of the swing via the use of the quadriceps muscle, which uses 50-70% of its muscle strength during this process.

The swing-related dorsiflexion muscle group, including the hip flexor muscle group, the biceps muscle group, the quadriceps muscle group, the hip extension muscle group and the abductor muscle group show consistent muscle activation variations (A. S. Arnold et al., 2007). Liu et al. (2008) performed slower (0.54m/s), slow (0.75m/s), comfortable (1.15m/s) and fast (1.56m/s) gait speed for population with no history of any injury. In their study, they used biomechanical testing, combined with OpenSim 2392 model (23 degrees of freedom and 92 muscle-tendon complex). The results from the simulation and experiments showed high consistency, which indicates that the muscle strength output obtained by the OpenSim musculoskeletal model simulation, has high reliability (Liu, Anderson, Schwartz, & Delp, 2008).

With alteration of the external load on the trunk (reducing by leaning forward or increasing by leaning backward 25%, 50% body weight), it was found that the joint kinematics, kinetics and muscle activation outputs from the lower extremity musculoskeletal model were highly inconsistent with the experimental data during walking. Muscle function exhibits the same degree of activation as the torso load increases, and the soleus muscle is the main muscle that satisfies the incremental load during the support and push-off phases (linear correlation coefficient between load increase and soleus muscle excitability R^2=0.95, highly relevant) (McGowan, Kram, & Neptune, 2009). The internal and external ground reaction forces (GRFs) during the stance phase and the push-off phase are respectively generated by the lower extremity abductor muscles and the knee extension, plantar flexor and adductor muscle groups (John, Seth, Schwartz, & Delp, 2012).

Subject-specific musculoskeletal model of joints have also been studied. It has been found

that not only the femoral articular surface load increased together with the increment of different (Slow velocity: 0.75m/s, Normal velocity: 1.25m/s, Fast velocity: 1.5m/s) walking speeds (Figure 6), but the flexion, extension and abduction moment of the knee joint, together with compression force of the tibial-femoral joint surface (Lerner, Haight, DeMers, Board, & Browning, 2014).

It is worthy to note that the similarity and difference of muscle strength exist between individuals in walking gait. The force of soleus muscle (1856.1N) acting on ankle joint is higher than that of gastrocnemius muscle (1232.5N); the foot length (-0.01); the foot width (-0.012) and the arch height index (-0.012) were closely related to the maximum moment of the subtalar joint ($p<0.01$, $r=0.678$) (Błażkiewicz, Wiszomirska, Kaczmarczyk, Naemi, & Wit, 2017). The individualized model combined with the subject-specific differences of the population improves the accuracy and pertinence of the simulation outputs, therefore it can be applied to basic research and clinical pathological diagnosis (Knarr & Higginson, 2015).

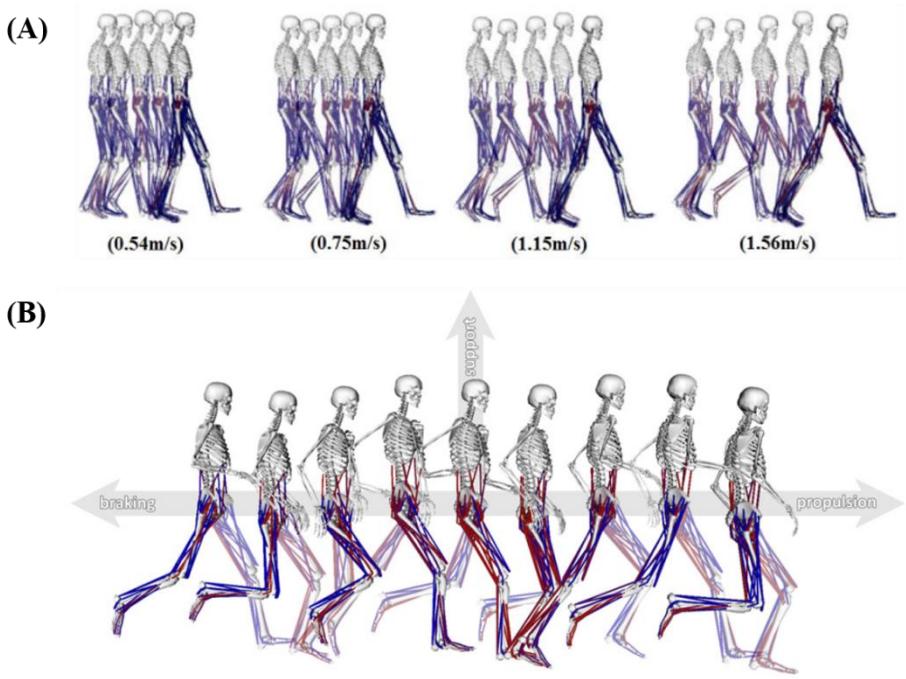

Figure 6 (A) Musculoskeletal model used to generate three-dimensional simulations of walking for eight subjects, each walking at four speeds (very slow, slow, free, and fast) (Liu et al., 2008); (B) Snapshots from a simulation of the running gait cycle (Hamner et al., 2010), used by permission.

RUNNING

Another important physical activity with the evolution of human biology to produce an upright walking movement is running. Studies have shown that in running gait, the stance phase accounts for about 31% of the gait cycle, and the swing phase accounts for about 69% of the gait cycle (Bramble & Lieberman, 2004). One important difference between running and gait (with double stance phase) is that running has a period, the so-called ‘Double Float’ when both of the feet are off the ground which creates gaps e.g. during ground reaction force

measurements, but means no hindrance in motion capture.

With increased running speed, the strike pattern transfer from heel strike to forefoot strike, which is the main difference between jogging and sprint running. The former is mainly used for endurance running by aerobic metabolism, the latter is commonly used in short distance sprinting using anaerobic metabolism (Mclean, 2008).

In view of the difference between running and walking, it is more complicated to coordinate the muscle function by the nervous system to provide vertical support and propulsion force for running (Hamner, Seth, & Delp, 2010).

The study found that during the stance phase of running, the quadriceps muscle is the main braking muscle and it balances the center of gravity as well. In the late stance phase of running, the gastrocnemius and the soleus muscles are the main muscles that initiate the acceleration and balance the body center of gravity (Debaere, Delecluse, Aerenhouts, Hagman, & Jonkers, 2013). The coordinated oscillation of the torso and upper arm has less effect on initiating or balancing the acceleration of the center of the body, but stabilizing the vertical angular momentum generated by the lower extremities.

Another study aimed to analyze the different running speeds (2.0m/s, 3.0m/s, 4.0m/s and 5.0m/s), to explore the characteristics of the related muscle activities on human running movements, and to find the soleus muscle contribution for the acceleration of the body center in the vertical direction under different speed conditions (Debaere, Delecluse, Aerenhouts, Hagman, & Jonkers, 2015). It was also reported that other muscle groups (such as gastrocnemius, tibialis anterior, quadriceps and gluteus maximus) also gradually increase the acceleration of the body center of gravity in the vertical and anteroposterior directions during the heel strike and the push-off phases, which indicates an increasing vertical ground reaction force (Debaere et al., 2015).

The muscle-tendon unit geometry that produces the force also changes with the exercise pattern, such as the maximal length of the rectus femoris (119±2%) and the hamstring muscle (125±4%) relative to the rest condition (Hamner & Delp, 2013; Riley, Franz, Dicharry, & Kerrigan, 2010). The running musculoskeletal model is also used to analyze the technical movements of the short-track sprinting. By analyzing the musculoskeletal movement of sprinting squat-type starting movement, it was found that the hip joint stretched during the first stance phase after the start. The knee flexor muscle group produced more significant power during the action transition, occupying about 54% (hip), 31% (knee) and 15% (ankle) respectively, while the speed was 3.1±0.25m/s. During the second stance phase, the speed increased to 4.28±0.27m/s, and the hip, knee and ankle joints performed 35%, 17% and 48% respectively. Exploring the effect of related muscle groups on increasing the starting speed, the ankle joint flexor muscles (gastrocnemius and soleus muscle) played a prominent role in the first and second steps, and the gastrocnemius muscle played an even more significant role in the second step, up to 92.9 % (in the first step is 67.1%) (Debaere et al., 2015). The role of the knee joint and the hip joint muscle group showed different effects due to the various starting

positions of the athletes.

As a conclusion of this study it was deduced that the knee joint accelerates the vertical direction of the body center of gravity and the hip joint has a significant effect on the forward and vertical directions of the center of gravity of the body. Further analysis of the starting movements of sprinters with different ages showed that adult athletes relied on the knee joint (35%) for work and produced larger steps and speeds in the first step of the start, while young athletes relied more on hip joints (57%). A study of musculoskeletal models for hurdlers and sprinters revealed differences in geometric and mechanical changes in the soleus and gastrocnemius-Achilles tendon units. Due to hurdle movements, geometric deformation (elongation: 0.031 m respectively for the soleus and the gastrocnemius-Achilles tendon) and the mechanical load on the AT (4066.91±322.56N) was found significantly higher compared to sprint movements (elongation: 0.016 m for the soleus and 0.021 m for the gastrocnemius-Achilles tendon) and load (3361±194.01N) (Li & Zhang, 2013). This research results provide a research basis for the risk of high damage to hurdles. Analysis and clarification of the characteristics of the starting movements at different levels have theoretical guiding significance for the formulation of training plans and strategies.

JUMPING

Jumping is a basic movement in several sports (such as basketball, volleyball, track and field, etc.). According to the difference in the support limb in the final step, the jump is divided into one-legged take-off, two-legged take-off, one-foot landing and two-foot landing (Hackney, Clay, & James, 2016). According to the difference in the completion of the action mode, the jump is further divided into jumping landing and free landing. Based on the differences in jumping movements, the biomechanical characteristics are also different (Vint & Hinrichs, 1996). Studies have shown that the single-leg take-off can provide higher center of gravity elevation by the auxiliary action of the swinging leg. On the contrary, the vacant period of the two-legged take-off is longer; the load distribution characteristics of the lower limb of the drop-landing and the free-falling are also different, resulting in potential injury characteristic differences. For example, anterior cruciate ligament (ACL) injury commonly occurs during landing.

The study found that the risk of ACL injury is not only related to the muscles of the knee joint (such as the quadriceps, the posterior femoral muscle and the gastrocnemius), but also to the muscles that do not cross the knee (such as the soleus muscle). For example, if the muscle strength of the gastrocnemius muscle is activated (flexed) then it will decrease the force submitted to the hamstring muscle during landing. Thus this muscle mechanism will produce immediate protection on the knee joint and it will prevent ACL from injury risk (Mokhtarzadeh et al., 2013).

The above-mentioned information not only reveals the biomechanical functional

characteristics of the jumping movement, but also has a guiding on preventing injury and carrying out intervention training programs, such as avoiding the injury of the ACL by enhancing the strength of the knee flexor muscle group (Figure 7) (Morgan, Donnelly, & Reinbolt, 2014).

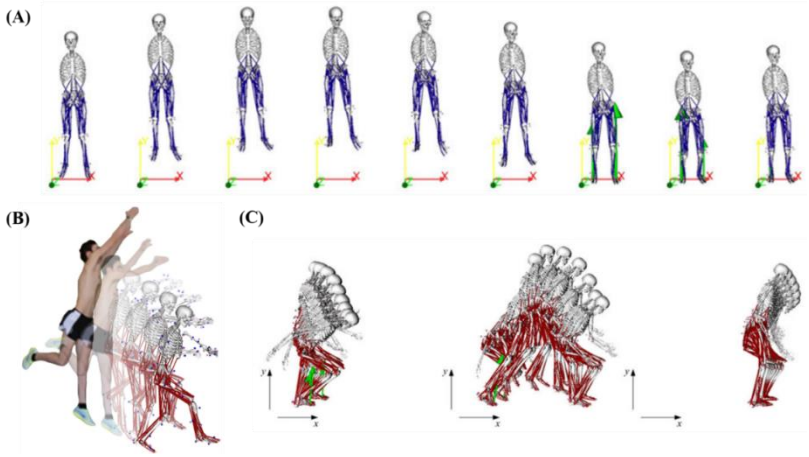

Figure 7 Illustration of OpenSim musculoskeletal model with different jumping and landing patterns; (A) Counter movement jump; (B) Single-leg jump landing; (C) Standing long jump. (Morgan et al., 2014) (Palmieri, Callegari, & Fioretti, 2015). Used by permission.

1.3.3 OpenSim lower extremity modeling in pathology gait

OpenSim musculoskeletal model is gradually applied to investigate the mechanism and the characteristics of movement patterns of numerous abnormalities such as joint dysfunction, obesity, diabetes, hemiplegia, hip dysplasia or knee arthritis. According to statistics from the World Health Organization (WHO) in 2016, the global adult population (over 18 years-old) has over 39% overweight and obesity. Children and adolescents (5-18 years old) have over 18% overweight and obesity (Harris et al., 2017). Obesity has been shown to be associated with several diseases and is a major preventable risk factor for degenerative changes in lower extremity joints, primarily knee joints. Moderate-intensity walking is often used as an exercise to intervene in obesity; however, studies have shown that with body weight gain by 5 kg the risk of knee arthritis will increase by 35% (Figure 8).

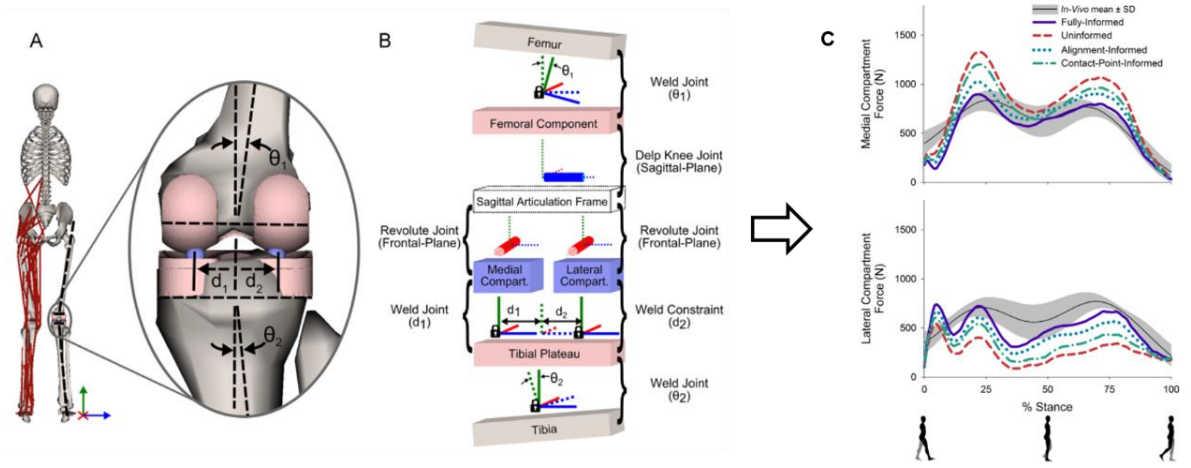

Figure 8 Graphical (A) and schematic (B) depictions of the medial/lateral compartment joint structures in the musculoskeletal model; (C) Medial (top) and lateral (bottom) compartment tibiofemoral contact forces during stance (Lerner, DeMers, Delp, & Browning, 2015), used by permission.

Another example where OpenSim musculoskeletal model can be effectively applied is the investigation of the effect of hemiplegia. This is an undesired brain malfunction which often leads to motor dysfunction in the neuromuscular system. For example, people with cerebral hemiplegic tend to exhibit a “Duchenne” gait, that is, the trunk leans toward dysplasia and keeps the pelvis stable or increases the swinging limb during the single stance phase. It is clinically interpreted as the mechanism of the resistance reduction of the hip abductor muscle group. By constructing an individualized three-dimensional musculoskeletal model, researchers explored the joint torque and power of the trunk to the frontal plane of the hip joint, and found that the trunk lumbar vertebrae in the frontal plane is more active than the normal population (32.48±8.04° vs 16.71±4.36°, $p<0.001$), and significantly reduced hip torque. While the torque and power of lumbar spine were significantly higher than the normal population, indicating that the hemiplegia needs compensatory improvement of the trunk muscle (Salami, Niklasch, Krautwurst, Dreher, & Wolf, 2017; Mei, Gu, Sun, & Fernandez, 2018).

In addition to lower limb modeling, problems related to the knee joint have been adequately handled by OpenSim application. For the musculoskeletal model of knee arthritis with different degrees of lesions, the knee joint contact force of early knee arthritis is not significantly different from that of normal and confirmed knee arthritis. It is necessary to evaluate the abduction and flexion moment of the knee joint to understand more the pathogenesis of the knee joint. One potential strategy is to shorten the duration of the high-intensity load during the gait stance phase (Meireles et al., 2016). The calculation of the adduction moment of the knee joint is also affected by the motion axis of the constructed model, such as Transepicondylar axis (TEA). The functional axis of rotation (FAR) is found to be different due to the difference of the movement axis of the constructed model (Richards & Higginson, 2010). In case of the factors, such as the relaxation of the joint ligament, the calculation of the knee arthritis load should consider the load-bearing condition. The function of the lower

extremity axis of motion is thus able to explain knee instability under load bearing conditions (Meireles, De Groote, Van Rossom, Verschueren, & Jonkers, 2017).

Conventional aerobic exercise is an effective intervention for the treatment of knee arthritis, which can slow knee pain and improve motor function. There is no consensus on whether to use continuous or intermittent aerobic walking intervention. The intensity of aerobic exercise (heart rate) was monitored by conducting a 45-minute and three 15-minute intermittent aerobic exercise tests. Subjective knee pain index and objective knee contact force data were recorded and the continuous exercise was monitored in the whole process. During the landing phase, the peak value of the knee joint contact force increased by 22-25% of the body weight, leading to increase of subjective pain. On the contrary, the intermittent aerobic exercise of the same intensity did not increase the pain of the knee joint and the joint contact force. Studies have shown that intermittent exercise of the same intensity is recommended for aerobic exercise regimens of more than 30 minutes, which can reduce knee pain. Another treatment for knee lesions is total knee arthroplasty (TKA) to relieve pain and improve function (Shawn Farrokhi et al., 2017). However, the compensatory response to motor function often results in asymmetry of lower limb movement and weight bearing. It also result in muscle and motor function alterations around the knee and hip joints, showing increased hip external rotation and reduced knee flexion, decreased muscle strength of the quadriceps and hip abductors during stair climbing. The above-mentioned compensation strategy aims to reduce the quadriceps muscle load in order to prevent joint instability after total knee arthroplasty and relief pain during knee arthritis.

A special application field for musculoskeletal modeling is related to lower limb amputations, which are due to terminal nerve disease and other unexpected factors (Gaffney et al., 2016). In the design process of prosthetic instruments, due to ergonomics and amputation of the population's own motor function compensation and other factors, the bilateral asymmetry of lower limbs often coexist, which may lead to lower back pain and increase the risk of contralateral knee and hip joint inflammation.

The ergonomics research on artificial limbs is also influenced by the musculoskeletal model. The traditional Plug-In-Gait (PIG) six-joints model are often used to calculate and analyze the kinematics, kinetics and muscle activities of the lower limbs (Karimi et al., 2017). The morphological parameters of the prosthesis have a great influence on the biomechanical performance. The results showed that the ergonomic study of the prosthesis needs to combine the characteristics of the prosthesis to build the whole-body musculoskeletal model and to obtain accurate and reliable estimation data output (Rigney, Simmons, & Kark, 2016). The effect of the personalized ankle brace during the walking process was found to be able to compensate the lower limb muscle function and provide active knee flexor muscles in the middle and late stance phases (Arch, Stanhope, & Higginson, 2016).

It is worthy to mention that juvenile idiopathic arthritis is a musculoskeletal disease that often occurs in children and adolescents. It usually affects the structure and function of the knee and ankle joints, and causes arthritis or cartilage lesions, severe cases can lead to disability. Combine MRI imaging to reconstruct individualized musculoskeletal model, define ankle joint axis and Achilles tendon anterior/posterior tibia, tibia long/short muscle, lumbar flexor/extensor and longus flexor/extensor starting and ending points. Comparing the motion axis of the ankle joint based on MRI and the ankle motion axis based on clinical gait analysis (CGA) on the ankle joint force. It has been found that the ankle joint force is affected by the starting point of the Achilles tendon (7.2%-13.4% difference). The results show that the reliability of the model has a great impact on the accuracy of the estimated results among special pathological populations. For specific populations, individualized musculoskeletal models need to be constructed to carry out reliable scientific research (Figure 9) (Prinold et al., 2016).

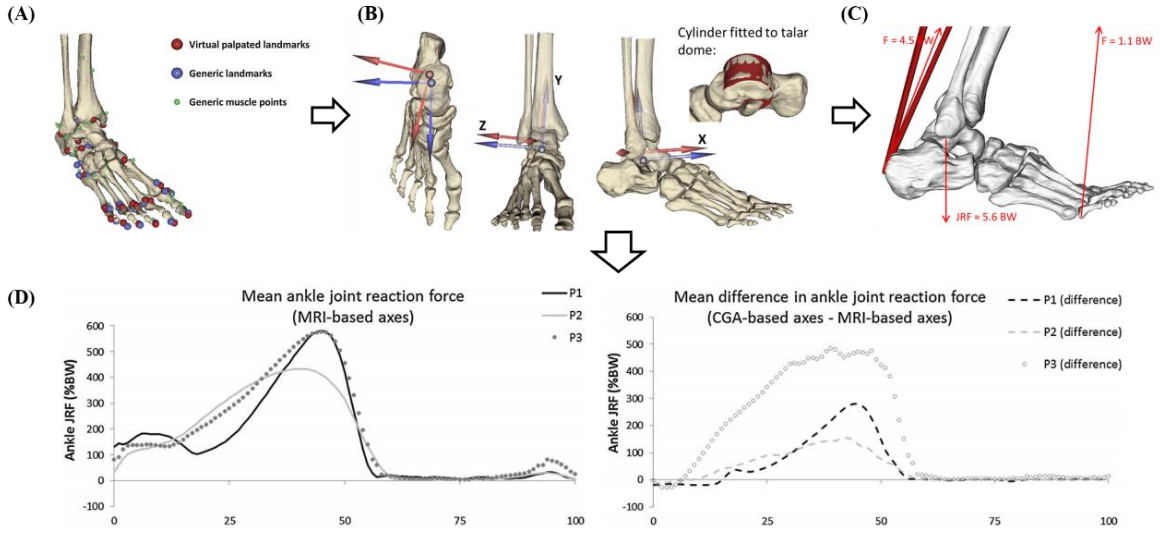

Figure 9 (A) MRI-based patient-specific foot-ankle model; (B, C) to define motion axis and muscle tendon insertion points; (D) for the comparative analysis of ankle joint reaction force. (Prinold et al., 2016), used by permission.

The above-mentioned studies about walking, running, jumping and pathological gait research have laid a solid research background and theoretical basis for the application of individualized OpenSim musculoskeletal model in the field of sports science and rehabilitation. The patient-specific OpenSim musculoskeletal model, based on medical images, can eliminate the differences in sport performance caused by different anthropometric characteristics between individuals. In addition, a large sample size data can be used to construct a musculoskeletal model database for different areas (Asia, Europe, America, India, Africa, etc.) and populations (such as children, adolescents, athletes, elderly and special diseases).

1.4 Achilles tendon rupture mechanism

1.4.1 Achilles tendon properties alteration

Achilles tendon rupture (ATR) is common and life altering injury. A patient who sustains an ATR should expect a year recovery with extensive rehabilitation (Leppilahti, Puranen, & Orava, 1996)(Raikin, Garras, & Krapchev, 2013). For elite athletes, especially in sprinters, basketball players and badminton players, it is a career-threatening injury. ATR most commonly associated with sports activities, such as bursts of pivoting, jumping and sprinting (Naim, Simşek, Sipahioğlu, Esen, & Cakmak, 2005). The ATR is a devastating injury that causes a functional deficit of the triceps surae muscle-tendon complex and plantar flexors. About 50%-60% of athletes with an ATR are unable to return to the court, and accompanied with an obvious decline of physical activity level due to disability after injury (Nicola Maffulli, 1999). AT elongation and decreased calf muscle function altered gait are permanent impairments and it is still a common problem for athletes with history of ATR (Jandacka, Zahradnik, Foldyna, & Hamill, 2013).

Recovery from an ATR involves alteration in the mechanical properties and morphology of the tendon. These alterations include disruption and disorganization of collage bundles, and increase in proportion of type III relative to type I collagen bundles. These changes affect the AT mechanical behavior and material properties (Shim et al., 2019). Voleti et al., (2012) displayed scar tissue, which was produced after ATR in the final stage of tendon healing. This process can last one year or more after injury (Voleti, Buckley, & Soslowsky, 2012). A systematic review concluded that there is consistent evidence that the AT elongates more for a similar tendon force, and has a lower stiffness and Young's modulus in people recovery from ATR. In addition, the morphology of AT is changed with ATR (Singh, 2017) by having an increased cross-sectional area. Suydam et al., (2015) collected 4 ATR patients between 6-12 months post-surgery and 5 healthy controls via ultrasound imaging. This study found that the AT lengths at 6-12 months post-surgery were significantly longer on the ruptured side compared to the un-ruptured side. The anatomical changes in the tendon and the weakness of AT related muscle (the calf) maybe due to a lack of force transmission capability (Suydam, Buchanan, Manal, & Silbernagel, 2015).

The AT will stretch when loaded and this stretch was believed, until very recently, to occur within the tendon fascicles, incorporating first crimp straightening and then fascicle extension under load. However, recent in-vitro data indicate that tendon stretch and recoil involves significant sliding or shearing in the connective tissue between the fascicles in the end of the tendon. Tendon strain is influenced by several factors, including muscle forces applied to the tendon during exercise, the individual tendon geometry and the material properties of the tendon. Previous in vivo and experimental studies suggest that tendon rupture mainly occurs in the tendon mid-section and predominantly more in men than women due to reasons yet to be identified.

1.4.2 Gait function impairments

One of the key factors that limits the tendon recovery is an abnormality of gait. Kinematic and kinetic data collected in a full gait cycle can assess gait abnormalities to some extent, which include patients suffered from sports injuries (Matt L. Costa, 2005; Garrido et al., 2010). Gait abnormalities have been found even 2 years after injury, where the weakness of calf muscles and tendon elongation should be assumed as main responsibility. Finding the relationship between ankle plantar-flexor muscle tendon unit properties can help to create rehabilitation programs during walking patterns (Schepsis, Jones, & Haas, 2002). Previous studies found the increased ankle dorsiflexion range of motion (ROM), decreased ankle plantarflexion ROM, decreased step length and co-activation of the lower limbs muscles were associated with gait abnormalities after 1-year Achilles tendon (AT) surgical repair (Don et al., 2007). The decreased calf muscles force and functionality have also been reported in a longitudinal study, which combined with the persistence of decreased step length and ankle plantarflexion weakness induce a decreased fitness activity and the quality of daily life (Matthew L. Costa, Logan, Heylings, Donell, & Tucker, 2006).

During human running, the AT is subjected to high repetitive and eccentric loads, up to 6 times the body weight. The AT is a key factor for efficient human movement, since after foot contact with the ground, the AT stretches and transfer forces through the kinetic chain via the joints (Farris et al., 2011). Then the AT is returned in the mid-stance phase, contributing more than the half of propulsive force and energy at the ankle joint during running. It is proven that athletes with a surgical repaired ATR are more likely to suffer another rupture again than those without ATR history (Kujala, Sarna, & Kaprio, 2005). Another significant factor that influence the outcome after ATR and limits recovery is the asymmetry of gait. Altered ankle kinematics during stance phase of 2 runners were found with an elongated AT. Kinematics and kinetics collected in a full gait analysis can assess the magnitude of gait abnormalities after ATR (Geremia et al., 2015). Asymmetry is described as a difference in kinematic and kinetic parameters between both lower limbs, and it often occurs in healthy populations (Sadeghi, Allard, & Duhaime, 1997). High gait asymmetry degrees are typically to be associated with pathology in previous studies (Alexander et al., 2009; Lathrop-Lambach et al., 2014).

It is important to note that threshold levels of gait asymmetry do exist, which can be used to predict injury risks. It was found that imbalances exceeding 15% in knee flexors and hip extensors were main causes of injuries for female elite runners (Knapik, Bauman, Jones, Harris, & Vaughan, 1991). Previous injuries that have not been properly rehabilitated can also lead to increased level of asymmetry. The effect of gait speed on the bilateral symmetry of gait has been primarily studied on the transition of walking to running in case of healthy individuals on treadmill (Plotnik, Bartsch, Zeev, Giladi, & Hausdorff, 2013). Quick motion alterations like high speed walking and running for ATR patients may be detrimental for the tendon rehabilitation. In addition, abnormal gait patterns combined with asymmetrical mechanical loading on the healed AT could also lead to potential injuries. Therefore, the above-mentioned

motions can possibly increase the re-rupture risk and lead to compensatory and functional changes of the muscular-skeletal system (Maquirriain, 2011). However, the effect of gait speed on unilateral ATR uninjured-injured coordination were seldom explicitly addressed during over ground gait in previous studies.

The gait asymmetry among participants of unilateral ATR after surgical repair has been found (Silbernagel, Steele, & Manal, 2012). However, few information was reported about how the muscles contribute to walking and running tasks.

To address this problem, the use of musculoskeletal models (MSMs) has prevalent in recent 10 years in the biomechanics community, due to its ability to evaluate muscle and joint contact forces during gait. AT forces during locomotion has been reported in relatively few studies. In most of those studies, AT force during running has been estimated by dividing net ankle joint moments, estimated by inverse dynamics approach, by the AT moment arm. However, a principle limitation of using the net joint moments calculated using inverse dynamics to estimate AT force is that this method does not account for co-contraction of the tibialis anterior observed during the loading phase (Scarton et al., 2018).

Therefore, the magnitude of AT force may have been underestimated during the loading phase. To solve this problem, the gait2392 model is used in our research, which is created to be subject specific by the insertion of lateral gastrocnemius, medial gastrocnemius and soleus muscles. By having this model, it is possible to higher the accuracy of muscle activation and force results in Static Optimization. Therefore, it becomes possible to gain knowledge how gastrocnemius and soleus muscles contribute to walking, jogging and running tasks, and in addition the investigation of the inter-limb (injured and uninjured side) symmetry or asymmetry characteristics via subject-specific MSMs is also converted into reality (Chen, Hu, Blemker, & Holmes, 2018).

The purpose of gait analysis in this dissertation is to prospectively investigate gait abnormality in athletes who underwent unilateral surgical repair of ATR. This is carried out by comparing asymmetry magnitude during walking and running, within an average period of 18-24 months after surgical repair via comparison of biomechanical parameters. The following investigations will include how gait abnormalities affect the kinematic (joint angles and angular velocities of ankle, knee and hip), kinetic parameters (ground reaction forces, vertical average loading rate), plantar pressure (peak pressure, pressure-time integral and contact area) as well.

1.4.3 Musculoskeletal disorders of Achilles tendon rupture

ATR is more common in male than in females with figures being quoted at 5:1 (Ganestam, Kallemose, Troelsen, & Barfod, 2016). It must be mentioned that tendons are not contractile tissues, and as such cannot provide necessary positive work to drive human motion. Evidence has been reported that ATR will cause persistent tendon elongation and it is associated with biomechanical deficits such as decreased plantar flexor muscle strength/volume, decreased ankle joint proprioception and reduced AT stiffness (Mullaney, McHugh, Tyler, Nicholas, & Lee, 2006; Barfod, Bencke, et al., 2015).

These functional deficits are reported regardless of the medical efforts and treatment modality for both short-term and long-term outcomes (Heikkinen et al., 2017). The elongated tendon combined with decreased muscle force and tendon stiffness has been shown to have a substantially decreased running and jumping performance, and they also have implications for daily functional activities such as normal gait and walking on stairs (Rosso et al., 2015). The alterations in calf muscle anatomical, mechanical and neuromuscular properties after ATR may increase plantar flexor muscle activity during movement, leading to AT weakness in a plantar-flexed position and reduce plantar flexor endurance (Suydam et al., 2015).

The rupture injury mechanism of ATR can be attributed to sudden unexpected powerful dorsiflexion of the foot or forced dorsiflexion of the plantar-flexed foot (Olsson et al., 2011). A case study reported that long-term functional deficits after ATR could be explained by permanent reductions in gastrocnemius muscle fascicle length (Jandacka et al., 2013). The muscle-tendon structure is detrimentally affected following ATR and the calf muscle strength deficits are positively correlated with the fascicle length reduction magnitude (Matthew L. Costa et al., 2006). The atrophy and eccentric strength impairment of calf muscles were still present after 24 months of ATR, which brings adaptive modifications in gait strategy involving ankle motion and coordinated muscular activities (Goren, Ayalon, & Nyska, 2005). To further improve treatment it is important to understand the underlying mechanisms for musculoskeletal deficits.

Biomechanical analyses are always carried out using experimental or computational methods. The traditional biomechanical analysis based on laboratory experiments have two inadequacies:

1. Large amount of important information, including muscle forces, is difficult to measure in the laboratory,
2. Separate laboratory data proved to be difficult to build a relationship with complex human dynamic systems.

OpenSim is an open-source software package developed for musculoskeletal model building simulation, and analysis without surgically-invasive procedures (Delp et al., 2007). In silico OpenSim models provide a modeling environment for identifying individual variables (kinematics, kinetics, muscle-tendon parameters) and predict muscle force contributions and joint contact loads during walking and running (Seth et al., 2018).

Extensive research has developed "generic" lower limb musculoskeletal models using cadaveric data. Medical images (ultrasound, computed tomography, magnetic resonance imaging, etc.,) may help to generate a high level of anatomical personalization for creating image-based subject-specific musculoskeletal models (Smale et al., 2019). With the combination of medical images, several authors used subject-specific models to estimate knee/tibiofemoral articular forces. The comparison of generic and subject-specific models have also been shown to be more accurate in the assessment of knee joint contact force using subject-specific anatomical parameters (Harris et al., 2017; Lerner et al., 2016). Up until now, there are few studies that have investigated the rupture-repaired AT subject-specific model for estimating muscle forces and joint articular forces. The identification of musculotendon parameters, i.e. tendon slack length l_s^t and optimal fiber length l_o^m should be critical aspects when creating subject-specific musculoskeletal models. This is important due to the sensitivity of muscle estimated forces to the muscle-tendon complex moment arms (Modenese et al., 2018).

Direct measurement of AT forces and stresses is not ethically viable, therefore computational modelling, such MSMs are needed. Experimental measures that quantify regional tendon strain are currently restricted to a small imaging region of a portion of the AT and to less dynamic slow activities such as isolated contraction and walking (Halonen et al., 2017). In addition, due to the complex behavior and structure of the AT, it is difficult to experimentally measure the contribution of parameters that will influence tendon strain. Therefore, subject-specific FEMs were recently developed to investigate the relative effects of variations in tendon geometry and material properties on local tendon stress and strain. Shim et al., (2019) used manually segmented ultrasound images to create subject-specific finite element models. As a results they concluded that the cross-sectional area of tendinopathy was approximately 31% greater compared to healthy tendons. The lower tendon stress in tendinopathy was due to a greater influence of cross sectional area, compared to a lower Young's modulus, which reduced the tendon stress by 30%. The changes in 3D geometry of the tendon contributed more to local stresses in the tendon than the material properties. The MSMs can estimate muscle-tendon unit and joint reaction forces, while they do not provide detailed information about the tendon inner stresses and strains (Shim et al., 2019). There is strong evidence for altered mechanical and morphological properties in the pathological AT combined with the assumption that mechanical loading triggers the adaptation of the tendon. It is suggested that non-uniform displacement could reduce loading of the tendon. Exercises need to deliver the appropriate mechanical trigger to stimulate the restoration of normal tendon properties.

Therefore, it is crucial that exercises are adequately tuned to account for these altered properties in order to design a rehabilitation protocol that delivers optimal stimulus for tendon regeneration and avoids tendon overloading. This dissertation aims to implement the joint motions from integrated 3D motion capture, ground reaction forces (from force plates) and medical images to build subject-specific MSMs. Then calculation joint moments, muscle forces and joint reaction forces by MSMs can estimate the stresses and strains in the tendon during daily activities, such as walking and running.

1.5 Aims and objectives

In my thesis, I would like to draw up three research questions that have been unanswered so far in the relevant literature.

The 1st research question:

It has been revealed in the literature study, that in case of musculoskeletal modeling, no authors have considered to alter two important musculotendon related parameters, namely: tendon slack length l_s^t and optimal fiber length l_o^m. Without considering these parameters, the musculotendon forces will be very likely overestimated in the pathological side for ATR patients. By changing these parameters, it is possible to alter the Achilles tendon to behave like if it was ruptured and therefore, we could obtain realistic muscle forces for the triceps surae and the joint reaction forces.

Therefore, my 1st objective is:

To create a new musculoskeletal model, combined with experimental techniques (involving motion capture, ground reaction force measurement and medical imaging) which can realistically calculate the musculotendon forces and joint reaction forces in case of simulated Achilles tendon rupture. As a novel augmentation, the tendon slack length l_s^t and optimal fiber length l_o^m are determined by medical imaging, and they are integrated into the model. Therefore, it is possible to quantify the percentile difference between the musculotendon forces with or without Achilles tendon rupture.

The 2nd research question:

It has been not discussed whether the Achilles tendon rupture has any critical effect on the knee joint and its area. However, it is assumed that it does and this effect is very likely resulted in higher knee adduction moment and joint forces during walking, which should be quantified.

Therefore, my 2nd objective is:

By creating the new musculoskeletal model, the effect of Achilles tendon rupture on the knee kinetics will be quantified. The aim of this part is to compare the magnitude of the knee adduction moments in frontal plane and estimate knee joint reaction forces between the injured side (with ATR) and the uninjured side (without ATR) during walking, jogging and running. On one hand, by knowing the realistic joint loading in the injured side, a safer physical activity guideline during ATR rehabilitation process can be proposed to avoid the risk of knee pain and knee osteoarthritis in case of overloading. On the other hand, it should be evaluated if the Achilles tendon can increase the chance of knee osteoarthritis or it is an irrelevant factor.

The 3rd research question:

In the previous studies, reduced ankle plantarflexion moments, plantarflexion joint power (moment multiply by angular velocity) were found during walking in the injured side of unilateral ATR patients. However, little is known regarding ankle joint mechanics during high demand sporting tasks such as jogging and running after an ATR. It is also unclear in what way is the ankle-knee relationship effected by the ATR and whether it can cause negative long-term effect on the joints?

Therefore, my 3rd objective is:

To reveal how the kinematics (including trajectory of the center of pressure) and the kinetics (joint moments, gastrocnemius medialis, gastrocnemius lateralis, soleus and ankle joint reaction forces) of the ankle joint can be realistically estimated during walking and especially high demand sporting tasks consists of jogging and running. In addition, long-term physical effects are also addressed and explained in this part.

2 Materials and methods

2.1 Introduction to the experimental and computational workflow

This dissertation combines experimental testing part and OpenSim simulation part to develop and validate a workflow that will allow non-invasive characterization of AT properties in terms of its geometry and injury bio-mechanism. Based on these results, the workflow will allow the selection of appropriate rehabilitation exercises that will deliver the optimal strain distribution in the tendon to optimize the recovery process.

In order to carry achieve these aims, an eight-camera motion capture system (VICON Metrics Ltd., Oxford, United Kingdom) was used to track the marker trajectories at the frequency of 200 Hz, and an in-ground force platform (AMTI, Watertown, MA, United States) was utilized to record the ground reaction force at the frequency at 1000 Hz. The force plate was located in the middle of the 15 m walkway. The experimental part consists motion capture data (Marker data) and ground reaction forces (GRF) data, which were collected for all the subjects.

The OpenSim simulation part relies on the data inputs from the experimental part, as shown in Figure 10. The details about the experimental testing are listed in 2.2.

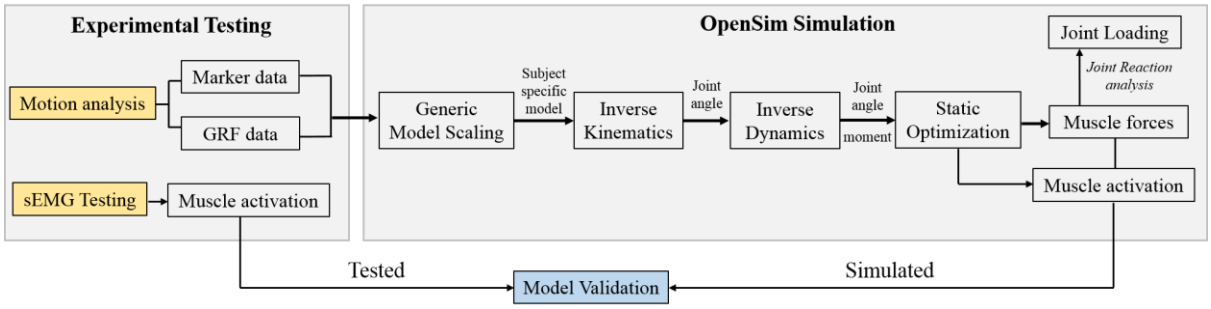

Figure 10 Data processing flow chart, from experimental testing to OpenSim simulation. Note. GRF: ground reaction force; sEMG: surface electromyography.

The OpenSim gait2392 generic musculoskeletal model (MSM) was used for this dissertation. This model included the torso and lower extremity, which had six degrees of freedom at the pelvis, a ball and socket joint with three degrees of freedom at the hip, pin joints at the ankle, subtalar and metatarsophalangeal joints. Data processing was performed in OpenSim version 4.0. Marker trajectories data and ground reaction forces data were low pass filtered at 12 Hz and 50 Hz with a zero-phase fourth order Butterworth filter. The musculoskeletal model was firstly scaled to each participant's anthropometric measures, collected from human static marker position, body mass and height. The "Inverse Kinematics" algorithm minimized errors between the virtual markers in the scaled model and the experimental marker trajectories to compute the joint angles. Then the joint angles, calculated from "Inverse Kinematics" tool, were integrated into "Inverse Dynamics" algorithm to calculate the joint moments.

Thereafter, the obtained joint angles and moments served as input in the "Static Optimization" to compute muscle forces and activation, which improves the accuracy of joint contact forces prediction. The "Joint Reaction Analysis" tool was used to compute the hip, knee and ankle joint contact forces, respectively.

The final part of the experiments end with the surface muscle electromyography (sEMG). In this process the sEMG signals were captured by Delsys system (Delsys, Boston, MA, United States) for muscle activities, including rectus femoris (RF), biceps femoris (BF), medial gastrocnemius (MG), and lateral gastrocnemius (LG). The importance of this last experiment is the following: the sEMG signals from experimental testing can be compared with the predicted muscle activations, obtained from the OpenSim, which serves as an excellent validation for the MSM model.

As a short summary, the complete workflow is carried out as follows: the subject-specific musculoskeletal model (Subject-specific model building) is built up by providing data from two sources (Figure 11):

1. Marker trajectories and ground reaction forces (Marker and ground reaction forces data capture);
2. Subject-specific anthropometric data from medical images (Subject-specific parameters).

Then the MSM is prepared for simulation, therefore walking, jogging and running motions are carried out on it (Inverse Kinematics and Inverse Dynamics) to obtain moments, muscle forces and joint reaction forces along with joint angles. Thereafter the last step is the procession of the data.

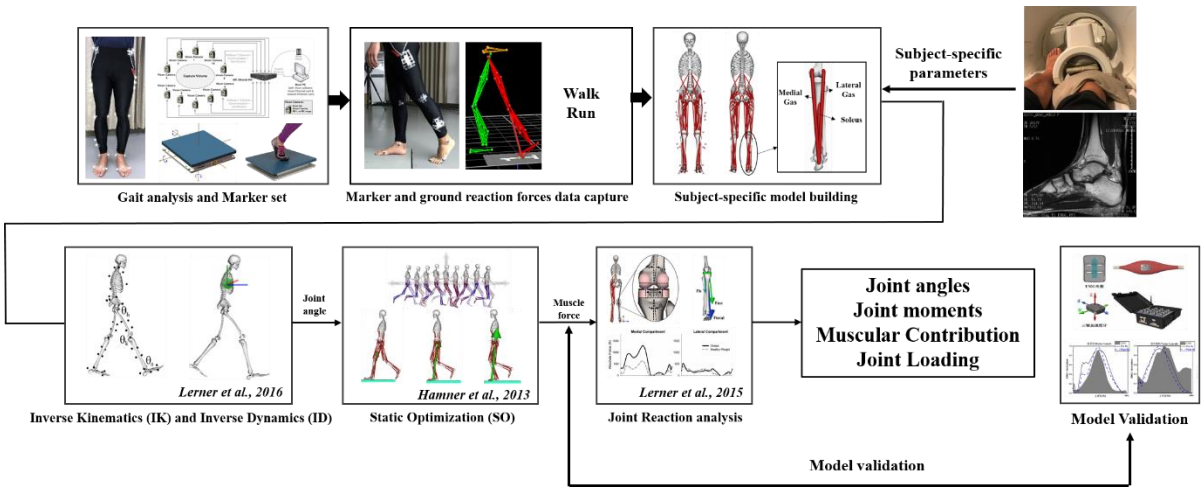

Figure 11 Experimental and computational process flowchart.

2.2 Experiments

2.2.1 Ethics statement

This dissertation was authorized by the Ethics Committee of Ningbo University (Authorization No. RAGH20181124). Before taking part in the dissertation, all subjects were informed of the objectives, experimental procedures and risks associated with this dissertation. All subjects gave consent to participate in this dissertation, as shown in Figure 12.

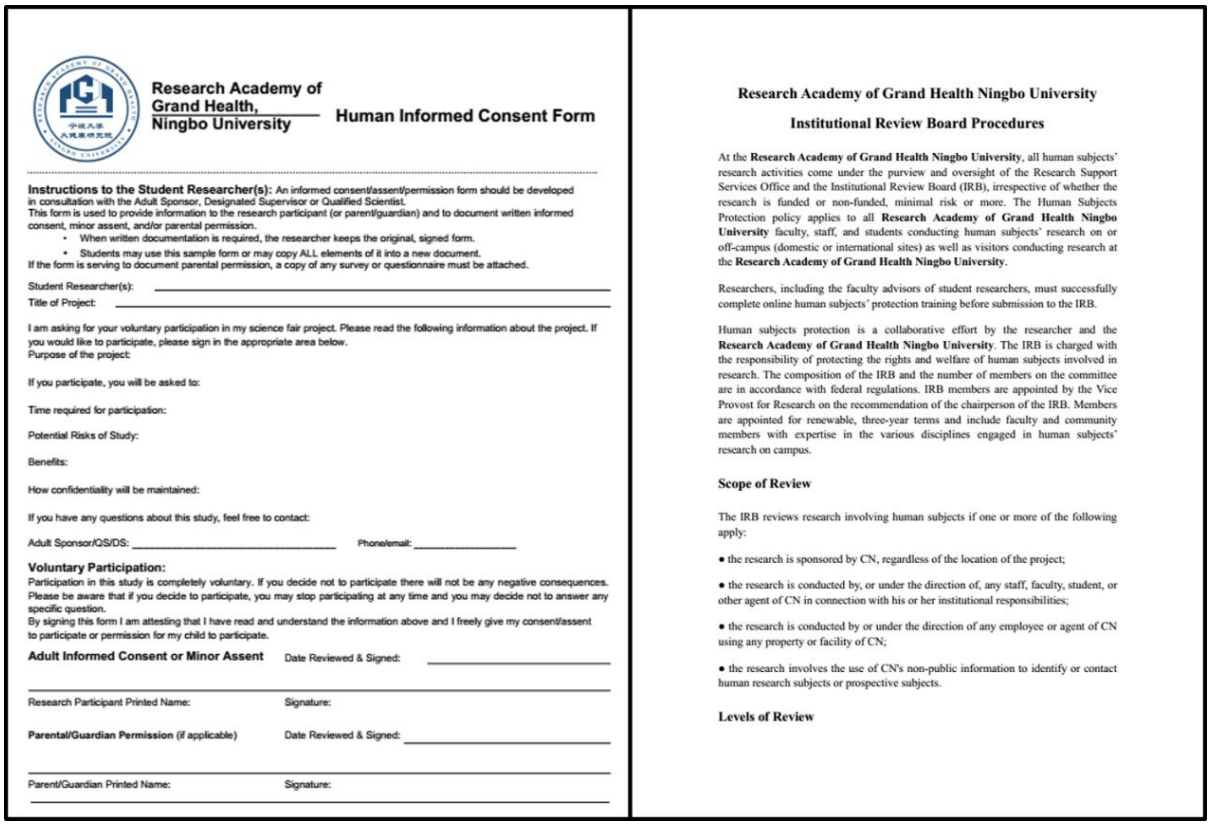

Research Academy of Grand Health, Ningbo University — Human Informed Consent Form

Instructions to the Student Researcher(s): An informed consent/assent/permission form should be developed in consultation with the Adult Sponsor, Designated Supervisor or Qualified Scientist.
This form is used to provide information to the research participant (or parent/guardian) and to document written informed consent, minor assent, and/or parental permission.

- When written documentation is required, the researcher keeps the original, signed form.
- Students may use this sample form or may copy ALL elements of it into a new document.

If the form is serving to document parental permission, a copy of any survey or questionnaire must be attached.

Student Researcher(s): _____

Title of Project: _____

I am asking for your voluntary participation in my science fair project. Please read the following information about the project. If you would like to participate, please sign in the appropriate area below.
Purpose of the project:

If you participate, you will be asked to:

Time required for participation:

Potential Risks of Study:

Benefits:

How confidentiality will be maintained:

If you have any questions about this study, feel free to contact:

Adult Sponsor/QS/DS: _____ Phone/email: _____

Voluntary Participation:
Participation in this study is completely voluntary. If you decide not to participate there will not be any negative consequences. Please be aware that if you decide to participate, you may stop participating at any time and you may decide not to answer any specific question.
By signing this form I am attesting that I have read and understand the information above and I freely give my consent/assent to participate or permission for my child to participate.

Adult Informed Consent or Minor Assent Date Reviewed & Signed: _____

_____

Research Participant Printed Name: Signature:

Parental/Guardian Permission (if applicable) Date Reviewed & Signed: _____

_____

Parent/Guardian Printed Name: Signature:

_____

Research Academy of Grand Health Ningbo University

Institutional Review Board Procedures

At the **Research Academy of Grand Health Ningbo University**, all human subjects' research activities come under the purview and oversight of the Research Support Services Office and the Institutional Review Board (IRB), irrespective of whether the research is funded or non-funded, minimal risk or more. The Human Subjects Protection policy applies to all **Research Academy of Grand Health Ningbo University** faculty, staff, and students conducting human subjects' research on or off-campus (domestic or international sites) as well as visitors conducting research at the **Research Academy of Grand Health Ningbo University**.

Researchers, including the faculty advisors of student researchers, must successfully complete online human subjects' protection training before submission to the IRB.

Human subjects protection is a collaborative effort by the researcher and the **Research Academy of Grand Health Ningbo University**. The IRB is charged with the responsibility of protecting the rights and welfare of human subjects involved in research. The composition of the IRB and the number of members on the committee are in accordance with federal regulations. IRB members are appointed by the Vice Provost for Research on the recommendation of the chairperson of the IRB. Members are appointed for renewable, three-year terms and include faculty and community members with expertise in the various disciplines engaged in human subjects' research on campus.

Scope of Review

The IRB reviews research involving human subjects if one or more of the following apply:

- the research is sponsored by CN, regardless of the location of the project;
- the research is conducted by, or under the direction of, any staff, faculty, student, or other agent of CN in connection with his or her institutional responsibilities;
- the research is conducted by or under the direction of any employee or agent of CN using any property or facility of CN;
- the research involves the use of CN's non-public information to identify or contact human research subjects or prospective subjects.

Levels of Review

Figure 12 The human informed consent form and institutional review board procedures.

2.2.2 Participants

Six male athletes with unilateral rupture surgical repaired AT were included (26.75±3.71years, 1.83±0.06m, 84.2±7.68kg). Five of the subjects were right side rupture and one of the subjects had a left side rupture, all the subjects were right-leg dominant. The inclusion criteria for the ATR subjects were between 20-40 years of age with no re-rupture or AT injury on the contralateral side. The exclusion criteria were physical or neurological conditions and problems existing preventing the subjects from walking normally. The AT total rupture score (ATRS) was used for measuring the patients' symptoms and physical activity levels(Nilsson-Helander et al., 2007). The range of ATRS was from 0 to 100, with lower scores indicating greater non-compliance with physical activity and more muscular impairments. The average (standard deviation, SD) ATRS for the six subjects was 87.3 (6) two-years after surgery.

2.2.3 Experimental instruments

An eight MX-Cameras VICON motion analysis system (Oxford Metrics Ltd., Oxford, UK) were used to capture the lower extremity kinematics at the frequency of 200Hz. Calibration of the motion capture system was performed before the gait trials. A 0.6 m×0.8 m force plate (AMTI, Watertown, USA) was fixed into the middle of the walkway and utilized to obtain the GRF data at a frequency of 1000 Hz (Figure 13). The marker trajectories and ground reaction force data were captured synchronously using the VICON Nexus software package (Version 2.8.5, VICON, UK).

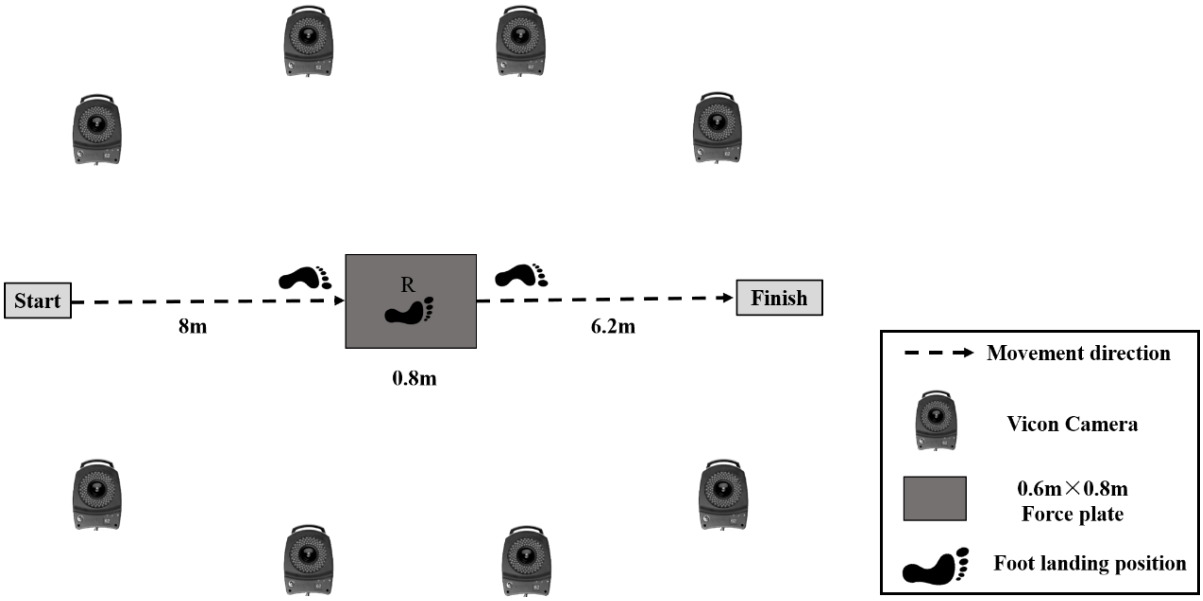

Figure 13 Experimental set-up (not on scale).

2.2.4 AT anthropometric measurement

AT length was taken with a 6.0 cm long linear transducer, scanning frequency of 10 MHz, distance resolution of 0.26 mm ultrasound imaging system (Aloka, Tokyo, Japan). In this dissertation, gastrocnemii and soleus AT lengths were measured from the ultrasound images and Magnetic resonance imaging (MRI) based on procedures of previous studies (Kunimasa et al., 2014). The length of gastrocnemii AT was defined from the calcaneal tubercle (AT insertion point) to the AT junction of medial and lateral gastrocnemii muscles. The length of the soleus AT length was defined from the calcaneal tubercle to the distal end of soleus muscle as previously described in the literature. The subjects were asked to lay in a prone position with their legs fully extended. The ImageJ ultrasound imaging analysis software was used for measuring the gastrocnemii and soleus AT lengths on both legs (NIH, Bethesda, Maryland, USA).

The measuring error of this method has been previously reported to be less than 0.01, and the retest reliability has been established with an intra-class correlation efficient (ICC) of 0.96 (Barfod, Riecke, et al., 2015). As shown in Figure 14 and 15.

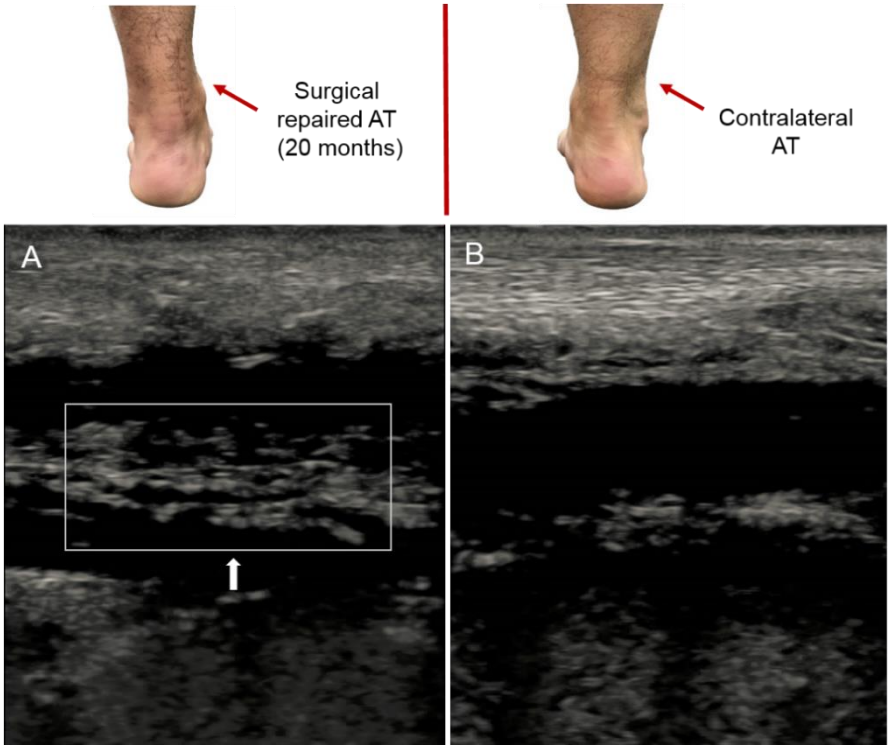

Figure 14 Ultrasonography images in the sagittal (longitudinal) plane of the (A) AT injured side and (B) AT uninjured side.

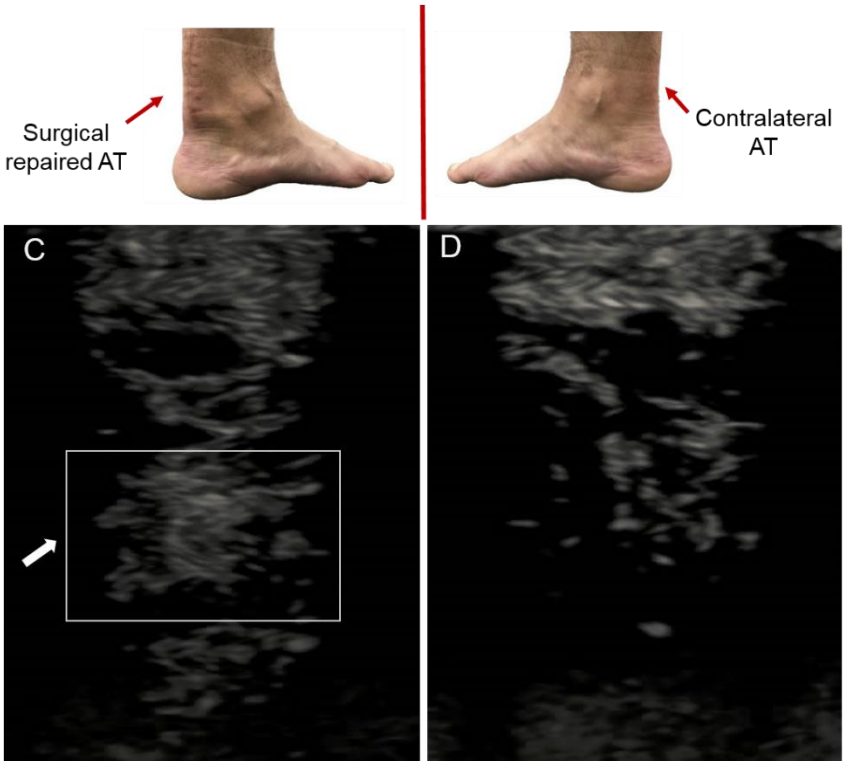

Figure 15 Ultrasonography images in the transverse plane of the (C) AT injured side and (D) AT uninjured side.

Complete injured side feet were captured using a Philips 3 Tesla MRI unit (Sigma Horizon LX 1.5 Tesla, General Electric, USA) through a single scan of three separate stacks. Repetition time/echo time was set to 500/14 millisecond, field of view: 18 cm, and slice thickness: 1 mm. Combinations of frontal and sagittal views of T1 and T2-weighted scans were used to segment the AT of the injured side (Figure 16). The segmentation of Achilles tendon geometry, based on the cross-sectional images, was performed by Mimics 17.0 software.

Figure 16 Magnetic resonance imaging for the participants.

2.2.5 Human motion and ground reaction forces capture

Prior to biomechanical tests, participants completed a self-directed warm-up and familiarization on the laboratory. Then, subjects were asked to walk and run barefoot at their self-controlled and comfortable speeds on a 15 m track. The subjects were also asked to land on the force plate and eight successive trails for each single right and single left foot strike conditions were collected bilaterally on all subjects. The experiments were carried out with the same technical background and devices. A pair of Brower timing lights (Brower Timing System, Draper, UT, USA) were set 2 m apart on the middle of the force plate to record the velocity. The three-dimensional marker trajectories were captured using a VICON motion analysis system (Oxford Metrics Ltd, Oxford, UK), with 8 cameras and sampling at 200 Hz. Ground reaction force measurement was synchronized by an in-ground force platform at 1000 Hz *(AMTI, Watertown, USA)*(Mei, Gu, Xiang, Baker, & Fernandez, 2019). The marker trajectory was low-pass filtered using a frequency of 12 Hz and the ground reaction forces were filtered at 50Hz using a zero-phase fourth-order Butterworth filter. Marker trajectory data file *(.trc)* and ground reaction force data file *(.mot)* were outputted using VICON Nexus software *(v2.8.5)*, as shown in Figure 17.

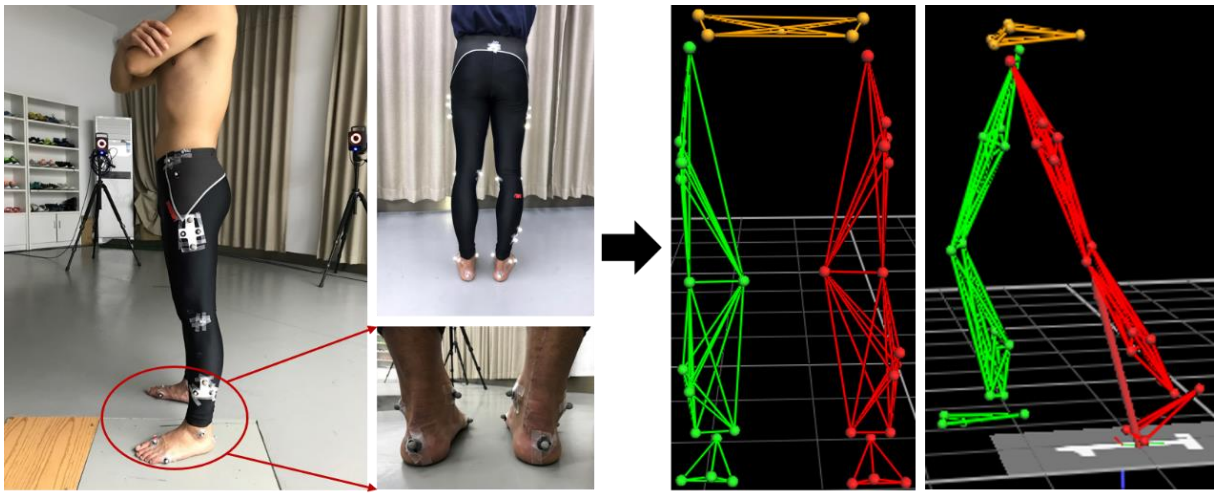

Figure 17 Three dimensional motion capture for the lower extremities.

Visual 3D (Version 6.10.0, C-motion, USA) gait analysis software was used to calculate the kinematics and the joint moments. The ankle, knee and hip joints were considered as a generalized linked-segment model. The joint angles and angular velocities of lower extremity were also computed, based on the Visual 3D requirement, for a skeletal framework. Inverse dynamics approach, based on Newton-Euler equations, was used for the calculation of lower limbs joint moments. All joint moments were normalized to body weight. For kinematic variables for analysis in this dissertation, peak angle values and peak angular velocity values in three planes of the hip, knee and ankle joints in the stance phase were included.

2.2.6 Plantar pressures collection

A Novel Emed force plate measurement system (Novel GmbH, Munich, Germany), 400×200×20 mm (millimeter) was mounted on top of the AMTI force plate, which was used to measure plantar loading with a frequency of 50 Hz. The foot was divided into 7 anatomical sub-areas, including big toe (BT), other toes (OT), medial forefoot (MFF), central forefoot (CFF), lateral forefoot (LFF), midfoot (MF) and heel (H). Variables collected with this system included peak pressure, pressure-time integral and contact area, a low pass fourth order Butterworth filter was used and filtered at 50 Hz. The stance phase (100%) of both the injured and uninjured limbs were divided by five cut-off events into four time periods based on the previous studies. The initial contact phase (ICP) starts from first foot contact (I) to first metatarsal contact (II), the forefoot contact phase (FFCP) starts from first metatarsal contact phase (II) to forefoot flat phase (III), the foot flat phase (FFP) starts from forefoot flat phase (III) to heel off phase (IV), the forefoot push-off phase starts from heel off phase (IV) to toe off phase (V) (Figure 18). The center of pressure (COP) trajectory under plantar were also recorded from heel-strike to toe-off within the injured side and the uninjured side.

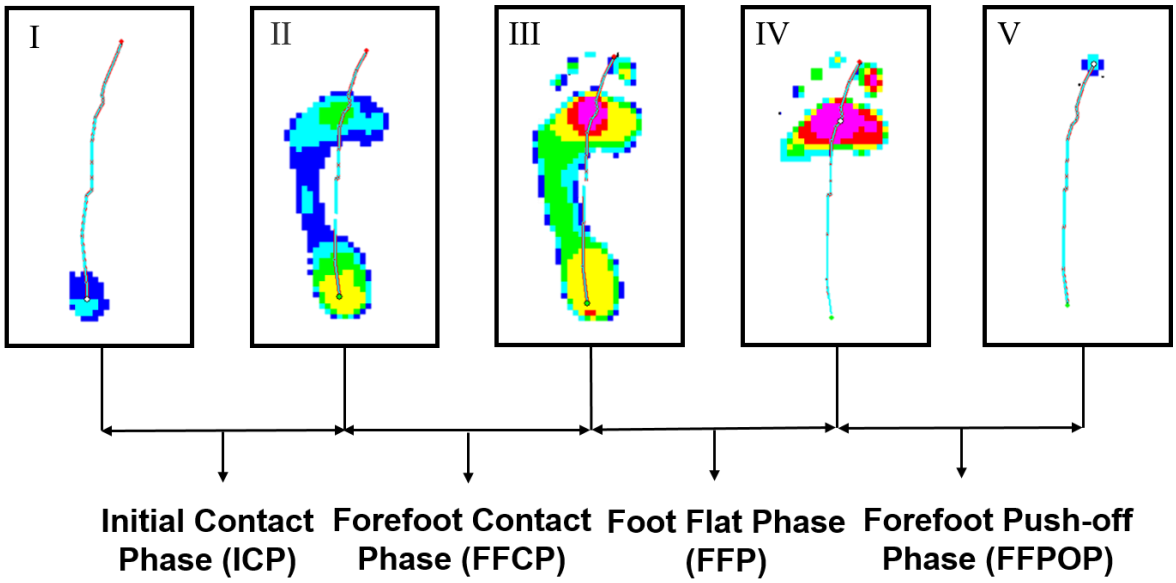

Figure 18 The illustration of cut-off points (I-V) for stance phase division. Note. I: first foot contact (FFC); II: first metatarsal contact (FMC); III: forefoot flat (FFF); IV: heel off (HO); V: toe off (TO).

2.2.7 Surface electromyography

Surface electromyography *(*sEMG*)* was recorded for one representative male subject during the stance phase of walking and running. Measurements were taken from the rectus femoris, biceps femoris long-head (lh), medial gastrocnemius and lateral gastrocnemius at a frequency of 1000 Hz, band-pass filtered between 16 to 380Hz, and was full-wave rectified. A low-pass filter at a frequency of 10 Hz (Delsys, Boston, Massachusetts, US) was used to smooth the data. The maximal voluntary isometric contraction (MVIC) trials were performed followed by the trials as reference data. EMG intensities for each muscle were normalized to the MVIC EMG activity from zero to one (Moissenet, Bélaise, Piche, Michaud, & Begon, 2019), as shown in Figure 19 and 20.

Figure 19 The Delsys surface electromyography devices (https://www.delsys.com/).

Figure 20 The placement of the EMG electrodes on the lower limbs.

2.3 Musculoskeletal modeling

2.3.1 Subject-specific musculoskeletal model building

An OpenSim Gait2392 generic musculoskeletal model with 23 degrees of freedom of the lower limbs, pelvis, torso, and head and 92 musculotendon actuators without any ligaments was scaled for each participant based on anthropometric characteristics. Muscle attachment points, segment inertial properties, joint articulations, and muscle lengths were scaled to match each participant's anthropometric profile. The scaling process is carried out as follows: the Scale Tool alters the anthropometry of a model so that it matches a particular subject as closely as possible. Scaling is typically performed by comparing experimental marker data to virtual markers placed on a model. In addition to scaling a model, the Scale Tool can be used to adjust the locations of virtual markers so that they better match the experimental data (Figure 21).

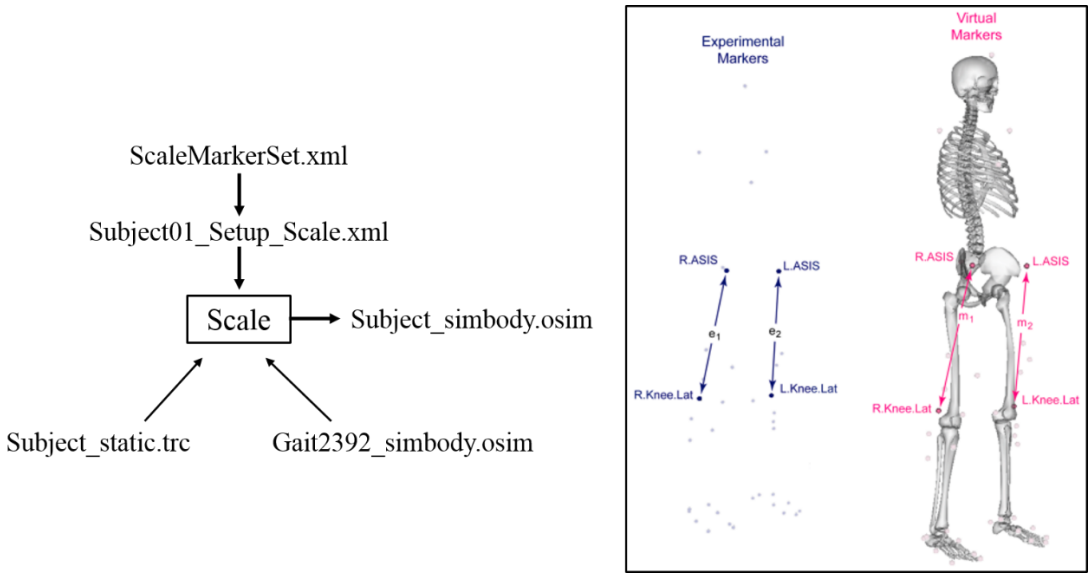

Figure 21 The scaling flowchart (left) and the operating principle (right). Experimental marker positions are measured with motion capture equipment (dark blue). Virtual markers are placed on a model in anatomical correspondence (https://simtkconfluence.stanford.edu/display/OpenSim/How+Scaling+Works).

Then each participant's scaled model were modified to create a subject-specific model by specifying the lower limb musculotendon architectural parameters based on the subject-specific AT length (ATL) between the injured side (IS) and uninjured side (US), Figure 22. The muscle fiber length was not measured in this dissertation, while a previous study has shown that if the ATL increases, the muscle length must decrease by the same amount. The optimal fiber length l_o^m and tendon slack length l_s^t of the three AT related muscles (gastrocnemius medialis, gastrocnemius lateralis and soleus) were proportionally adjusted based on the AT length ratio between the IS and US, equations outlined below.

$$\frac{IS\ l_o^m}{US\ l_o^m} = \frac{US_{ATL}}{IS_{ATL}} \quad \text{Eq. 1}$$

$$\frac{IS\ l_s^t}{US\ l_s^t} = \frac{IS_{ATL}}{US_{ATL}} \quad \text{Eq. 2}$$

In equation 1 and 2, IS l_o^m is the optimal fiber length in the injured side, and US l_o^m is the optimal fiber length in the uninjured side. IS l_s^t is the tendon slack length in the injured side, and US l_s^t is the tendon slack length in the uninjured side, shown in table 1. Musculotendon parameters modified using the two equations resulted in consistently longer l_s^t and shorter l_o^m on the IS compared to the US, as shown in Figure 22.

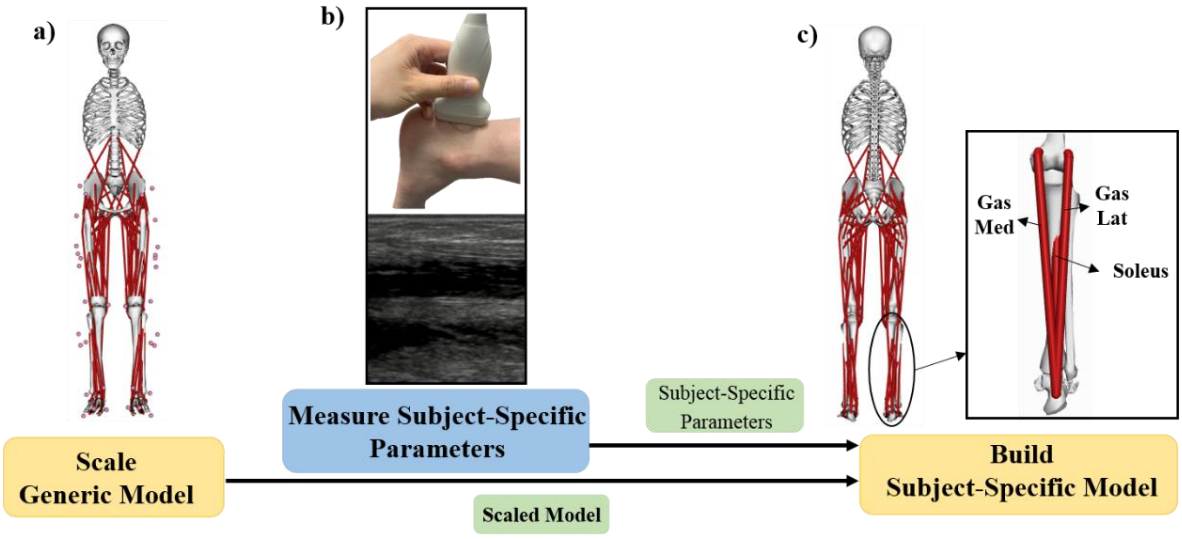

Figure 22 Schematic depiction of the subject-specific musculoskeletal modeling used in this dissertation. a) The generic musculoskeletal model is scaled for each subject using experimental markers placed on anatomical landmarks. b) The slack AT length of the injured side was measured with an ultrasound of each subject to obtain subject-specific parameters. c) Graphic depiction of modifying gas_med, gas_lat and soleus musculo-tendon parameters. Note. Gas Med: gastrocnemius medialis, Gas Lat: gastrocnemius lateralis.

It must be noted that the use of altering the optimal fiber length and the tendon slack length in patient-specific MSM is a novel step to model ATR. The joint kinematics were computed using Inverse kinematics (IK) tool, which tracks skin markers and minimizes errors between experimental maker trajectory and the virtual marker set at locations corresponding to the experimental marker in the model. The *IK* tool steps through each time frame of experimental data and positions the model in a pose that "best matches" experimental marker and coordinate data for that time step. This "best match" is the pose that minimizes a sum of weighted squared errors of markers and/or coordinates.

The joint moments were computed with the inverse dynamics (ID) OpenSim tools. The *ID* Tool determines the generalized forces (e.g., net forces and torques) at each joint responsible for a given movement.

If the kinematics and the external load are given, the ID Tool uses these data to perform an inverse dynamic analysis based on the Eq. 3.

$$\mathrm{M(q)}\ddot{q} + \mathrm{C(q}, \dot{q}) + \mathrm{G(q)} = \tau \qquad \text{Eq. 3}$$

In equation 3, $q, \dot{q}, \ddot{q} \in R^N$ are the vectors of generalized positions, velocities, and accelerations, respectively; $M(q) \in R^{N\times N}$ is the system mass matrix; $C(q, \dot{q}) \in R^N$ is the vector of Coriolis and centrifugal forces; $G(q) \in R^N$ is the vector of gravitational forces; $\tau \in R^N$ is the vector of generalized forces. The motion of the model is completely defined by the generalized positions, velocities, and accelerations. Consequently, all of the terms on the left-hand side of the equations of motion are known. The remaining term on the right-hand side of the equations of motion is unknown. The ID tool uses the known motion of the model to solve the equations of motion for the unknown generalized forces.

A static optimization (SO) approach was used to estimate the muscle force and activation. The SO method minimizes the sum of squared muscle activation at each time step. The muscle weighing constants were modified as 2 for the hamstrings, 1.5 for the gastrocnemius and 1 for the other muscles in this dissertation to reduce muscle forces prediction error based on previous protocols. As described in Inverse Dynamics, the motion of the model is completely defined by the generalized positions, velocities, and accelerations. The Static Optimization Tool uses the known motion of the model to solve the equations of motion for the unknown generalized forces (e.g., joint torques) subject to one of the following muscle activation-to-force conditions:

$$\tau j = \sum_{m=0}^{n} (a_m F_m^0) r_{m,j} \qquad \text{Eq. 4}$$

$$\tau j = \sum_{m=0}^{n} [a_m f(F_m^0, l_m, v_m)] r_{m,j} \qquad \text{Eq. 5}$$

$$J = \sum_{m=1}^{n} (a_m)^p \qquad \text{Eq. 6}$$

In equation 4, 5 and 6, there several parameters:

- n is the number of muscles in the model,
- a_m is the activation level of muscle m at a discrete time step,
- F^0_m is its maximum isometric force,
- l_m is muscle length,
- v_m is its shortening velocity,
- $f(F^0_m, l_m, v_m)$ is its force-length-velocity surface,
- $r_{m,j}$ is its moment arm about the joint axis,
- τj is the generalized force acting about the joint axis,
- p is a user defined constant.

Joint Reaction algorithm is an OpenSim Analysis tool for calculating resultant forces and moments at joint. Specifically, it calculates the joint forces and moments transferred between consecutive bodies as a result of all loads acting on the model.

2.4 Model validation

To evaluate the model reliability, the recording sEMG were qualitatively compared with the model-simulated muscle activations. The calculated root mean square (RMS) of the four muscles during the walking, jogging and running trails were normalized to the maximum RMS from zero to one during the MVIC testing. The model simulated muscle activation was also reported from zero to one, with zero representing no muscle activation and one representing full muscle activation. The comparison results are shown in Figure 23 and were in good agreement between the predicted muscle activation and sEMG during the stance phase.

Since the model can represent closely the same results as the experiments, with adequate probability the calculated kinetic (joint moments and contact forces) and kinematic (joint angles) parameters will correspond well to reality.

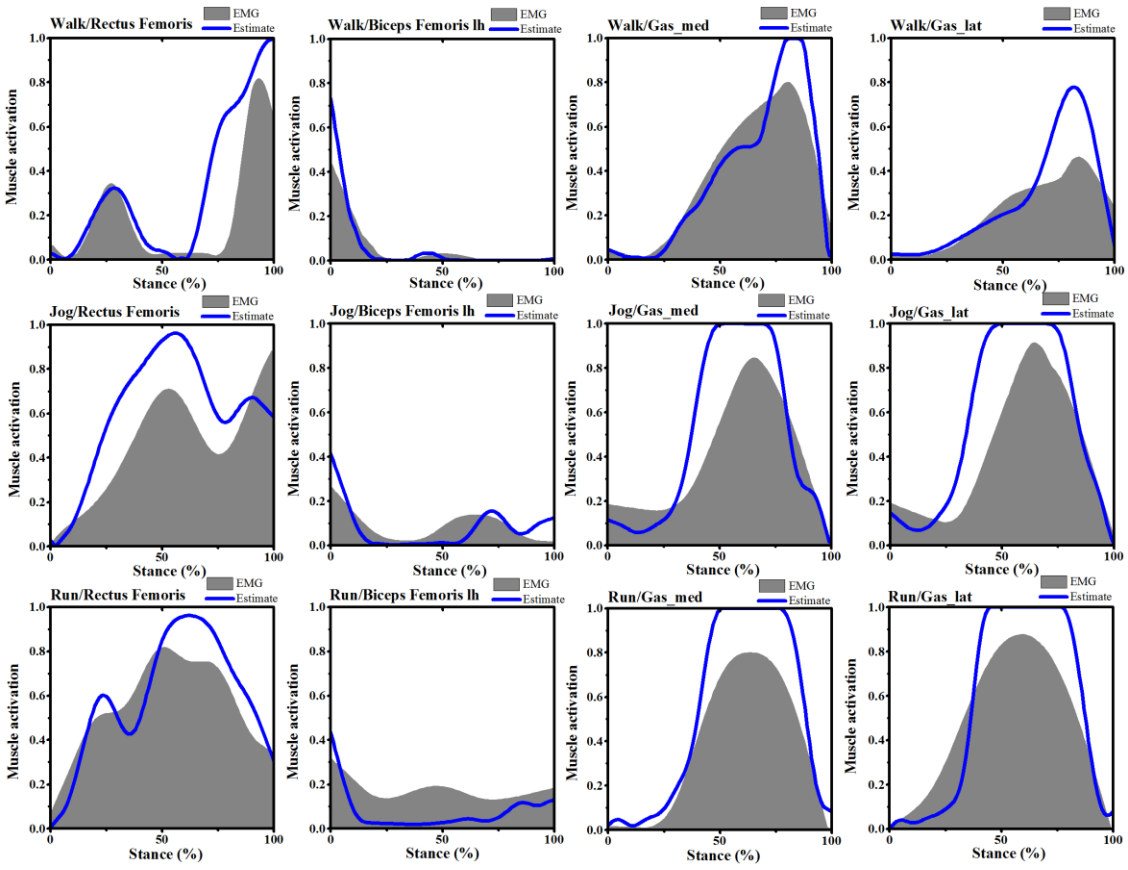

Figure 23 Comparison of muscle activations from static optimization estimated (blue line) and filtered electromyography (EMG) signals measured from the subjects during the same trial of normal walking, jogging and running. Note. EMG and activations were normalized from zero to one for each subject based upon the minimum and maximum values over the stance phase.

2.5 Data analysis

The statistical analyses were performed in SPSS version 22.0 (SPSS Science, Chicago, Illinois, USA). Twelve successful measurements were recorded when subjects landed with six injured and six uninjured foot on the force platform. The GRF was normalized to the subjects' body weight (BW). The vertical average loading rates (VALR) were also calculated through the average and normalized GRF divided by time. All data were normally distributed which assessed by the Shapiro-Wilk test and are presented as mean ± SD (standard deviation). The average walking and running speed in this dissertation were 1.32±0.11 m/s and 2.98±0.24 m/s. Paired sample t-tests were used to assess differences in biomechanical variables between injured and uninjured limbs during walking and running, respectively. The symmetry angle (SA) proposed by Zifchock et al., eliminates the need to choose a reference value and show great effective for identifying intra-limb differences (Zifchock, Davis, Higginson, & Royer, 2008).

$$\mathrm{SA} = \frac{\left(45° - \arctan\left(\frac{\mathrm{X.\,un}injured}{\mathrm{X.}\,injured}\right)\right)}{90°} \times 100\% \qquad \text{Eq. 7}$$

In equation 7, "X. uninjured" and "X. injured" represent biomechanical variables of uninjured limb and injured limb, respectively. SA of 0% corresponds to perfect symmetry of variables. Paired sample t-tests of SA values were utilized to evaluate changes in asymmetry magnitude between walking and running movements. Significance level were set as $p<0.05$.

The joint angles, moments, predicted muscle forces and joint contact forces during the stance phase for each walking, jogging and running trail from heel strike to toe-off on both legs were normalized to 101 data points from 0% to 100%. The joint angles (degrees) and moments (Nm/kg) were reported including sagittal plane, hip, knee, ankle and the frontal plane subtalar. The lower limb muscle forces and joint contact forces presented for the hip, knee and ankle joints were normalized to body weight (BW). The stance phase of walking was sub-divided into a loading response (0-20%), mid-stance (20-50%), push-off (50-100%) (Hebenstreit et al., 2015). The stance phase of jogging and running were sub-divided into initial contact (0-50%), mid-stance (-50%-) and push-off (50-100%) as indicated in previous studies (Lohman, Balan Sackiriyas, & Swen, 2011). To detect significant differences between the normalized waveforms of injured and uninjured sides, the open-source (www.spm1d.org) one-dimensional statistical parametric mapping was (SPM1d 0.4) applied to independent two-sample t-tests. Random field theory (RFT) outlined by Pataky et al., (2013) was employed to determine the potential statistical significance differences between the two sides for biomechanical variables over the whole stance phase in Matlab (R2018a, Mathworks Inc., Natick, MA, USA; Pataky, Robinson, & Vanrenterghem, 2013). Significance was set at $p<0.05$.

3 Results

3.1 AT anthropometric

As shown in Table 1, the gastrocnemii and soleus ATL were found to be significantly longer on the injured side compared to the uninjured side. The gastrocnemii ATL was 233.0±6.3 mm on the injured side compared with 210.4±7.1 mm on the uninjured side ($p<0.01$). The soleus ATL was 59.5±4.7mm on the injured side compared with 56.7±4.1 mm on the uninjured side ($p=0.13$). The average increase of Achilles tendon length in the injured side is 10.3% on average compared to the uninjured side.

Table 1 Subject AT length details (n=6). The gastrocnemii and soleus AT lengths (ATL) of each subject were measured for both the injured and uninjured sides.

Subjects	Gastrocnemii ATL (mm)				Soleus ATL (mm)			
	IS	US	IS_{ATL}/ US_{ATL}	US_{ATL}/ IS_{ATL}	IS	US	IS_{ATL}/ US_{ATL}	US_{ATL}/ IS_{ATL}
01	228.6	201.4	1.14	0.88	56.1	54.2	1.04	0.97
02	242.2	221.3	1.09	0.91	62.2	58.6	1.06	0.94
03	235.5	212.2	1.11	0.90	53.1	51.2	1.04	0.96
04	236.1	205.7	1.15	0.87	66.5	63.3	1.05	0.95
05	224.5	207.2	1.08	0.92	58.7	55.6	1.06	0.95
06	231.2	214.8	1.08	0.93	60.4	57.5	1.05	0.95

Note. IS: injured side; US: uninjured side; IS/US: AT length of injured side divide uninjured side; US/IS: AT length of uninjured side divide injured side.

3.2 Gait abnormality and asymmetry

3.2.1 Lower extremity kinematics

Table 2 shows a comparison of three-dimensional joint angle changes at the ankle, knee and hip joints in stance phase between injured limb and uninjured limb during walking and running. Through the paired t-test, significant differences were mainly observed in the sagittal and frontal planes. In the sagittal plane, peak ankle dorsiflexion angle was significant increase on injured limb, peak knee flexion angle and peak hip flexion angle of uninjured limb were significantly larger during walking and running. Peak hip extension angle was shown to be significantly smaller in the uninjured limb compared to uninjured limb during walking and running. In the frontal plane, comparing the inversion extent of ankle joint, the injured limb shows a remarkable difference compared with uninjured limb during walking and running, with an average increase of 1.02° and 2.88°. At knee joint, the adduction extent of injured limb also shows a remarkable difference compared to uninjured limb, with an average increase of 9.34° and 10.66°. The peak hip adduction showed a significant increase in the injured limb, while a significantly decreased peak hip abduction was found in injured limb.

In the transverse plane, significant difference was only found in the ankle joint, which showed a larger external rotation angles in the injured limb during walking and running, with an average increase of 3.87° and 2.43°.

Table 2 Comparisons of kinematic variables between injured side and un-injured side during walking and running.

Kinematic Variables	Walking		*p*	Running		*p*
	Injured	Uninjured		Injured	Uninjured	
Ankle kinematics (°)						
Dorsiflexion (max)	12.29±1.19	8.61±1.50	**<0.001**	26.61±0.83	22.64±0.85	**<0.001**
Plantarflexion (max)	-22.34±2.32	-24.66±1.20	0.12	-26.14±1.42	-28.16±0.75	0.29
Inversion (max)	4.58±1.25	3.56±0.38	**0.001**	7.29±0.22	4.41±0.16	**<0.001**
Inversion (min)	0.80±0.13	0.66±0.16	0.117	0.94±0.16	0.88±0.40	0.230
Int. rotation (max)	1.28±0.63	1.94±1.55	0.256	2.10±0.81	2.37±2.03	0.440
Ext. rotation (max)	-18.16±1.56	-22.03±3.22	**<0.001**	-21.10±0.89	-23.53±0.70	**0.001**
Knee kinematics (°)						
Flexion (max)	55.27±1.73	63.08±1.11	**<0.001**	61.96±2.87	72.39±1.58	**<0.001**
Extension (max)	-5.85±1.73	-5.33±1.99	0.190	7.71±2.61	9.98±2.48	0.095
Adduction (max)	8.81±2.53	5.47±1.36	**<0.001**	11.20±1.12	10.54±0.77	0.463
Adduction (min)	-0.28±0.67	-0.15±0.94	0.549	-4.85±0.86	-3.20±0.90	**0.001**
Int. rotation (max)	9.12±1.98	7.04±1.65	0.094	10.74±0.55	9.36±0.46	0.160
Ext. rotation (max)	-9.33±2.76	-8.64±3.10	0.161	-8.21±0.73	-7.51±0.61	0.093
Hip kinematics (°)						
Flexion (max)	23.85±1.43	25.91±1.34	**0.03**	20.36±1.57	22.75±1.32	**0.008**
Extension (max)	-26.17±1.53	-21.06±1.59	**<0.001**	-18.55±1.58	-16.56±0.61	**0.018**
Adduction (max)	7.89±1.11	4.32±2.29	**<0.001**	15.11±0.75	6.73±1.16	**<0.001**
Abduction (max)	-6.37±1.54	-12.07±1.61	**<0.001**	-6.01±1.22	-10.15±0.53	**<0.001**
Int. rotation (max)	26.23±1.72	24.12±2.28	0.342	27.40±2.22	24.80±2.51	0.097
Int. rotation (min)	7.78±2.78	7.98±1.40	0.632	17.01±1.91	16.90±0.92	0.480

Note. Int. rotation means internal rotation; Ext. rotation means external rotation; max means maximum; min means minimum (same as below).

The significant difference on angular velocity was observed in the sagittal and frontal planes (Table 3). In the sagittal plane, ankle dorsiflexion and plantarflexion angular velocities were reported larger in the uninjured limb compared to injured limb during walking and running. In the frontal plane, significant distinction ($p<0.001$) has been found in the ankle inversion velocity, which showed an average increase of 11.81 °/s and 20.00 °/s in the injured limb during walking and running. Significant increase of peak knee adduction and abduction velocities in this plane was also observed in the injured limb compared with the uninjured limb during walking and running. This result showed an average increase of 74.87 °/s and 44.97 °/s of peak knee adduction velocity during walking and running.

In terms of hip joint, hip abduction velocity showed constant difference between injured and uninjured limb, which showed an average increase of 12.31 °/s and 18.50 °/s in the injured limb during walking and running.

Table 3 Comparison of Angular velocity variables between injured side and uninjured side during walking and running.

Variables	**Walking**		***p***	**Running**		***p***
(peak values)	**Injured**	**Uninjured**		**Injured**	**Uninjured**	
Ankle angular velocity (°/s)						
Dorsiflexion	219.82±17.55	249.51±10.97	**0.007**	256.05±16.63	289.01±18.80	**<0.001**
Plantarflexion	-324.68±17.39	-366.79±16.53	**<0.001**	-549.60±23.22	-589.16±24.18	**0.004**
Inversion	52.83±6.66	41.02±2.16	**<0.001**	79.28±13.86	59.28±14.41	**<0.001**
Eversion	-29.54±4.67	-28.15±5.84	0.125	-66.05±3.24	-62.86±3.10	0.343
Int. rotation	180.13±19.80	171.86±26.02	0.136	303.36±15.22	285.85±17.47	0.139
Ext. rotation	-231.88±26.73	-225.25±27.51	0.292	-367.90±64.68	-322.3±61.26	0.303
Knee angular velocity (°/s)						
Flexion	373.92±11.01	367.14±9.49	0.096	542.03±23.58	517.08±26.88	0.634
Extension	-395.82±13.93	-444.22±11.53	0.347	-587.16±39.35	-604.16±26.68	0.082
Adduction	189.53±21.18	114.66±7.73	**<0.001**	194.76±10.72	149.79±14.64	**<0.001**
Abduction	-214.02±28.70	-169.57±16.84	**<0.001**	-236.53±20.82	-158.51±21.14	**0.002**
Int. rotation	179.65±12.27	186.58±18.56	0.357	281.71±17.72	267.87±24.49	0.196
Ext. rotation	-157.43±27.27	-150.52±11.54	0.448	-221.32±16.74	-243.10±20.40	0.424
Hip angular velocity (°/s)						
Flexion	234.68±10.00	230.63±7.30	0.093	285.10±18.16	272.40±12.88	0.193
Extension	-155.98±9.66	-137.37±14.57	0.104	-280.76±11.61	-260.39±13.38	0.103
Adduction	99.01±18.69	106.47±11.22	0.107	140.11±11.25	148.33±9.12	0.221
Abduction	-106.55±11.33	-94.24±6.83	**0.005**	-117.87±7.28	-99.37±10.20	**0.005**
Int. rotation	202.80±29.40	211.48±40.80	0.096	163.39±33.58	176.35±35.90	0.103
Ext. rotation	-119.88±13.69	-129.31±22.45	0.275	-126.98±14.13	-114.28±12.9	0.338

3.2.2 Lower extremity joint moments and ground reaction forces

Significant differences of kinetic variables between injured and uninjured limbs have been determined via paired t-tests, indicating limb asymmetry (as shown in Table 4). The GRFs on both walking and running for injured and uninjured limbs exhibited two main peaks during the loading response and pre-swing phase. The first vertical peak and VALR of injured limb were significantly larger than uninjured limb during walking and running. Significant differences of lower limbs joint moments can be found for all variables in Table 4 except for hip extension moments during walking. The increased knee adduction angles and adduction moments should be noticed in the injured limb compared to the uninjured. The increased knee joint reaction forces were also find in the injured limb during walking and jogging, which indicates higher knee joint loading in the injured side, and especially in the medial part of the knee joint, as shown in Figure 24.

Table 4 Comparison of kinetic variables between injured limb and uninjured limb during walking and running.

Variables (peak values)	**Walking**		***p***	**Running**		***p***
	Injured	**Uninjured**		**Injured**	**Uninjured**	
Ground reaction forces						
First vertical peak	1.28±0.06	1.22±0.10	**0.044**	1.45±0.25	1.38±0.22	**0.006**
Second vertical peak	1.24±0.03	1.22±0.02	0.232	2.87±0.12	2.86±0.13	0.487
Peak braking force	0.21±0.02	0.20±0.03	0.295	0.28±0.04	0.30±0.03	0.249
Peak propulsive force	0.28±0.02	0.30±0.02	0.091	0.27±0.04	0.28±0.04	0.616
VALR (BW/s)	10.99±0.69	9.39±1.14	**0.003**	170.56±18.7	152.23±14.5	**0.002**
Ankle moments (Nm/kg)						
Dorsiflexion moment (max)	2.29±0.10	2.38±0.07	**0.011**	4.38±0.22	4.68±0.25	**<0.001**
Inversion moment (max)	0.37±0.11	0.18±0.03	**<0.001**	0.52±0.15	0.36±0.08	**<0.001**
Knee moments (Nm/kg)						
Flexion moment (max)	0.63±0.12	0.41±0.10	**<0.001**	3.50±0.36	2.92±0.31	**<0.001**
Extension moment (max)	0.66±0.12	0.57±0.09	**0.038**	0.60±0.13	0.55±0.11	**0.012**
Adduction moment (max)	0.17±0.05	0.13±0.07	**0.006**	0.62±0.12	0.46±0.22	**<0.001**
Hip moments (Nm/kg)						
Extension moment (max)	1.59±0.14	1.75±0.24	**0.021**	0.94±0.23	1.07±0.04	0.415
Adduction moment (max)	1.90±0.08	1.49±0.17	**<0.001**	3.68±0.12	3.09±0.08	**<0.001**

Note. *VALR=vertical average loading rate.*

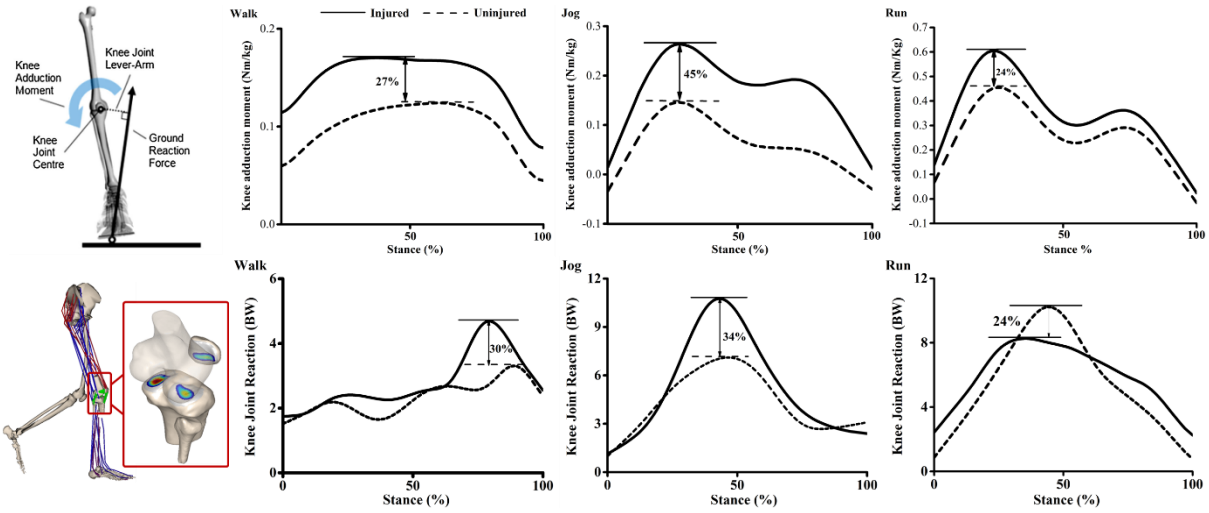

Figure 24 The knee joint adduction moments and joint reaction forces between injured and uninjured limbs during walking, jogging and running.

The knee joint kinetics in the injured limb were found significantly difference between the injured and uninjured sides during walking, jogging and running. As shown in Figure 24, The increased knee adduction moment (walking: peak 27%, average difference 19%; jogging: peak 45%, average difference 26%; running: peak 24%, average difference 13%) accompanied with higher knee joint reaction forces (walking: peak 30%, average difference 14%; jogging: peak 34%, average difference 15%; running: peak 24%, average difference 3%) were found in the injured side compared with the uninjured side, the average increase of knee joint reaction forces in the injured side is 14%.

3.2.3 Plantar pressures distribution

Peak pressure, pressure-time integral and contact area were collected in the experiment to evaluate foot loading symmetry during walking and running (Figure 25 and Figure 26). For walking condition, peak pressure and pressure-time integral in the big toe (BT) and other toes (OT) were found significantly higher in the uninjured limb compared with the injured limb. However, the injured limb showed higher peak pressure and pressure-time integral in the central forefoot (CFF) compared with uninjured limb. Measured contact area in the CFF of injured limb was significantly higher than uninjured limb. While contact area in the midfoot (MF) of uninjured limb was significantly higher in the injured limb. For running condition, peak pressure in the BT, OT and medial forefoot (MFF) exhibited higher values in the uninjured limb compared with the injured limb. Peak pressure in the lateral forefoot (LFF) and heel (H) showed significantly higher in the injured limb. Pressure-time integral in the OT showed higher in the uninjured limb. On the contrary, pressure-time integral in the CFF and lateral forefoot (LFF) showed higher in the injured limb. The injured limb showed higher contact area in LFF and lower contact area in MFF.

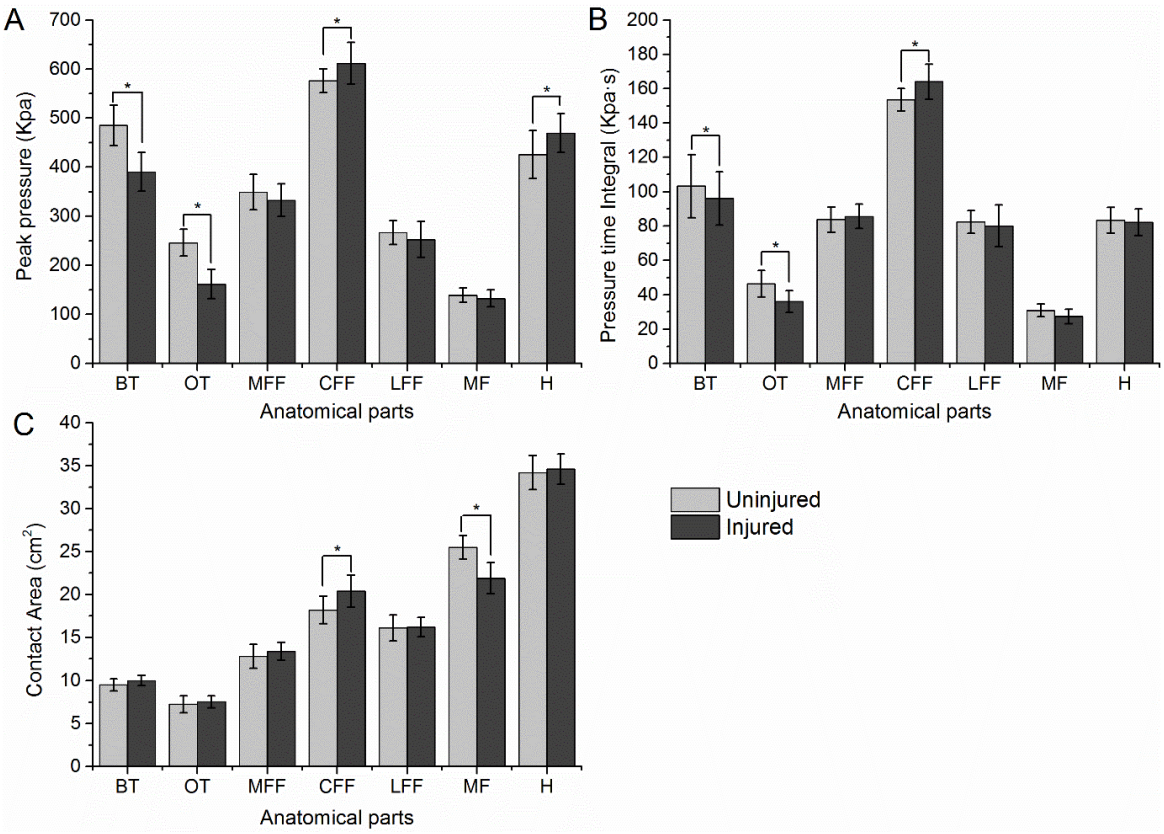

Figure 25 The comparison of plantar pressure during walking between injured and uninjured side.

Note. Footprint image and anatomical parts divisions in the bottom right. “A” represents peak pressure; “B” represents pressure-time integral; “C” represents contact area; “*” indicates significance between injured and uninjured limb (same as below).

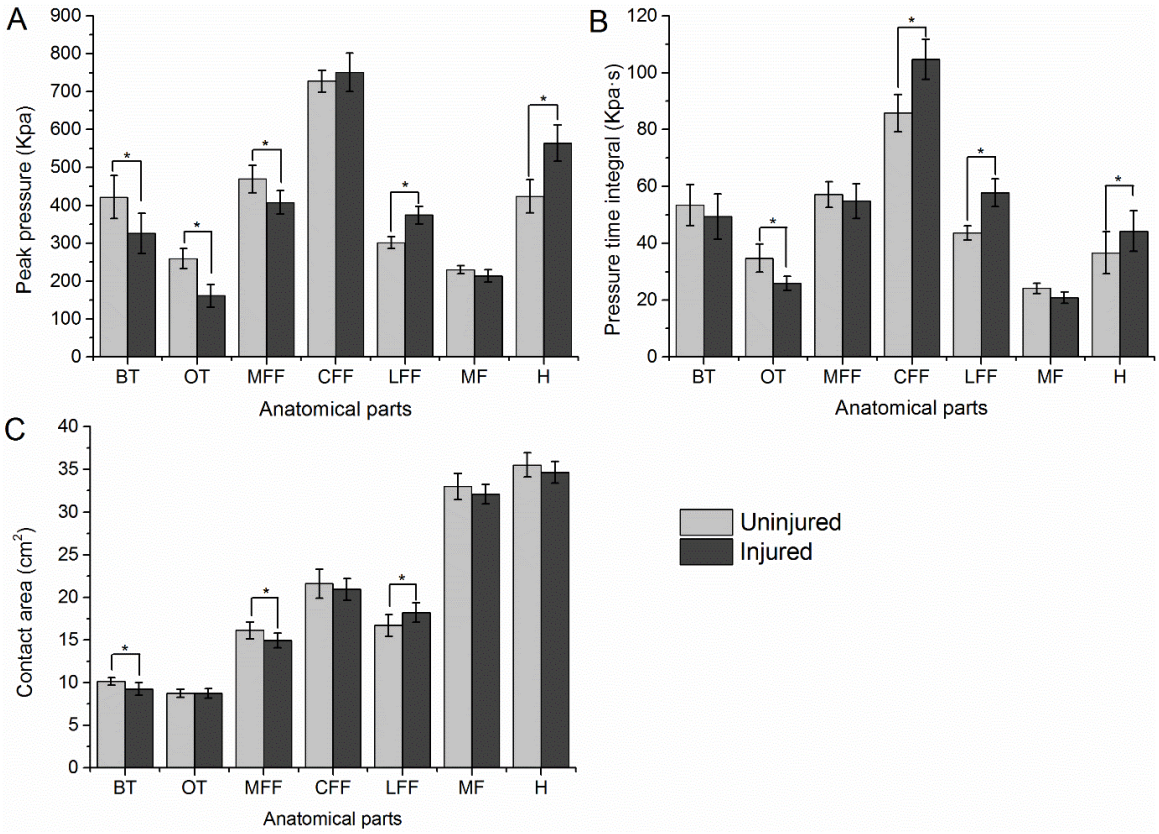

Figure 26 The comparison of plantar pressure during running between injured and uninjured side.

The center of pressure (COP) lines under the injured and uninjured sides were extracted during walking and running, as shown in Figure 27. WUW-S, WIW-S means the width between starting point with uninjured and injured sides during walking; RUW-S, RIW-S means the width between starting point with uninjured and injured sides during running; WUW-M, WIW-M means the width between middle flatfoot stances with uninjured and injured sides during walking; RUW-M, RIW-M means the width between middle flatfoot stances with uninjured and injured sides during running; WUW-E, WIW-E means the width between ending point with uninjured and injured sides during walking; RUW-E, RIW-E means the width between ending point with uninjured and injured sides during running. The width of WIW-M and RIW-M was significantly longer than WUW-M and RUW-M, which implicate the over-eversion of the injured side feet.

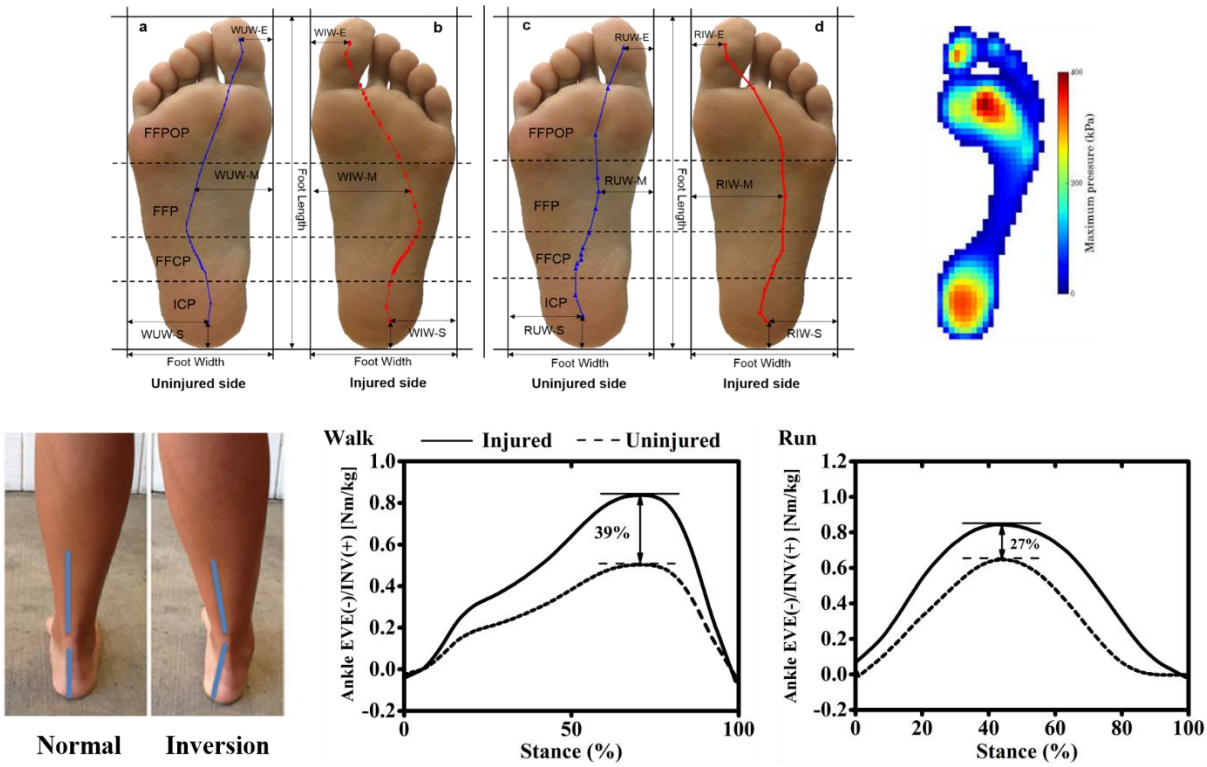

Figure 27 In the first line (center of pressure trajectories), "a" and "b" represent COP trajectory between Uninjured and injured leg during walking, "c" and "d" represent COP trajectory between Uninjured and injured leg during running; In the second line, higher ankle inversion moments were found in the injured side during walking and running.

The laterally excursion of center of pressure (COP) accompanied with significantly increased ankle inversion moments (walking: peak 39% and average difference 21%; running: peak 27% and average difference 12%) were found in the injured side. Which indicates the ankle lateral sprain in the injured limb compared with the uninjured limb during daily activities such as walking and running.

3.2.4 Gait asymmetry results

Significant differences in symmetry angles (SA) between walking and running conditions were presented in Table 5. The paired t-test *p* values showed significance (p<0.001) in ankle dorsiflexion angle, knee adduction velocity, ankle inversion moment and knee flexion moment. This indicates changes in asymmetry magnitude due to walking and running. The average SA angles during walking and running vary between 1.2% and 21%, however most of them have higher values than the physiological value (5%).

Table 5 Differences of selected biomechanical variables in symmetry angles (SA) between walking and running.

Variables (peak values)	Walking symmetry Angle (%)±SD	Running symmetry Angle (%)±SD	*p*-value
Ankle dorsiflexion angle	11.13±2.62	5.14±1.72	**<0.001**
Ankle inversion angle	8.04±2.36	13.41±4.95	**<0.001**
Ankle inversion velocity	7.93±3.15	9.12±3.37	0.35
Knee flexion angle	4.26±1.81	4.90±1.61	0.213
Knee adduction angle	14.53±4.66	13.42±4.83	0.346
Knee adduction velocity	15.46±5.25	8.32±3.89	**<0.001**
Ankle dorsiflexion moment	1.21±2.37	2.13±2.42	**0.012**
Ankle inversion moment	21.26±6.50	11.53±4.32	**<0.001**
Knee flexion moment	13.35±3.82	5.74±2.46	**<0.001**
Knee adduction moment	10.93±3.35	14.64±5.16	**0.004**
VALR	4.94±2.25	3.63±1.95	**0.033**

Note. VALR=vertical average loading rate.

3.3 Musculoskeletal modeling estimation

3.3.1 Joint kinematics

During self-selected speed walking, the hip flexion angle of the injured side increased at 0%~7% (p=0.027) and 79%~90% (p=0.010) (Figure 28a). The knee flexion angle of the uninjured side increased at 63%~80% (p<0.001) (Figure 28b). The ankle dorsiflexion angle of the injured side increased at 0~78% (p<0.001) (Figure 28c). The subtalar inversion angle of the injured side increased at 18~80% (p<0.001) (Figure 28d).

During self-selected speed jogging, the hip flexion angle of the injured side increased at 52%~100% (p<0.001) (Figure 28e). The knee flexion angle of the uninjured side increased at 0~14% (p=0.015) and 41%~95% (p<0.001) (Figure 28f). The ankle dorsiflexion angle of the injured side increased at 13%~100% (p<0.001) (Figure 28g). The subtalar inversion angle of the injured side increased at 19~80% (p<0.001) (Figure 28h).

During self-selected speed running, the hip flexion angle of the injured side increased at 0~7% (p=0.040) and 53%~100% (p<0.001) (Figure 28i). The knee flexion angle of the uninjured side increased at 28%~52% (p=0.047) (Figure 28j).

The ankle dorsiflexion angle of the injured side increased at 0~26% (p=0.002) and 53%~100% (p<0.001) (Figure 28k). The increased subtalar joint inversion angle of the injured side was observed to be between 8%~23% (p=0.002) and 65%~78% (p=0.006), while the decreased subtalar inversion angle was observed to be 93%~100% (p=0.026) of the injured side compared with the uninjured side (Figure 28l).

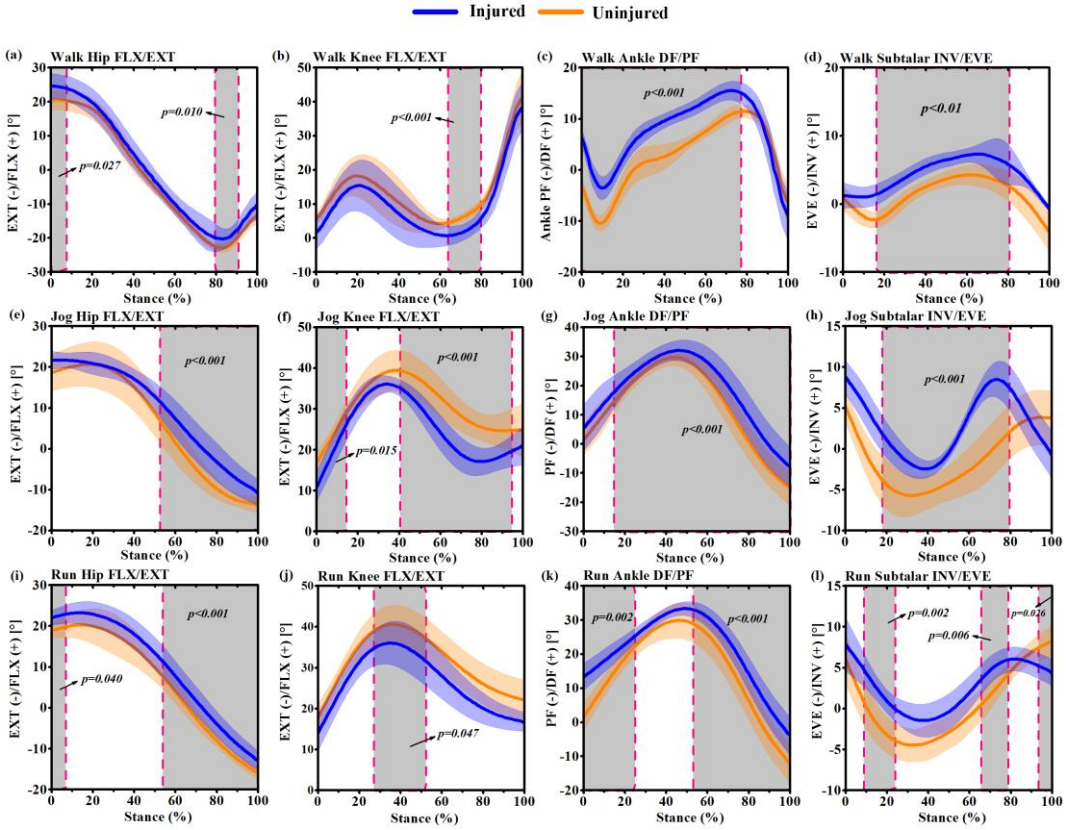

Figure 28 Mean and standard deviation lower extremity joint angle waveforms over stance phase (100%) for the uninjured side (yellow) and injured side (blue) during self-selected speed walking, jogging and running. Grey shaded regions on graphs indicate a significant difference between the two sides (p<0.05) from SPM1d analyses.

3.3.2 Joint moments

During walking movement, no significant differences were found between the injured and uninjured sides for the hip joint (Figure 29a). Reduced knee flexion moment was observed in the injured side between 62%~81% (p<0.001), whereas the knee extension moment of the injured side increased at 90%~95% (p=0.034) (Figure 29b), Increased subtalar inversion moment was found in the injured side between 62~78% (p<0.001). During jogging movements, the knee extension moment of the injured side increased at 49%~74% (p<0.001) (Figure 29f). The ankle plantarflexion moment of the uninjured side increased at 22%~70% (p<0.001) (Figure 29g). The injured side had an increased subtalar inversion moment during the whole waveform, especially during 20%~29% (p=0.014) and 56%~96% (p<0.001) of the stance phase (Figure 29h).

During running movements, the hip extension moment of the injured side decreased between 23%~25% (p<0.001) (Figure 29i). The knee extension moment of the injured side increased at 0~3% (p=0.035) and 30%~42% (p=0.017) (Figure 29j). The ankle plantarflexion moment of the uninjured side increased at 44%~63% (p=0.022) (Figure 29k). The subtalar inversion moment of the injured side increased at 27%~85% (p<0.001) (Figure 29l).

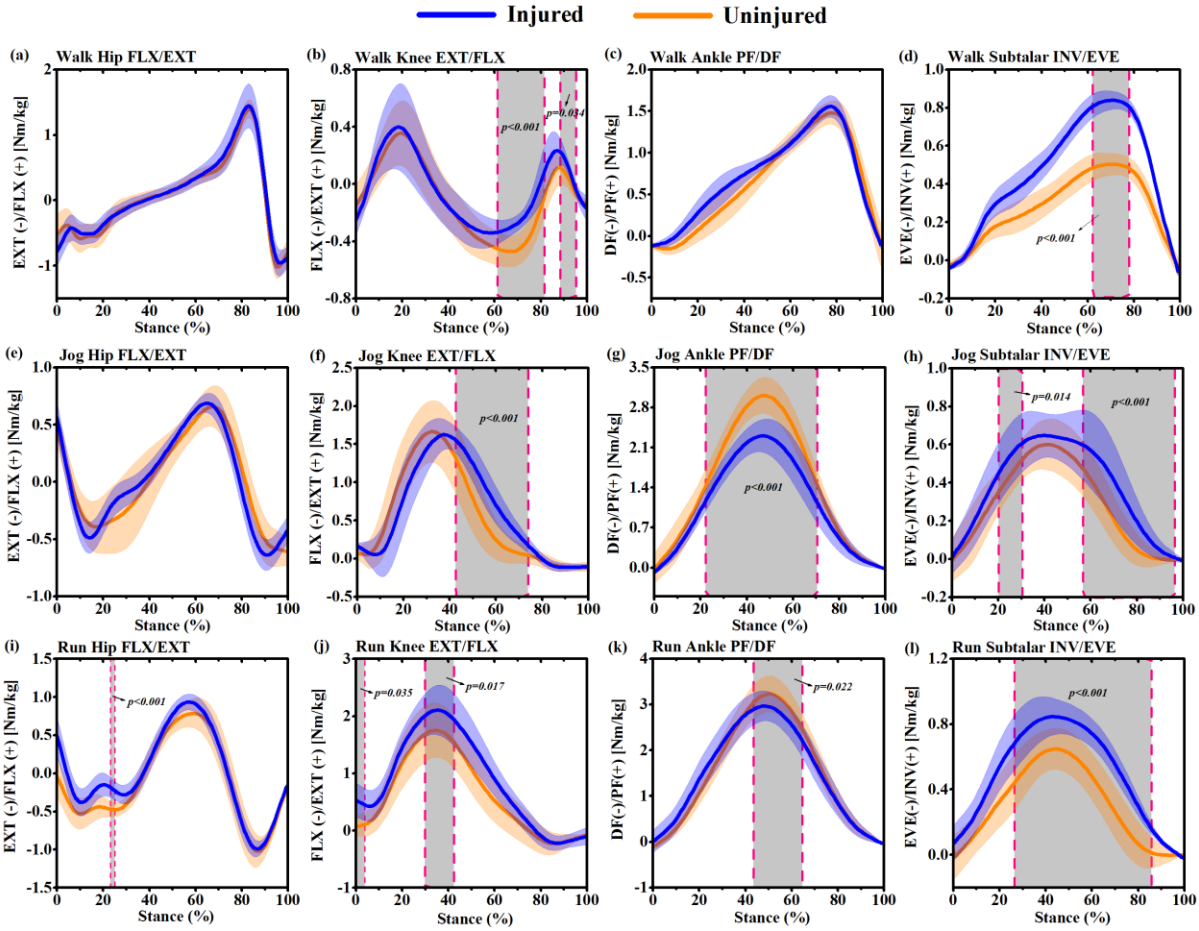

Figure 29 Mean and standard deviation of lower extremity joint moment waveforms over stance for the uninjured side (yellow) and injured side (blue) during self-selected speed walking, jogging and running. Grey shaded regions on graphs indicate a significant difference between the two sides (p<0.05) from SPM1d analyses.

3.3.3 Muscular contribution

The SPM1d analysis of the muscle force data found significant differences in all three movements (Figure 30). The vastus medialis (vas_med), vastus lateralis (vas_lat) and vastus intermedius (vas_inter) force waveforms were found to have similar trajectory changes during walking, jogging and running, respectively. During walking, the uninjured side was found to increase in vas_med (19%~46%, $p<0.001$), vas_lat (17%~43%, $p<0.001$) and vas_inter (16%~42%, $p<0.001$) forces compared to the injured side (Figure 30a-c). While the injured side recorded increased vas_med (26%~47%, $p<0.001$), vas_lat (30%~42%, $p<0.001$) and vas_inter (30%~44%, $p<0.001$) forces during running (Figure 30i-k).

During the mid-stance and push-off phases of jogging movements, the vas_med, vas_lat and vas_inter forces showed increases in the injured side (Figure 30e-g). The rectus femoris force during walking was observed higher in the injured side at the push-off phase (60%~85%, $p<0.001$). During jogging, the rectus femoris force of the injured side increased at 44%~64% ($p<0.001$), whereas it decreased at 84%~100% ($p<0.001$). The rectus femoris force was significantly ($p<0.001$) greater from 34%~62% of the stance phase in the injured side during running (Figure 30l). The three AT related triceps surae muscles were also significantly different between the two sides during the three movements. During walking, the gastrocnemius medialis (gas_med) force of the uninjured side increased at 20%~48% ($p<0.001$) and 68%~92% ($p<0.001$) (Figure 31a). The gastrocnemius lateralis (gas_lat) force of the uninjured side increased at 5%~44% ($p<0.001$) and 68%~88% ($p<0.001$) (Figure 31b). The soleus force was found to decease in the injured side during the push-off phase (70%~93%, $p<0.001$) during walking (Figure 31c). During jogging movements, gas_med and gas_lat force waveforms were found completely similar during the whole stance phase. The gas_med and gas_lat forces of the uninjured side were significantly higher than the injured side at 20%~43% ($p<0.001$) and 22%~51% ($p<0.001$), respectively. During running, the gas_med force was significantly greater from 40%~52% ($p=0.007$) in the injured side (Figure 31g), while no significant differences were found in gas_lat force between the injured and uninjured sides. The soleus forces during both jogging and running were also non-significant between the injured and uninjured sides.

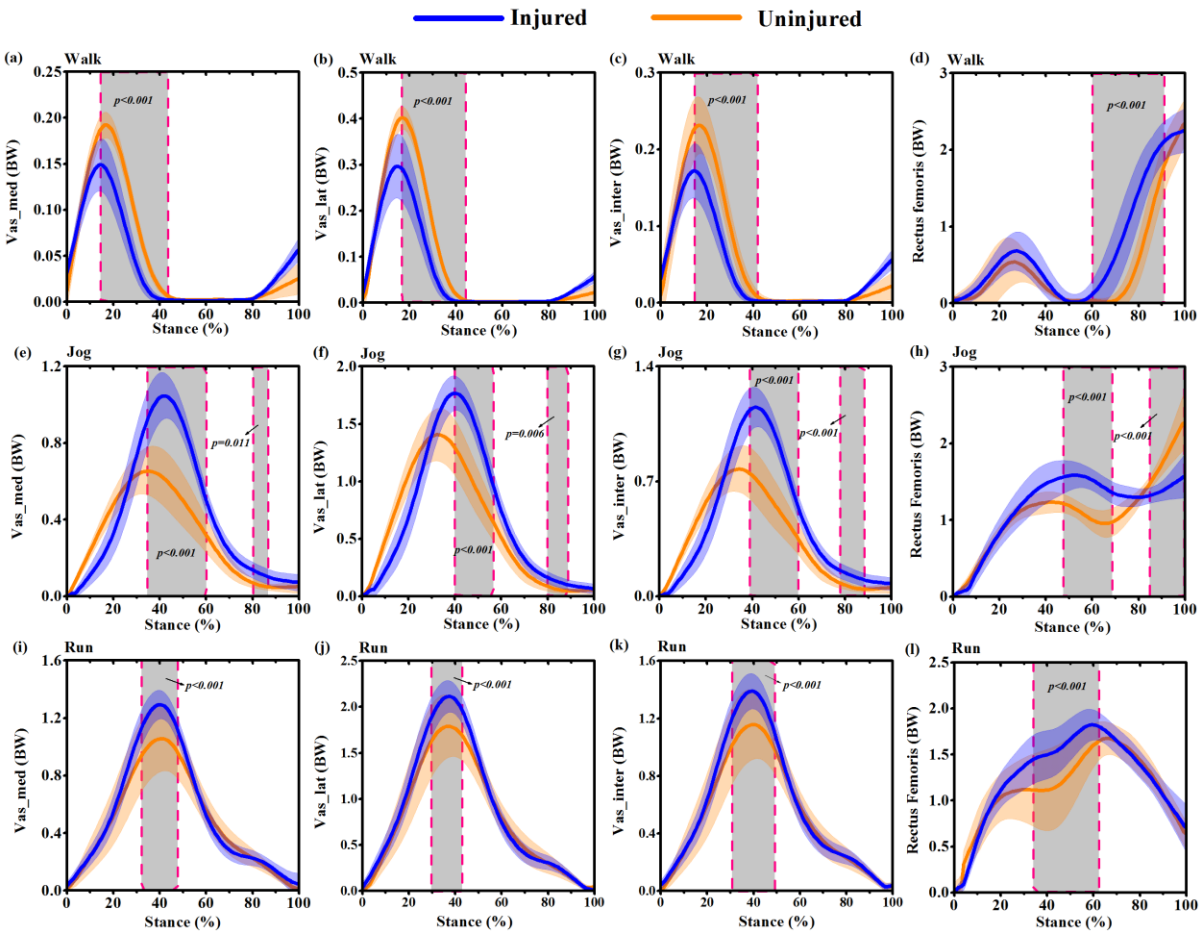

Figure 30 Mean and standard deviation of estimated vas_med (vastus medialis), vas_lat (vastus lateralis), vas_inter (vastus intermedius) and rectus femoris musculo-tendon forces waveforms over stance between uninjured side (yellow) and injured side (blue) during walking, jogging and running. Grey shaded regions on graphs indicate a significant difference between the two sides ($p<0.05$) from SPM1d analyses.

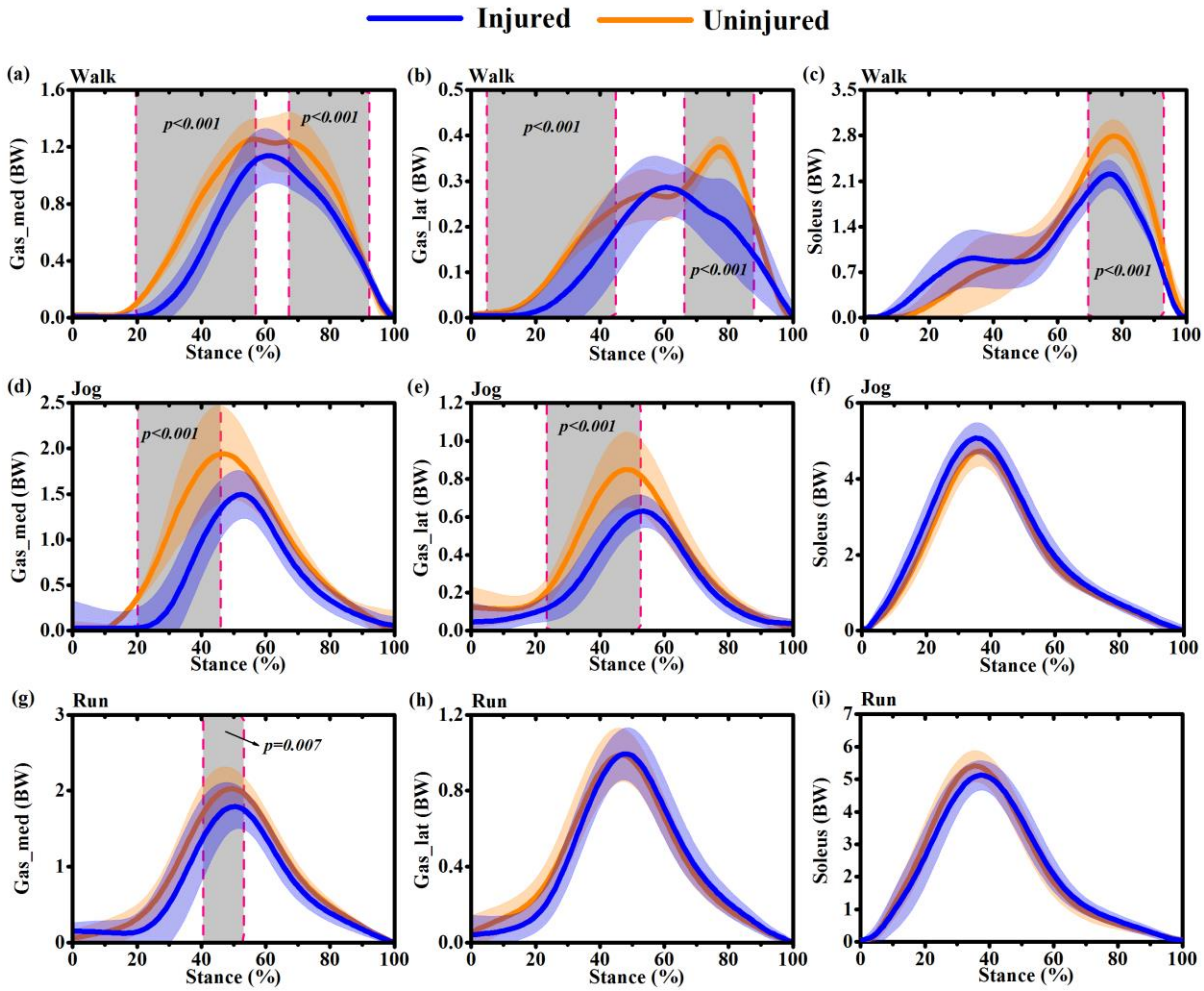

Figure 31 Mean and standard deviation of estimated gas_med (gastrocnemius medialis), gas_lat (gastrocnemius lateralis) and soleus musculo-tendon forces waveforms over stance between uninjured side (yellow) and injured side (blue) during walking, jogging and running. Grey shaded regions on graphs indicate a significant difference between the two sides ($p<0.05$) from SPM1d analyses.

The patient-specific OpenSim musculoskeletal model with the modification of Achilles tendon related musculotendon parameters can avoid the overestimating risk of triceps surae muscle forces. When comparing the estimated triceps surae muscle forces from this dissertation with a previous OpenSim model outputs using healthy subjects (Modenese et al., 2018), as shown in Figure 32. The patient-specific musculoskeletal model in this dissertation can reduce the muscle forces estimation error of gastrocnemius medialis during walking movement: 26% peak and 12% average difference; gastrocnemius lateralis: 25% peak and 11% average difference; soleus: 23% peak and 9% average difference compared to the study of Modenese et al., 2018.

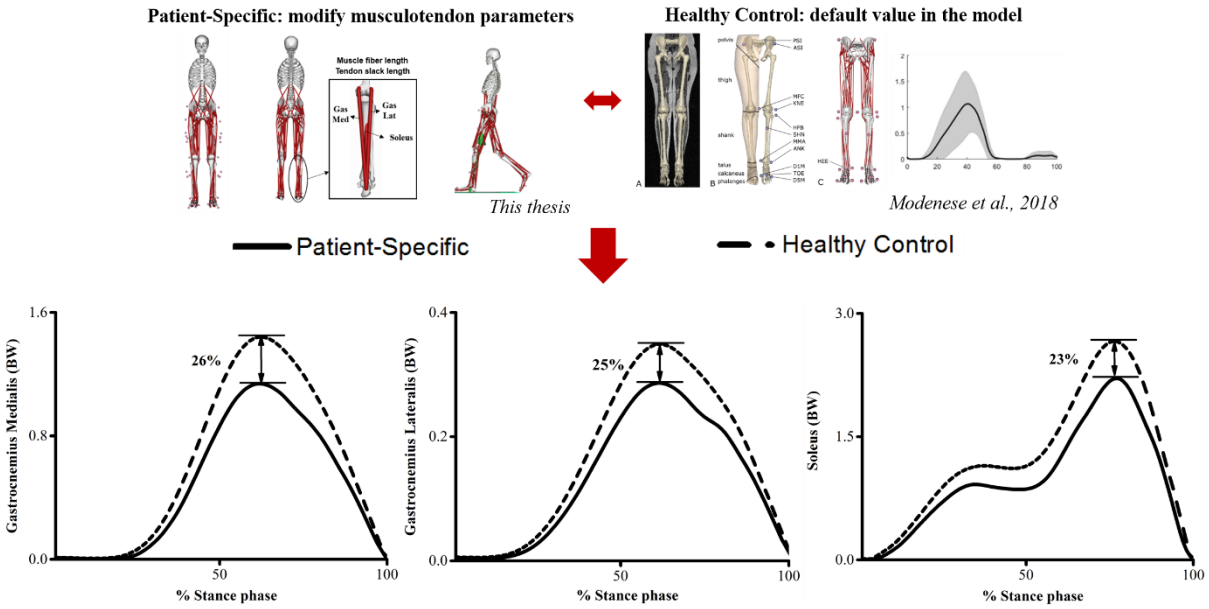

Figure 32 The compared estimated triceps surae muscle forces between patient-specific from this dissertation and study from Modenese et al., 2018, used by permission.

3.3.4 Joint loading

During walking, the hip joint reaction force of the injured side increased at 0%~85% ($p<0.001$) (Figure 33a). The knee joint reaction force of the injured side increased from 24% to 39% ($p<0.001$) and from 69% to 88% ($p<0.001$) (Figure 33b). The uninjured side showed increased ankle joint force from 48%~90% ($p<0.001$) compared to the injured side (Figure 33c). During jogging, increased hip joint reaction forces of the injured side were observed during the mid-stance at 10%~60% ($p<0.001$), while decreased hip joint reaction forces of the injured side were found during push-off between 86%~95% ($p=0.027$) (Figure 33d).

Increased knee joint reaction force of the injured side was found during the mid-stance at 29%~59% ($p<0.001$). Decreased ankle joint reaction force in the injured side was found during 38%~44% ($p=0.035$), respectively (Figure 33e-f). During running movements, increased hip joint contact forces of the injured side were observed at 0%~7% ($p=0.017$) during initial contact, while decreases were observed at 59%~85% ($p<0.001$) during the push-off phase.

On the knee joint, there were significant differences at three separate instances in the stance phase, increased knee contact forces of the injured side during initial contact (0%~8%, $p=0.012$) and push-off (77%~97%, $p<0.001$) and decreased knee contact force of the injured side during mid-stance (43%~52%, $p=0.009$) (Figure 33h). The ankle joint force of the uninjured side increased at 7%~43% during initial contact ($p<0.001$) (Figure 33i).

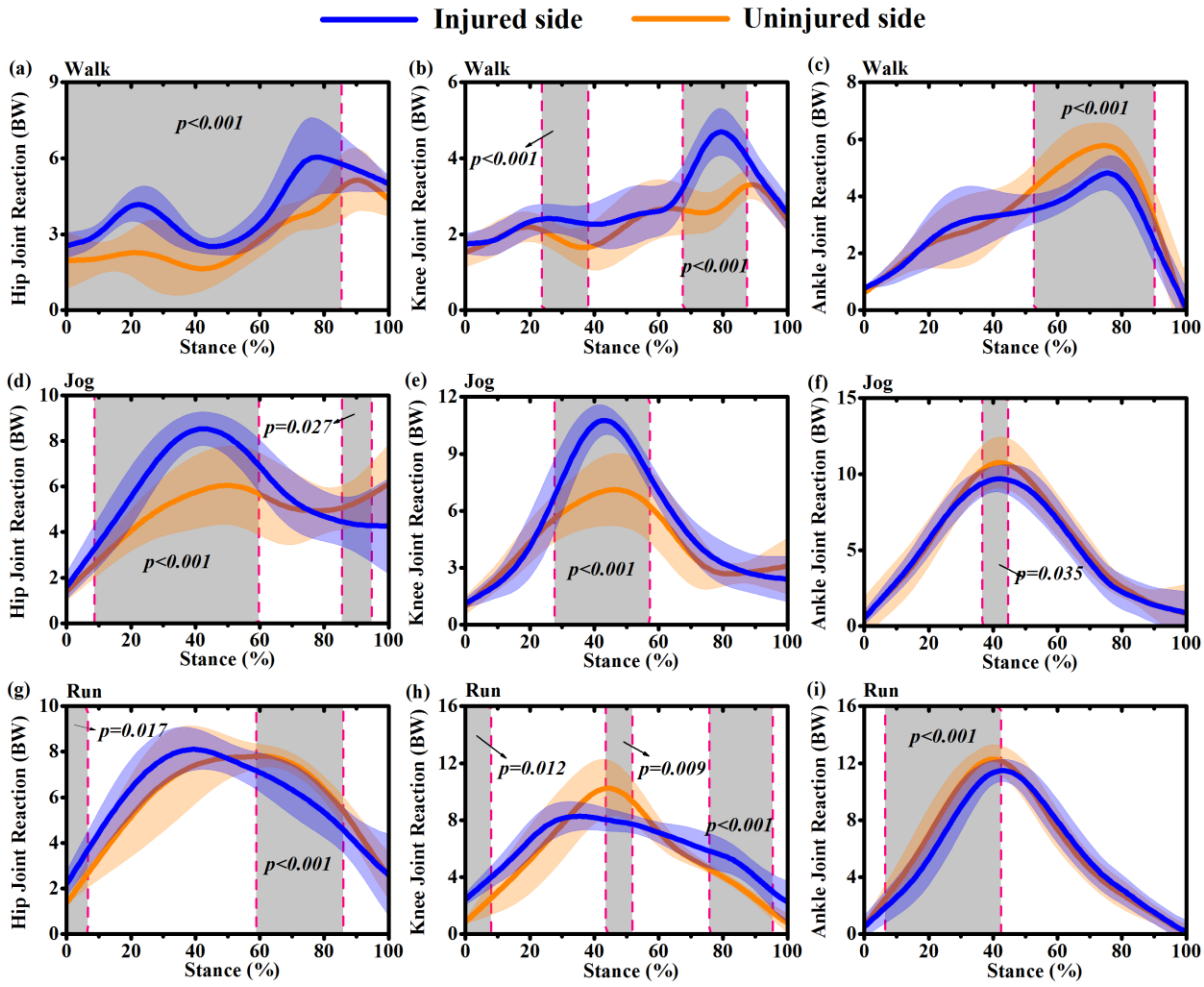

Figure 33 Mean and standard deviation of estimated joint reaction forces waveforms over stance at the hip, knee and ankle joints for uninjured side (yellow) and injured side (blue) during walking, jogging and running. Grey shaded regions on graphs indicate a significant difference between the two sides ($p<0.05$) from SPM1d analyses.

4 Discussion

4.1 Gait abnormality and asymmetry

In 3.2, large differences in lower limbs kinematics and kinetics between injured and uninjured sides in athletes with a previous ATR were found, at both self-selected speed walking and running. The main differences between both sides were:

1) Increased peak ankle dorsiflexion angle, peak ankle inversion angle and peak knee adduction angle on the injured limb;
2) Decreased peak knee and hip flexion angle on the injured limb;
3) Increased vertical GRF, VALR, ankle inversion moment and knee adduction moment on the injured limb;
4) Peak plantar pressure showed lateral excursion;
5) Walking symmetry angle showed was larger than running symmetry angle in some key biomechanical parameters.

In this dissertation, significant differences on kinematics of injured and uninjured limbs were primarily found in the sagittal and frontal planes. Increased peak ankle dorsiflexion angle and angular velocity of injured limb were found during walking and running stance phases. However, decreased peak ankle plantarflexion angle and knee flexion angle and angular velocity were shown on injured limb during walking and running. Similarly to previous studies where AT repaired athletes were selected, here it was also observed than an elongated AT, which indicates an imbalance of the triceps surae muscle-tendon complex and may influence the sagittal kinematics and kinetics of the ankle and knee joints (Stenroth, Peltonen, Cronin, Sipila, & Finni, 2012). Increased ankle dorsiflexion and decreased knee flexion on injured limb maybe two possible compensation mechanisms to ensure sufficient tension of the elongated triceps surae-tendon complex during the stance phase. Another assumption is also presented: greater ankle dorsiflexion on injured limb is probably arisen due to the fact that athletes with past AT injuries tries to compensate the insufficient function of the ankle dorsal flexors through greater ankle dorsiflexion (Don et al., 2007). Decreased ankle plantarflexion on repaired limb maybe due to a functional deficit of plantar flexors, which was also reported in a previous study, where patients with ATR history suffers from a functional deficit even two years after surgical repair (N Maffulli, 1998). An average ankle dorsiflexion increase of 3° and ankle plantarflexion decreased by 13% have been reported at a mean of 3.1 years after AT surgical repair (Brorsson, Willy, Tranberg, & Grävare Silbernagel, 2017). The plantar flexion weakness and the healed AT elongation maybe two main explanations for the increased ankle dorsiflexion observed during walking and running. Increased peak ankle inversion, knee and hip adduction angles and angular velocities were found on injured limbs during walking and running in the frontal plane. In previous modeling studies, limited ability of power generation in the plantar flexors may result in an increase in frontal plane motion of ankle joint, i.e. inversion/eversion, potentially placing the individuals at greater injury risk (Neptune, Kautz, & Zajac, 2001).

Another cause of increased ankle inversion maybe a deficit in ankle position and motor control which may increase the risk of tripping over and generating an injury risk (Konradsen, 2002). Increased hip adduction angle and knee adduction angle and angular velocities have been previously related to knee overuse injuries (Kean, Bennell, Wrigley, & Hinman, 2015).

The first vertical peak GRF which was called passive force and the second vertical peak GRF which was called active force were found greater in the injured limb as against the uninjured one. Relatively large and rapid impact forces during running has been suggested as an increased risk of an overuse injury of the lower limbs (Nigg, 2001). Increased maximal vertical GRF during loading response maybe due to an increased ankle dorsiflexion during stance phase (Kondo & Someya, 2016). Our subjects exhibited significantly greater VALR and frontal plane joint moments in the injured limb. Increased loading rate and knee adduction moment have been previously correlated with tibia stress fracture. The external knee adduction moment can be used as a common indirect measure of the medial tibiofemoral contact force (Kutzner, Trepczynski, Heller, & Bergmann, 2013). Higher loading on the medial compartment may increase the incidence of medial compartment knee pain and osteoarthritis (OA) (Chang et al., 2010). Larger knee extension moment was exhibit in the injured limb during walking and running. Higher knee adduction loading, small knee flexion angles and large knee extensor moments are considered as three important mechanisms coupled to non-contact knee anterior cruciate ligament (ACL) strain and injury (Shin, Chaudhari, & Andriacchi, 2009). A significantly decreased external ankle dorsiflexion moment and hip extension moment was found in the injured limb during walking, the difference may be explained by reduced ankle plantar flexor strength on ATR limb (Mueller, Minor, Schaaf, Strube, & Sahrmann, 1995). However, the increased contralateral ankle and hip moments during walking of athletes with a history of ATR maybe a strategy to lower AT loading and maybe useful during low intensity movements like normal walking (Grävare Silbernagel, Willy, & Davis, 2012). It appears that a functional deficit in the AT may cause increased values of some biomechanical risk factors. Increased lower limbs joint moments on contralateral side may directly indicate increased load on contralateral uninjured side (Kristianslund, Krosshaug, & Van den Bogert, 2012).

The plantar pressure results of this current dissertation shows that ATR history would lead to difference on foot loading patterns, which is evident in the results of peak pressure, pressure-time integral and contact area distribution. Compared with the uninjured limb, peak pressure and pressure-time integral were find greater in the injured limb in the initial contact phase (ICP) during walking and running, respectively (Mei QC et al., 2015). This could be explained by the compensation mechanism of increased length of repaired AT and plantar flexor strength deficit combined with a greater angle dorsiflexion motion and first vertical peak GRF which were found in the injured limb. In the foot flat phase (FFP), peak pressure and pressure-time integral showed higher in the medial forefoot (MFF) with uninjured limb, and showed higher in the central forefoot (CFF) and lateral forefoot (LFF) with injured limb during walking and running. Decreased pressures in the MFF region and increased pressure in the lateral LFF region in the

ATR limb, which indicates athletes adopt a more lateral loading pattern when walking and running. Meanwhile, the changes of plantar pressure in the forefoot region implies higher magnitude of ankle inversion. This may increase injury risk of ankle sprain and ankle ligament lesions, since the mechanism of these ankle related injuries are frequently an inversion of the ankle and foot (M. L. Costa, 2005).

Symmetry angles (SA) of selected biomechanical parameters showed significant differences between walking and running. While walking and running are considered relatively symmetric activities, asymmetric movement patterns of these two simple movements can disrupt the natural rhythm of gait. It has been demonstrated that some degree of functional asymmetry exist between dominant and non-dominant lower limbs in walking and running of healthy individuals (Sadeghi, 2003). However, when gait asymmetry is above functional levels, the difference will significantly increase chronic lower limb injury risks. Zifchock et al., have shown that the runners who had undergone unilateral limb injury with bilateral imbalance in strength, gait mechanics or structure may be associated with higher impact loading on injured side during running (Zifchock, Davis, Higginson, McCaw, & Royer, 2008). High levels of gait asymmetry between limbs are typically considered to be associated with pathology on lower limbs. Significant asymmetry could also bring out new or recurring injuries (Polk, Stumpf, & Rosengren, 2017). Restoration of gait symmetry was set by clinicians as a goal for rehabilitation results of ATR patients. In the current dissertation, paired t-tests statistics between the comparison of walking SA and running SA indicated that almost all biomechanical parameters in Table 4 showed different levels of asymmetry. Furthermore, the walking SA level showed larger of many, but not all biomechanical parameters compared with running SA level. The walking SA was found greater significance $(p<0.001)$ for ankle dorsiflexion angle, ankle inversion moment, knee adduction velocity, knee flexion moment, indicating that these variables become more asymmetrical during walking activity compared to running SA. Increased ankle dorsiflexion angle reflect more compensation to the functional deficit of elongated AT. Greater knee flexion moment and knee adduction velocity have been previously associated with knee overuse injury (Radzak, Putnam, Tamura, Hetzler, & Stickley, 2017). These changes in asymmetry induced by walking, as indicated by increased SA values, therefore future studies should pay more attention on the effect of walking of ATR patients. The findings of this present dissertation indicate that gait abnormality of well-trained ATR athletes generate higher magnitude of asymmetry, which are associated with higher risk of ankle sprain injury, knee overuse injury and greater loading on contralateral uninjured limb, compared to running.

In summary, the results of this dissertation indicate that the athletes with history of surgically repaired ATR have increased ankle dorsiflexion and decreased knee flexion during stance phase of walking and running on their injured limb compared with the uninjured limb. These kinematic results may be explained by a compensation mechanism, which is against the functional deficit in the elongation of AT and muscle-tendon complex of the triceps suare.

However, the compensation mechanism during movements have been previously linked to knee osteoarthritis and knee overuse injury. Increased impact peak and loading rate was accompanied with higher hip and knee adduction angles, angular velocities and moments on the injured limb, which have been previously associated with chronic knee pain tibia stress fracture. Laterally excursion of center of pressure (COP) were also found together with increased ankle inversion on the injured limb, which indicate higher injury risk of ankle sprain. Overall, many of the biomechanical variables were found to be asymmetric during walking and running associated with previous ATR. Ankle dorsiflexion, knee adduction velocity, ankle inversion moment and knee flexion moment were found to be more asymmetric with walking compared to running. The ankle and knee joints were found to be more impressionable to asymmetries after ATR during lower intensity activity like walking. Future research is needed to compare the mechanics of the lower extremities between ATR individuals and healthy control group during lower and higher intensity activities.

4.2 Musculoskeletal modeling and estimation

This part integrates an in vivo gait analysis, ultrasound imaging based subject-specific AT repaired lower limb musculoskeletal model to investigate if geometry modification of the AT was present after 2 years operative treatment of the unilateral ATR. This dissertation also investigated if as a consequence, lower limb kinematics, kinetics, and muscular contributions were different between the injured and uninjured legs. In the current dissertation, the mean ATRS value (83.7) of these patients reported fairly normal physical activity and function and recovered well after two years ATR (Nilsson-Helander et al., 2007). As hypothesized, a discrepancy was found between the patient-reported outcomes and the tests, which showed large impairment and significant functional deficits with an elongated AT persisting on the injured side in patients with a surgically repaired AT at two years. The previous findings showed higher AT length 2-6 years after surgical repair on the previously injured leg, which supports our first hypothesis (Agres et al., 2015).

Gait analysis has been used to identify intrinsic gait-related risk factors, which revealed altered ankle joint sagittal plane kinematics and plantarflexion moments compared to the uninjured side (De Monte, Arampatzis, Stogiannari, & Karamanidis, 2006). Increased ankle dorsiflexion was accompanied with decreased plantarflexion and was observed almost during the whole stance phase of walking, jogging and running movements. This has also been found in previous studies (Don et al., 2007; Barfod, Bencke, et al., 2015). It has been suggested that increased ankle dorsiflexion may reveal a sustained eccentric dynamic control deficit even 4.5 years after an ATR (Speedtsberg, Kastoft, Barfod, Penny, & Bencke, 2019). An association between increased ankle dorsiflexion and consistent ankle plantar flexor eccentric contraction deficits 2 years after an ATR was also reported (Rosso et al., 2013). The plantarflexion moment of the injured limb was lower during the mid-stance phase of jogging and running.

The intra-patient AT length and stiffness asymmetries were found related to deficits in plantarflexion moments during gait in a previous study (Agres et al., 2015). While this dissertation failed to find any difference between the injured and uninjured sides during normal walking. This discrepancy in such results could be attributed to the physical activity level and follow-up time in my dissertation.

Willy et al., (2017) suggested that the side to side deficits and discrepancies were larger in ATR patients with high-demand and higher angular velocity activities, i.e. jogging and hopping compared with walking (Willy et al., 2017). The decreased plantarflexion angle during the push-off phase in jogging and running movements of the injured leg suggested decreased triceps surae muscle contribution in the center of mass displacement during locomotion (Nilsson-Helander et al., 2010). The ankle joint kinematic and kinetic data obtained in this dissertation suggest that the ankle plantar flexor function is more impaired during higher-demand movements and higher end-range ankle joint plantarflexion after an ATR. A previous study showed the plantar flexor muscles suffered from a functional deficit in patients with an ATR even more than 2 years after surgery (Olsson et al., 2011). It was speculated that the increased ankle dorsiflexion degree accompanied by a decreased plantarflexion moment may be a compensatory mechanism of insufficient ankle dorsal flexor function and the anomalous co-contraction of tibialis anterior and calf muscles, which has been confirmed in previous gait analysis with 41 ATR patients one year after surgery (Chan et al., 2011).

Another important finding in this dissertation was that increased knee joint loading associated with decreased ankle joint loading was present in patients two years after an ATR. It was reported that if the AT length of the injured side increased, the muscle fascicles length will decrease by an equal amount (Suydam et al., 2015). The AT is not a contractile tissue compared to muscle and can't provide positive work to produce human motion. Thus the shorter triceps surae fascicles in the injured limb may promote a deficit in plantar flexor power generation (Drazan, Hullfish, & Baxter, 2019). The compromised plantar flexor function of the injured leg following an ATR may compensate by increased work done by the ipsilateral knee joint (Jandacka et al., 2018). In this dissertation, increased knee extension angle and elevated knee joint moment were found in the injured limb during all activities. Furthermore, increased knee joint contact forces were also present during walking, jogging and running except in the mid-stance phase of running movements. This dissertation showed increased knee extension in the injured limb during initial contact and push-off phases of jogging and mid-stance phase of running. The increased knee extension during jogging and running maybe a potential regulatory mechanism to ensure sufficient elongated triceps surae complex tension (Grävare Silbernagel et al., 2012). A previous study supports the findings of this dissertation, which found a compensation mechanism of the overextension knee joint during running against the AT elongation and deficit of gastro-soleus muscle-tendon complex (Jandacka et al., 2013). The calf muscle crosses two joints, which play an important role to prevent knee overextension and anterior knee laxity as a stabilizer.

Thus the deficit and weakness of the calf muscle in the injured limb may place the knee in an overextension position and at risk for further injury (Cooper, Alghamdi, Alghamdi, Altowaijri, & Richardson, 2012). It was found that the hip joint was more flexed during the push-off phase of jogging and running, which may be a compensation mechanism following overextension of the knee joint to prevent injury risk during high-demand tasks.

The resultant pattern of greater knee extension moment and knee joint contact forces in the injured limb may result in an overloaded knee extensor mechanism. The increased knee joint loading may be attributed to weakened ankle plantar flexor function and elongation of the AT during higher demand tasks like jogging, running and even basic locomotion like walking (Willy et al., 2017; Jandacka et al., 2018). The greater knee/patellofemoral joint loading was reported positively correlated with patellofemoral pain and even knee osteoarthritis in previous studies (S. Farrokhi, Keyak, & Powers, 2011; Draper et al., 2012). The average ATRS value of the previous study is 87.0 compared with 83.7 in this dissertation, and the follow-up time of the previous study is 6.2 years on average compared to 2 years in this dissertation. It is probable that the AT of the patients in this dissertation were still in the remodeling stage and the symptoms and functions will reach a plateau two years after ATR (Peng et al., 2019). Further study should assess the knee symptoms in patients recovering from an ATR.

In the frontal plane, the subtalar joint angle and moment patterns were also changed between the injured and uninjured sides. During walking, jogging and running, the foot was found more inverted combined with greater subtalar inversion moment during almost the whole stance phase. Foot over-inversion was observed associated with several running-related injuries, including medial tibial stress syndrome and knee pain (Bennett et al., 2001). The deficit of plantar flexor muscle operation in the sagittal plane may be substituted by increased loading in the frontal plane of the lower limb joints (Baxter, Hullfish, & Chao, 2018). Consistently, Jandacka et al., (2018) reported the weakened and elongated AT may be the main reason causing altered sagittal plane knee and ankle joint kinematics and increasing lower extremity frontal-plane loading as a consequence (Jandacka et al., 2018).

To the extent of our knowledge, this is the first dissertation to investigate the side-to-side muscular contribution during normal activities via subject-specific OpenSim musculoskeletal modeling after a unilateral ATR. The knee extension femur muscles strength were found conversely increased during jogging and running. While during walking, only the rectus femoris force was found higher in the injured side during the push-off phase, the vas_med, vas_lat and vas_inter forces were still showed deficits in the injured side. In accordance with the present results, which have demonstrated that significantly greater knee joint power was observed in the injured side as compensation for reduced plantar flexor function during high-demand activities only but was not observed during walking (Powell, Silbernagel, Brorsson, Tranberg, & Willy, 2018). The greater knee extension muscular forces in the injured side in this dissertation were also in accordance with higher knee extension degree and moments during jogging and running.

In my dissertation, it was found that significant lower limb muscle strength deficits during normal movements persist on the injured side two years after an acute ATR. The gastrocnemius and soleus muscle forces were found significantly decreased in the injured side during the stance phase of walking, jogging and running. There are several possible explanations for this result. The first interpretation was that with the elongated AT in the injured side, the shank muscles are atrophied, the AT properties may tend to more compliant and hysteresis, which may have a negative effect on the stretch-shortening cycle and muscle-tendon interaction during the stance phase of the injured limb (Geremia et al., 2015, McNair, Nordez, Olds, Young, & Cornu, 2013; Wang et al., 2013). The second interpretation was when the ankle joint in plantar flexion position during push-off phase, the triceps surae muscle was in a shortened posture and below the optimal angle for force generation (Silbernagel et al., 2012). These findings are in accordance with a study that reported the additional slack of the AT may lead to decreased plantarflexion strength (Suydam et al., 2015). The weakened plantar flexor muscles on the injured side and asymmetry may overload the muscle-tendon complex in the uninjured side (Zellers, Marmon, Ebrahimi, & Grävare Silbernagel, 2019). Furthermore, the plantar flexor muscle deficit may affect the mediolateral acceleration of the center of mass based on a previous study and thus disturb the frontal plane ankle stability of the injured side. This may be an additional explanation for the increased foot eversion in the injured side in this dissertation (Knarr, Reisman, Binder-Macleod, & Higginson, 2013). The increased AT length and decreased triceps surae strength to stretch the AT indicate that the functional deficit in the injured side may be primarily caused by anatomical alterations of the tendon. Thus the calf muscle asthenia may be due to inefficacies in force transmission capacity across the joint.

There are 3 limitations that should not be ignored in the OpenSim simulation part:

1. The first limitation relates to the small sample size in this part. However, we have still observed significant musculoskeletal abnormalities between the injured and uninjured side in patients recovering from an ATR.
2. The second limitation was the lack of a healthy control group and to assess inter-limb differences, while an inter-limb gait function test may be a conservative assessment after an ATR.
3. The third limitation of this dissertation was that the movement speed (about 3.5m/s during running) during testing in the laboratory was relatively slow compared to the real outdoor activities. The ATR mostly occurred during a rapid plantar flexor eccentric loading phase. Thus further studies should investigate lower limb musculoskeletal functional differences during high-intensity movements like cutting and landing in both ATR patients and uninjured subjects.

In summary, this part provides subject-specific lower limb musculoskeletal models on 6 patients recovering from a unilateral ATR based on ultrasound imaging data for the prediction of joint kinematics, joint moments, muscle strength and joint reaction forces during daily activities.

Increased AT length is associated with persistent triceps surae muscle strength deficits and decreased plantarflexion moments after surgical repair of ATR during walking, jogging and running. The greater knee extension femur muscle forces combined with increased knee extension moments and higher joint reaction forces during normal daily activities were predicted as a compensation strategy for ankle impairment and plantar flexor function deficit. In the frontal plane, the elevated subtalar joint inversion degrees and moments in the injured side may be due to weakened plantar flexor muscle and perhaps disturb the frontal plane ankle stability, which is confirmed by greater knee loading in the medial part. A speculation of this dissertation is that patients after an ATR may suffer from increased knee overuse injury risk compared to healthy controls. Future studies should develop subject-specific musculoskeletal knee joint models to predict medial and lateral knee/ tibiofemoral contact forces during explosive movements like cutting, landing and hopping of the affected limb with participants after an ATR.

5 Conclusions and future work

5.1 Conclusions

The experimental results indicate that the athletes with history of surgically repaired ATR have increased ankle dorsiflexion and decreased knee flexion during stance phase of walking and running on their injured limb compared with the uninjured limb. These kinematic results may be explained by a compensation mechanism, which is against the functional deficit in the elongation of AT and muscle-tendon complex of the triceps suare. However, the compensation mechanism during movements have been previously linked to knee osteoarthritis and knee overuse injury. Increased impact peak and loading rate was accompanied with higher hip and knee adduction angles, angular velocities and moments on the injured limb, which have been previously associated with chronic knee pain tibia stress fracture. Laterally excursion of center of pressure were also found together with increased ankle inversion on the injured limb, which indicate higher injury risk of ankle sprain. Overall, many of the biomechanical variables were found to be asymmetric during walking and running associated with previous ATR. Ankle dorsiflexion, knee adduction velocity, ankle inversion moment and knee flexion moment were found to be more asymmetric with walking compared to running. The ankle and knee joints were found to be more impressionable to asymmetries after ATR during lower intensity activity like walking. Greater symmetry angle were found during walking. It is supposed that side to side gait variable differences, found between lower limbs, may be related to the AT elongation of surgical repaired side. Increased symmetry angle found in walking of AT ruptured athletes should pay additional attention in the future studies.

Individualization of muscle and tendon parameters in musculoskeletal models is necessary to attain valid results, especially since Achilles tendon properties changes in patients recovery from Achilles tendon ruptures. This dissertation showed that simulation-based calculations of muscle forces are more sensitive to the individualization of Achilles tendon moment arm, Achilles tendon slack length and stiffness compared to the individualization of optimal muscle fascicle length. This dissertation provides subject-specific lower limb musculoskeletal models on patients recovering from a unilateral ATR based on ultrasound imaging data for the prediction of joint kinematics, joint moments, muscle strength and joint reaction forces during daily activities. Increased AT length is associated with persistent triceps surae muscle strength deficits and decreased plantarflexion moments after surgical repair of ATR during walking, jogging and running. The greater knee extension femur muscle forces combined with increased knee extension moments and higher joint reaction forces during normal daily activities were predicted as a compensation strategy for ankle impairment and plantar flexor function deficit. In the frontal plane, the elevated subtalar joint eversion degrees and moments in the injured side may be due to weakened plantar flexor muscle and perhaps disturb the frontal plane ankle stability, which is confirmed by greater knee loading in the medial part.

One assumption of this dissertation is that patients after an ATR may suffer from increased knee overuse injury risk compared to healthy controls. This dissertation combines an experimental and computational workflow to generate gait asymmetry and musculoskeletal disorders during normal activities to determine optimal rehabilitation movements. The combined workflow will lead to urgently needed new insight in which factors contribute to rehabilitation process and how these can be changed by alteration in external load, position and execution of the exercises. For the first time, a detailed description of the loading progression in the exercises have been documented allowing better insight in the contribution parameters to stresses in the tendon. The individual tendon properties and computational workflow could be used to investigate which rehabilitation exercise could provide an optimal loading stimulus for this subject.

5.2 Recommendations for future works

1. To investigate the efficacy of the individualized treatment protocol. Results from this dissertation provide a validated computational workflow to start a randomized clinical controlled trial comparing the individualized treatment protocol to usual therapeutic schedule (a standardized eccentric treatment protocol). The current dissertation will provide the clinically relevant proof-of-concept for this future work. Based on the results in the project, the potential effect size of the new treatment protocol can be calculated. The collaboration with key clinical partners, which are crucial for such a clinical trial, is further established during the purposed study. The aim of the future work is to develop a new rehabilitation protocol of ATR, and to determine its relative efficacy in comparison with the existing usual care physiotherapy treatment.
2. To investigate the effect of footwear and orthosis on tendon loading during normal activities. A further intervention that has been advocated for the rehabilitation of ATR is foot orthoses. The theoretical mechanism for the use of foot orthoses for this condition is that they align the calcaneus to a more vertical position and reduce stress applied to the AT, particularly in a pronated foot. However, there is still no consensus on the effect of orthosis on tendon loading and ATR. Some studies indicate that the mechanical effects of foot orthoses are non-specific and small, and that their mechanism of action is likely to be more complicated, possibly involving neuro-motor effects. Despite the mechanism by which foot orthoses exert their effects being unclear, there is evidence from a small number of studies to suggest that they may reduce symptoms in those patients recovery from ATRs. Better knowledge of the mechanism by which foot orthoses exert their effects when used to treat ATRs could significantly improve this non-surgical treatment option. In addition, motion control running shoes are also developed to change the ankle in/eversion. The future work will give some insights in the potential effect of ankle in/eversion on tendon loading during an isometric contraction.

A future work can expand this knowledge to more dynamic movement and investigate the effect of changing in rear foot angle through orthosis or footwear on the tendon loading during functional movements such as running. The future work will get insight in the effect of orthoses and footwear on tendon loading during functional activities. This future project will first need to further expand the developed computational workflow to include orthosis and footwear, extent the basic knowledge regarding effect of footwear and orthosis on tendon loading before a clinical trial is organized.

Thesis points

1st Thesis point: *I created an augmented musculoskeletal model[1] where the Achilles tendon-related musculotendon parameters, tendon slack length (l_s^t) and optimal fiber length (l_o^m), are obtained by medical imaging techniques[2] from patients with Achilles-tendon rupture. Together with the computational model and experiments, I could prove that without considering the alteration of these parameters, the musculoskeletal models tend to overestimate the Achilles tendon-related muscle forces (as shown in Figure 32) during walking as follows: gastrocnemius medialis: 26% peak and 12% average difference; gastrocnemius lateralis: 25% peak and 11% average difference; soleus: 23% peak and 9% average difference. Therefore, my subject-specific model has increased prediction accuracy and reliability with regard to Achilles tendon-related muscle forces.*

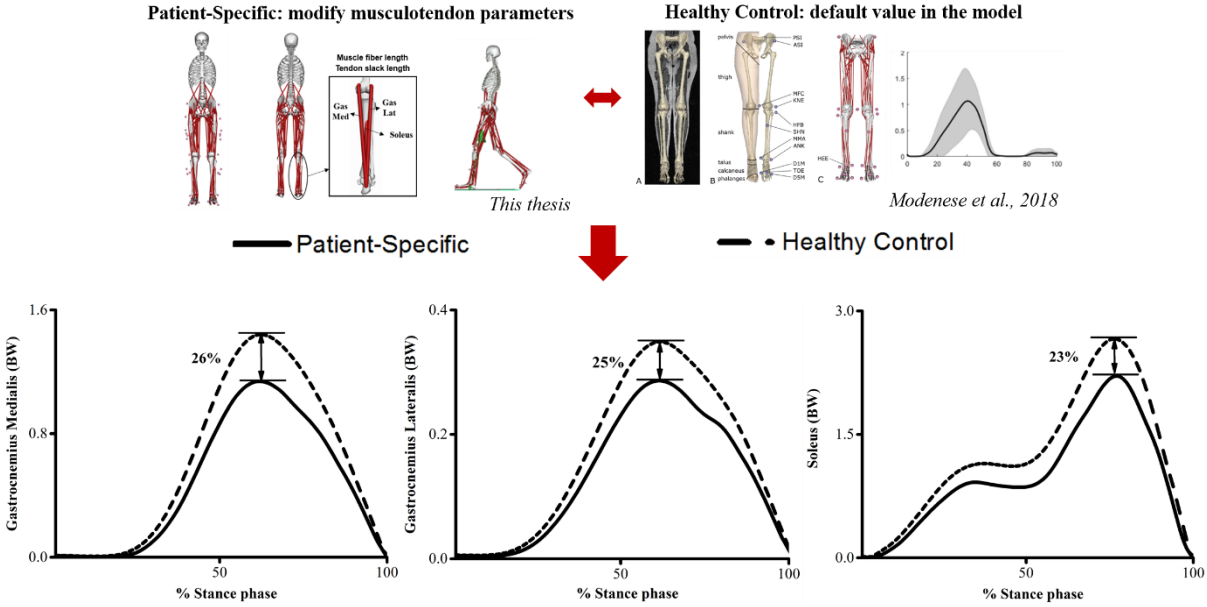

Figure 32 The compared estimated triceps surae muscle forces between patient-specific from this dissertation and study from Modenese et al., 2018, used by permission.

Related articles to the 1st thesis point:

[1] **Sun, D**., Fekete G., Baker J S., & Gu, Y. (2020). Inter-limb musculoskeletal abnormalities in patients in recovery from a unilateral rupture-repaired Achilles tendon. SAGE Open, under review. **IF: 0.68, Q4**

[2] **Sun, D**., Fekete, G., Mei, Q., & Gu, Y. (2019). Gait abnormality and asymmetry analysis after 18–24 months surgical Repair of unilateral Achilles tendon rupture. Journal of Medical Imaging and Health Informatics, 9(3), 552-560. **IF: 0.50, Q4**

2nd Thesis point: *Based on the augmented musculoskeletal model[1], I concluded that the rupture-repaired Achilles tendon will act as a compensator and it causes increased knee joint loading in the injured side[1] (see Figure 24). The increased knee adduction moment (walking: peak 27%, average difference 19%; jogging: peak 45%, average difference 26%; running: peak 24%, average difference 13%) accompanied with higher knee joint reaction forces (walking: peak 30%, average difference 14%; jogging: peak 34%, average difference 15%; running: peak 24%, average difference 3%) in the injured side will likely cause accelerated onset of knee osteoarthritis[2] due to the uneven (medially shifted) loading. The computational results are supported by experimentally obtained data, which shows that during different movements the trajectory of center of pressure will laterally translate[3] (Figure 34). This translation will increase the moment arm of the ground reaction forces, which are experimentally proven to be bound to the speed of locomotion[4], and consequently the knee adduction moment, resulting a mild type of genu varum (bow-legs).*

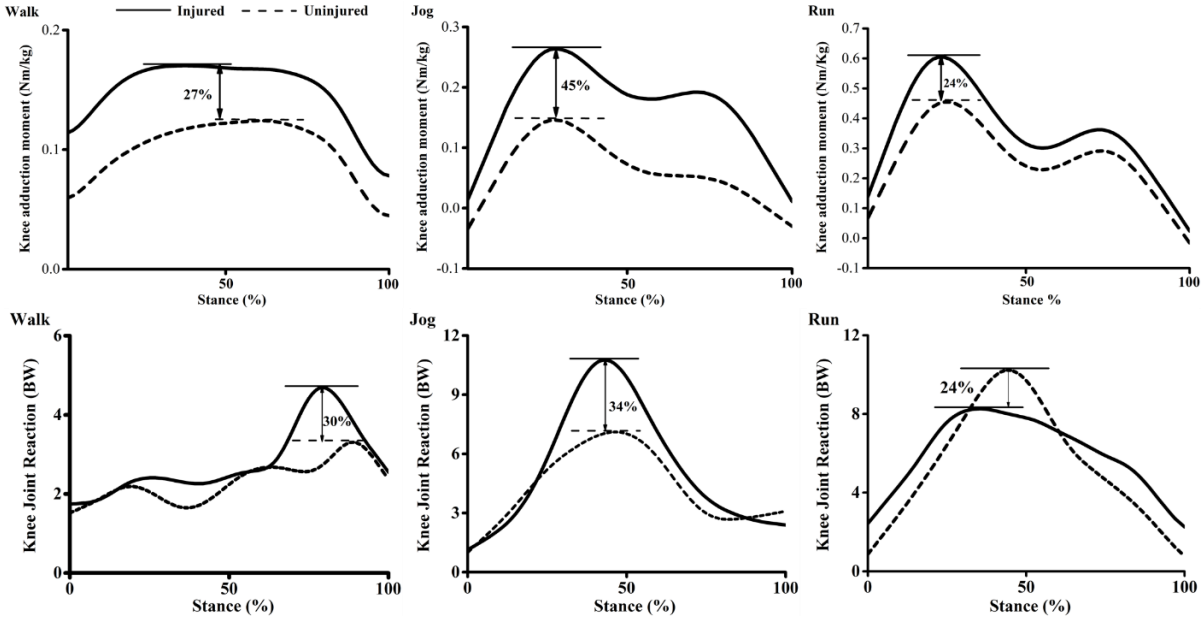

Figure 24 The knee joint adduction moments and joint reaction forces between injured and uninjured limbs

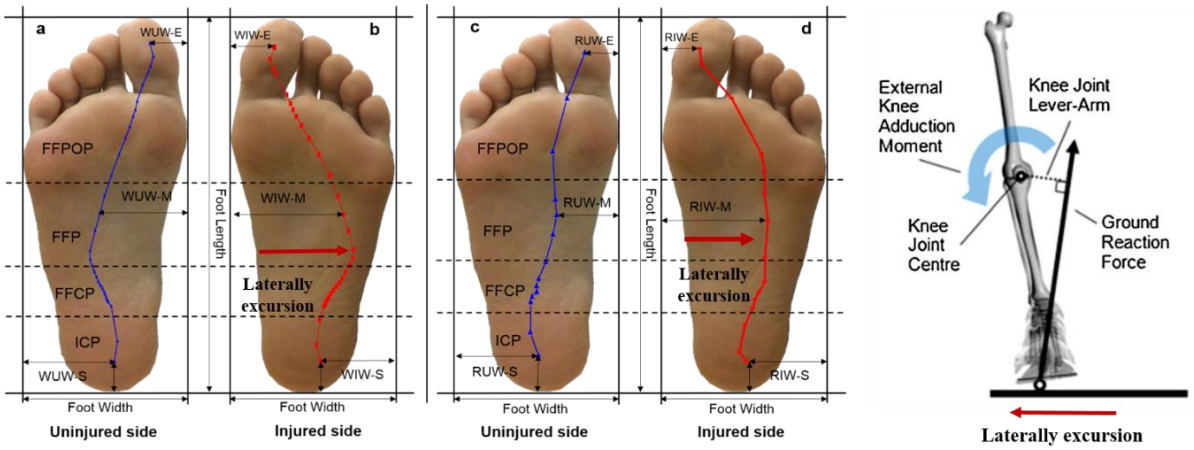

Figure 34 The center of pressure (COP) trajectories in the injured and uninjured sides

Related articles to the 2nd thesis point:

[1] **Sun, D**., Fekete G., Baker J S., & Gu, Y. (2020). Inter-limb musculoskeletal abnormalities in patients in recovery from a unilateral rupture-repaired Achilles tendon. SAGE Open, under review. **IF: 0.68, Q4**

[2] Fekete, G., **Sun, D**., Gu, Y., Neis, P. D., Ferreira, N. F., Innocenti, B., & Csizmadia, B. M. (2017). Tibiofemoral wear in standard and non-standard squat: implication for total knee arthroplasty. Muscles, ligaments and tendons journal, 7(4), 520. **Q1**

[3] **Sun, D**., Gu, Y., Mei, Q., Shao, Y., Sun, J., & Fernandez, J. (2017). Effect of heel heights on female postural control during standing on a dynamic support surface with sinusoidal oscillations. Journal of Motor Behavior, 49(3), 281-287. **IF: 1.31, Q3**

[4] **Sun, D**., Fekete, G., Mei, Q., & Gu, Y. (2018). The effect of walking speed on the foot inter-segment kinematics, ground reaction forces and lower limb joint moments. PeerJ, 6, e5517. **IF: 2.35, Q1**

3rd Thesis point: *Based on my experiments I concluded that the Achilles tendon rupture causes a significant lateral excursion with regard to the center of pressure trajectory*[1]*. Due to this phenomenon, the ankle joint is subjected to increased ankle inversion moments*[2] *(walking: peak 39% and average difference 21%; running: peak 27% and average difference 12%) resulting in a high injury risk for over-inversion, or commonly known, lateral ankle sprain, during walking and high demand activities like running (see Figure 27).*

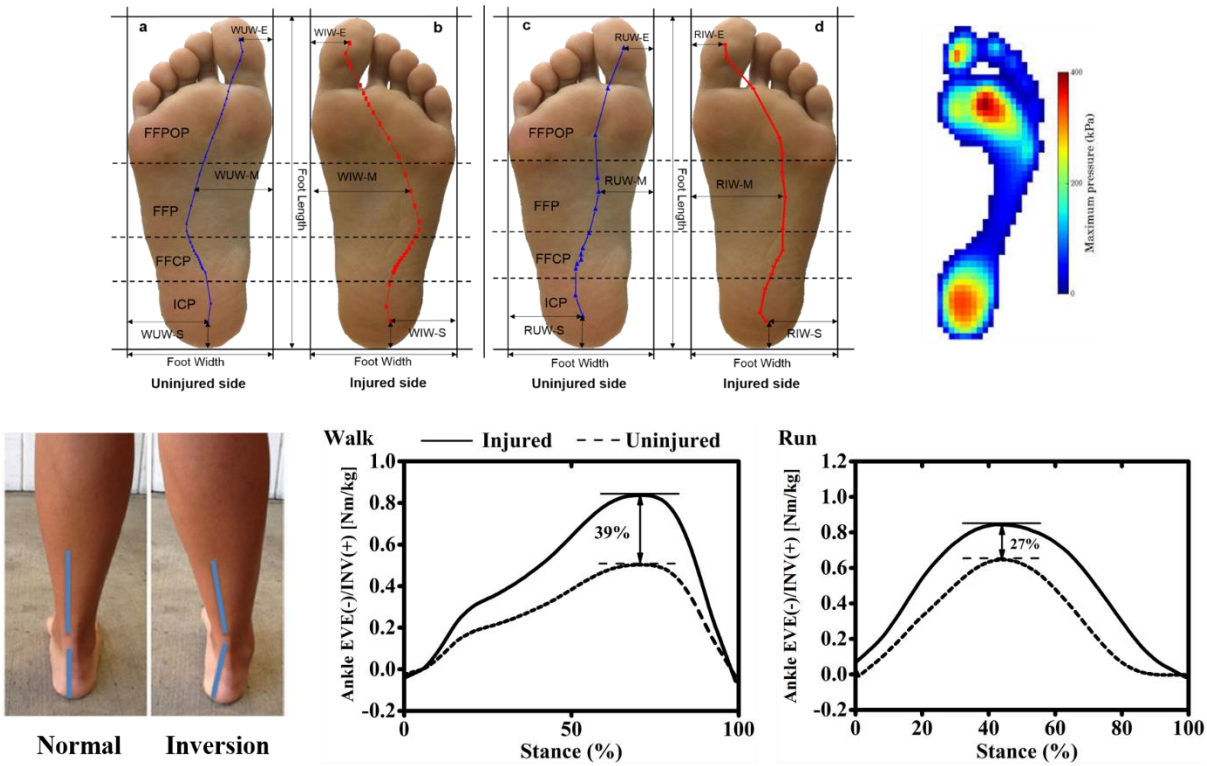

Figure 27 In the first line (center of pressure trajectories), "a" and "b" represent COP trajectory between Uninjured and injured leg during walking, "c" and "d" represent COP trajectories between Uninjured and injured leg during running; In the second line, higher ankle inversion moments were found in the injured side during walking and running.

Related articles to the 3rd thesis point:

[1] **Sun, D**., Gu, Y., Mei, Q., Shao, Y., Sun, J., & Fernandez, J. (2017). Effect of heel heights on female postural control during standing on a dynamic support surface with sinusoidal oscillations. Journal of Motor Behavior, 49(3), 281-287. **IF: 1.31, Q3**

[2] **Sun, D**., Fekete G., Baker J S., & Gu, Y. (2020). Inter-limb musculoskeletal abnormalities in patients in recovery from a unilateral rupture-repaired Achilles tendon. SAGE Open, under review. **IF: 0.68, Q4**

List of publications

Referred articles related to this thesis:

1. Sun, D., Fekete, G., Mei, Q., & Gu, Y. (2018). The effect of walking speed on the foot inter-segment kinematics, ground reaction forces and lower limb joint moments. PeerJ, 6, e5517. **IF: 2.35, Q1**

2. Sun, D., Fekete, G., Baker, J. S., & Gu, Y. (2020). Foot motion character during forward and backward walking with shoes and barefoot. Journal of Motor Behavior, 52(2), 214-225. **IF: 1.31, Q3**

3. Sun, D., Fekete, G., Mei, Q., & Gu, Y. (2019). Gait abnormality and asymmetry analysis after 18–24 months surgical Repair of unilateral Achilles tendon rupture. Journal of Medical Imaging and Health Informatics, 9(3), 552-560. **IF: 0.50, Q4**

4. Sun, D., Gu, Y., Mei, Q., Shao, Y., Sun, J., & Fernandez, J. (2017). Effect of heel heights on female postural control during standing on a dynamic support surface with sinusoidal oscillations. Journal of Motor Behavior, 49(3), 281-287. **IF: 1.31, Q3**

5. Sun, D., Fekete G., Baker J S., & Gu, Y. (2020). Inter-limb musculoskeletal abnormalities in patients in recovery from a unilateral rupture-repaired Achilles tendon. SAGE Open, under review. **IF: 0.68, Q4**

6. Fekete, G., **Sun, D**., Gu, Y., Neis, P. D., Ferreira, N. F., Innocenti, B., & Csizmadia, B. M. (2017). Tibiofemoral wear in standard and non-standard squat: implication for total knee arthroplasty. Muscles, ligaments and tendons journal, 7(4), 520. Q1

7. Mei, Q., Gu, Y., **Sun, D.**, Li, J., & Fernandez, J. (2020). Progress on biomechanics research of image-based subject-specific OpenSim lower extremity musculoskeletal model. Journal of Medical Biomechanics (original Chinese title: 医用生物力学), 35(2).

International conference abstracts related to this thesis:

1. Sun D, Fekete G, Gu Y, Mei Q. The influence of walking speed on foot kinematics and kinetics using a multi-segment foot model. World Congress on Osteoporosis, Osteoarthritis and Musculoskeletal Diseases (WCO-IOF-ESCEO 2018) At: Krakow, Poland.

2. Sun D, Fekete G, Zheng Z, Li Y, Mei Q, Gu Y. Gait abnormality and asymmetry after 18-24 months surgical repair of unilateral ATR. The 8th World Congress of Biomechanics (WCB2018), Dublin, Irish.

3. Sun D, Fekete G, Zheng Z, Li Y, Mei Q, Gu Y. A comparison of foot inter-segment kinematics and plantar pressures during forward and backward walking with shoes and barefoot. The 7th Asian Society of Sport Biomechanics Conference in South Korea (ASSB 2018).

Other publications:

1. **Sun, D**., Mei, Q., Baker, J. S., Jia, X., & Gu, Y. (2017). A pilot study of the effect of outsole hardness on lower limb kinematics and kinetics during soccer related movements. Journal of Human Kinetics, 57(1), 17-27. **IF. 1.41, Q2**

2. **Sun, D**., Gu, Y. D., Mei, Q. C., & Baker, J. S. (2017). Different soccer stud configurations effect on running and cutting movements. Int. J. of Biomedical Engineering and Technology, 24(1), 19-32. **Q3**

3. Sun, D., Gu, Y. D., Fekete, G., & Fernandez, J. (2016). Effects of different soccer boots on biomechanical characteristics of cutting movement on artificial turf. In Journal of Biomimetics, Biomaterials and Biomedical Engineering (Vol. 27, pp. 24-35). Trans Tech Publications Ltd. **Q4**

4. Sun, D., Li, F. L., Zhang, Y., Li, C. F., Lian, W. L., & Gu, Y. D. (2015). Lower Extremity Jogging Mechanics in Young Female with Mild Hallux valgus. In Journal of Biomimetics, Biomaterials and Biomedical Engineering (Vol. 22, pp. 37-47). Trans Tech Publications Ltd. **Q3**

5. Sun, D., Gu, Y., & Feng, N. (2014). Comparison of plantar pressure distribution between different heel heights during incline treadmill walking. International Journal of Biomedical Engineering and Technology, 16(4), 279-292. **Q3**

6. Sun D., Fekete, G., Gu, Y., Li, J. (2018). Biomechanical analysis of soccer players on different turf conditions with different studded soccer shoes. China Sport Science and Technology (original Chinese title: 中国体育科技), 54(1), 71-79.

7. Song, Y., Ren, F., **Sun, D**., Wang, M., Baker, J. S., István, B., & Gu, Y. (2020). Benefits of Exercise on Influenza or Pneumonia in Older Adults: A Systematic Review. International Journal of Environmental Research and Public Health, 17(8), 2655. **IF: 2.47, Q2**

8. Jiang, X., Song, Y., **Sun, D**., Rong, M., Mao, L., & Fekete, G. (2020). Sports Related Injury Mechanism on Ice Hockey Skills: A System Review. Journal of Medical Imaging and Health Informatics, 10(5), 1149-1158. **IF: 0.50, Q4**

9. Lv, X., He, Y., **Sun, D**., Baker, J. S., Xuan, R., & Gu, Y. (2020). Effect of stud shape on lower limb kinetics during football-related movements. Proceedings of the Institution of Mechanical Engineers, Part P: Journal of Sports Engineering and Technology, 234(1), 3-10. **IF: 0.72, Q2**

10. Song, Y., Zhang, W., Zhao, L., **Sun, D**., Huang, Y., & Gu, Y. (2020). Sports-Related Injuries Sustained by Disabled Athletes in Winter Paralympic Games: A Systematic Review. Journal of Medical Imaging and Health Informatics, 10(5), 1136-1143. **IF: 0.50, Q4**

11. Mei, Q., Xiang, L., **Sun, D**., Li, J., Fernandez, J & Gu, Y. (2019). Foot Pronation after Prolonged Running Increased the Medial Contact Force in the Knee Joint：A Study Based on OpenSim Modelling and Machine Learning Prediction. China Sport Science (original Chinese title: 体育科学), 39(9), 51-59.

12. Mei, Q., Gu, Y., **Sun, D**., & Fernandez, J. (2018). How foot morphology changes influence shoe comfort and plantar pressure before and after long distance running?. Acta of Bioengineering and Biomechanics, 20(2). **IF: 1.11, Q3**

13. Fekete, G., **Sun, D**., Liu, G. J., Gu, Y., Balassa, G. P., Bíró, I., & Jánosi, E. (2018). Preliminary results of size and slide-roll effect on the kinematics of total knee replacements. Acta Polytechnica Hungarica, 15, 143-153. **IF: 1.29, Q2**

14. Gu, Y, **Sun D**, Fekete G, Mei Q, Li, J. (2019). Review on the Research of Barefoot Locomotion for Alterations of Lower Extremity Biomechanical Functions. China Sport Science and Technology(original Chinese title: 中国体育科技), 55(1), 61-74.

15. Gu, Y., **Sun, D**., Li, J. S., Graham, M. R., & Ren, X. J. (2013). Plantar pressure variation during jogging with different heel height. Applied Bionics and Biomechanics, 10(3), 89-95. **IF: 1.53, Q3**

16. Liu, G., Fekete, G., Yang, H., Ma, J., **Sun, D**., Mei, Q., & Gu, Y. (2018). Comparative 3-dimensional kinematic analysis of snatch technique between top-elite and sub-elite male weightlifters in 69-kg category. Heliyon, 4(7), e00658. **Q1**

17. Ye, J., **Sun, D**., & Fekete, G. (2018). Ba Duan Jin preliminary analysis of the second type of plantar pressure. Physical Activity and Health, 2(1).

18. Li, C., **Sun, D**., Li, Y., Chang, L., & Lian, W. (2016). Energy consumption character due to different forward position change during jogging movement. International Journal of Biomedical Engineering and Technology. **Q3**

19. Yin, L., **Sun, D**., Mei, Q. C., Gu, Y. D., Baker, J. S., & Feng, N. (2015). The kinematics and kinetics analysis of the lower extremity in the landing phase of a stop-jump task. The open biomedical engineering journal, 9, 103.

20. Shu, Y., **Sun, D**., Hu, Q. L., Zhang, Y., Li, J. S., & Gu, Y. D. (2015). Lower Limb Kinetics and Kinematics during Two Different Jumping Methods. In Journal of Biomimetics, Biomaterials and Biomedical Engineering (Vol. 22, pp. 29-35). Trans Tech Publications Ltd. **Q4**

21. Zhang, Y., Mei, Q., **Sun, D**., Gu, Y., & Shen, W. (2014). Gait kinematic features in rural older women of China. International Journal of Biomedical Engineering and Technology, 16(1), 71-78. **Q3**

Reviewer for international journal articles:

1. Journal of Medical Imaging and Health Informatics
2. Physical Activity and Health
3. International Journal of Biomedical Engineering and Technology

ORCID: http://orcid.org/0000-0002-7634-5668

Total independent citations:

Scopus Database: 19 (https://www.scopus.com/authid/detail.uri?authorId=56443080100)

Hirsch index: 3

Total Impact Factor: 15.68 (Web of Science)

References

Agres, A. N., Duda, G. N., Gehlen, T. J., Arampatzis, A., Taylor, W. R., & Manegold, S. (2015). Increased unilateral tendon stiffness and its effect on gait 2-6 years after Achilles tendon rupture. *Scandinavian Journal of Medicine and Science in Sports*. https://doi.org/10.1111/sms.12456

Alexander, L. D., Black, S. E., Patterson, K. K., Gao, F., Danells, C. J., & Mcllroy, W. E. (2009). Association between gait asymmetry and brain lesion location in stroke patients. *Stroke*, *40*(2), 537–544. https://doi.org/10.1161/STROKEAHA.108.527374

Arampatzis, A., Peper, A., Bierbaum, S., & Albracht, K. (2010). Plasticity of human Achilles tendon mechanical and morphological properties in response to cyclic strain. *Journal of Biomechanics*. https://doi.org/10.1016/j.jbiomech.2010.08.014

Arch, E. S., Stanhope, S. J., & Higginson, J. S. (2016). Passive-dynamic ankle-foot orthosis replicates soleus but not gastrocnemius muscle function during stance in gait: Insights for orthosis prescription. *Prosthetics and Orthotics International*. https://doi.org/10.1177/0309364615592693

Arnold, A. S., Schwartz, M. H., Thelen, D. G., & Delp, S. L. (2007). Contributions of muscles to terminal-swing knee motions vary with walking speed. *Journal of Biomechanics*. https://doi.org/10.1016/j.jbiomech.2007.06.006

Arnold, E. M., Ward, S. R., Lieber, R. L., & Delp, S. L. (2010). A model of the lower limb for analysis of human movement. *Annals of Biomedical Engineering*. https://doi.org/10.1007/s10439-009-9852-5

Axer, H., Axer, M., Sauer, H., Witte, O. W., & Hagemann, G. (2010). Falls and gait disorders in geriatric neurology. *Clinical Neurology and Neurosurgery*. https://doi.org/10.1016/j.clineuro.2009.12.015

Barfod, K. W., Bencke, J., Lauridsen, H. B., Dippmann, C., Ebskov, L., & Troelsen, A. (2015). Nonoperative, dynamic treatment of acute achilles tendon rupture: Influence of early weightbearing on biomechanical properties of the plantar flexor muscle-tendon complex-a blinded, randomized, controlled trial. *Journal of Foot and Ankle Surgery*. https://doi.org/10.1053/j.jfas.2014.11.018

Barfod, K. W., Riecke, A. F., Boesen, A., Hansen, P., Maier, J. F., Døssing, S., & Troelsen, A. (2015). Validation of a novel ultrasound measurement of achilles tendon length. *Knee Surgery, Sports Traumatology, Arthroscopy*. https://doi.org/10.1007/s00167-014-3175-2

Baur, H., Müller, S., Hirschmüller, A., Cassel, M., Weber, J., & Mayer, F. (2011). Comparison in lower leg neuromuscular activity between runners with unilateral mid-portion Achilles tendinopathy and healthy individuals. *Journal of Electromyography and Kinesiology*. https://doi.org/10.1016/j.jelekin.2010.11.010

Baxter, J. R., Hullfish, T. J., & Chao, W. (2018). Functional deficits may be explained by plantarflexor remodeling following Achilles tendon rupture repair: Preliminary findings. *Journal of Biomechanics*. https://doi.org/10.1016/j.jbiomech.2018.08.016

Bennett, J. E., Reinking, M. F., Pluemer, B., Pentel, A., Seaton, M., & Killian, C. (2001). Factors contributing to the development of medial tibial stress syndrome in high school runners. *Journal of Orthopaedic and Sports Physical Therapy*. https://doi.org/10.2519/jospt.2001.31.9.504

Błażkiewicz, M., Wiszomirska, I., Kaczmarczyk, K., Naemi, R., & Wit, A. (2017). Inter-individual similarities and variations in muscle forces acting on the ankle joint during gait. *Gait and Posture*. https://doi.org/10.1016/j.gaitpost.2017.07.119

Bovi, G., Rabuffetti, M., Mazzoleni, P., & Ferrarin, M. (2011). A multiple-task gait analysis approach: Kinematic, kinetic and EMG reference data for healthy young and adult subjects. *Gait and Posture*. https://doi.org/10.1016/j.gaitpost.2010.08.009

Bramble, D. M., & Lieberman, D. E. (2004). Endurance running and the evolution of Homo. *Nature*. https://doi.org/10.1038/nature03052

Brorsson, A., Willy, R. W., Tranberg, R., & Grävare Silbernagel, K. (2017). Heel-Rise Height Deficit 1 Year After Achilles Tendon Rupture Relates to Changes in Ankle Biomechanics 6 Years After Injury. *American Journal of Sports Medicine*, *45*(13), 3060–3068. https://doi.org/10.1177/0363546517717698

Carse, B., Meadows, B., Bowers, R., & Rowe, P. (2013). Affordable clinical gait analysis: An assessment of the marker tracking accuracy of a new low-cost optical 3D motion analysis system. *Physiotherapy (United Kingdom)*. https://doi.org/10.1016/j.physio.2013.03.001

Ceseracciu, E., Sawacha, Z., & Cobelli, C. (2014). Comparison of markerless and marker-based motion capture technologies through simultaneous data collection during gait: Proof of concept. *PLoS ONE*. https://doi.org/10.1371/journal.pone.0087640

Chan, A. P. H., Chan, Y. Y., Fong, D. T. P., Wong, P. Y. K., Lam, H. Y., Lo, C. K., … Chan, K. M. (2011). Clinical and biomechanical outcome of minimal invasive and open repair of the Achilles tendon. *Sports Medicine, Arthroscopy, Rehabilitation, Therapy and Technology*. https://doi.org/10.1186/1758-2555-3-32

Chang, A., Hochberg, M., Song, J., Dunlop, D., Chmiel, J. S., Nevitt, M., … Sharma, L. (2010). Frequency of varus and valgus thrust and factors associated with thrust presence in persons with or at higher risk of developing knee osteoarthritis. *Arthritis and Rheumatism*, *62*(5), 1403–1411. https://doi.org/10.1002/art.27377

Chen, K., Hu, X., Blemker, S. S., & Holmes, J. W. (2018). Multiscale computational model of Achilles tendon wound healing: Untangling the effects of repair and loading. *PLoS Computational Biology*. https://doi.org/10.1371/journal.pcbi.1006652

Cimolin, V., & Galli, M. (2014). Summary measures for clinical gait analysis: A literature review. *Gait and Posture*. https://doi.org/10.1016/j.gaitpost.2014.02.001

Cooper, A., Alghamdi, G. A., Alghamdi, M. A., Altowaijri, A., & Richardson, S. (2012). The Relationship of Lower Limb Muscle Strength and Knee Joint Hyperextension during the Stance Phase of Gait in Hemiparetic Stroke Patients. *Physiotherapy Research International*. https://doi.org/10.1002/pri.528

Costa, M. L. (2005). Gait abnormalities following rupture of the tendo Achillis: A PEDOBAROGRAPHIC ASSESSMENT. *Journal of Bone and Joint Surgery - British Volume*, *87-B*(8), 1085–1088. https://doi.org/10.1302/0301-620X.87B8.16540

Costa, Matt L. (2005). Gait abnormalities following rupture of the tendo Achillis. A pedobarographic assessment. *Journal of Bone and Joint Surgery - Series B*. https://doi.org/10.1302/0301-620X.87B8.16540

Costa, Matthew L., Logan, K., Heylings, D., Donell, S. T., & Tucker, K. (2006). The effect of Achilles tendon lengthening on ankle dorsiflexion: A cadaver study. *Foot and Ankle International*. https://doi.org/10.1177/107110070602700605

Davis, R. B., Õunpuu, S., Tyburski, D., & Gage, J. R. (1991). A gait analysis data collection and reduction technique. *Human Movement Science*. https://doi.org/10.1016/0167-9457(91)90046-Z

De Monte, G., Arampatzis, A., Stogiannari, C., & Karamanidis, K. (2006). In vivo motion transmission in the inactive gastrocnemius medialis muscle-tendon unit during ankle and knee joint rotation. *Journal of Electromyography and Kinesiology*. https://doi.org/10.1016/j.jelekin.2005.10.001

Debaere, S., Delecluse, C., Aerenhouts, D., Hagman, F., & Jonkers, I. (2013). From block clearance to sprint running: Characteristics underlying an effective transition. *Journal of Sports Sciences*. https://doi.org/10.1080/02640414.2012.722225

Debaere, S., Delecluse, C., Aerenhouts, D., Hagman, F., & Jonkers, I. (2015). Control of propulsion and body lift during the first two stances of sprint running: A simulation study. *Journal of Sports Sciences*. https://doi.org/10.1080/02640414.2015.1026375

Delp, S. L., Anderson, F. C., Arnold, A. S., Loan, P., Habib, A., John, C. T., … Thelen, D. G. (2007). OpenSim: Open-source software to create and analyze dynamic simulations of movement. *IEEE Transactions on Biomedical Engineering*. https://doi.org/10.1109/TBME.2007.901024

Don, R., Ranavolo, A., Cacchio, A., Serrao, M., Costabile, F., Iachelli, M., … Santilli, V. (2007). Relationship between recovery of calf-muscle biomechanical properties and gait pattern following surgery for achilles tendon rupture. *Clinical Biomechanics*, *22*(2), 211–220. https://doi.org/10.1016/j.clinbiomech.2006.10.001

Doral, M. N., Alam, M., Bozkurt, M., Turhan, E., Atay, O. A., Dönmez, G., & Maffulli, N. (2010). Functional anatomy of the Achilles tendon. *Knee Surgery, Sports Traumatology, Arthroscopy*. https://doi.org/10.1007/s00167-010-1083-7

Draper, C. E., Fredericson, M., Gold, G. E., Besier, T. F., Delp, S. L., Beaupre, G. S., & Quon, A. (2012). Patients with patellofemoral pain exhibit elevated bone metabolic activity at the patellofemoral joint. *Journal of Orthopaedic Research*. https://doi.org/10.1002/jor.21523

Drazan, J. F., Hullfish, T. J., & Baxter, J. R. (2019). Muscle structure governs joint function: linking natural variation in medial gastrocnemius structure with isokinetic plantar flexor function. *BioRxiv*. https://doi.org/10.1101/547042

Dubbeldam, R., Buurke, J. H., Simons, C., Groothuis-Oudshoorn, C. G. M., Baan, H., Nene, A. V., & Hermens, H. J. (2010). The effects of walking speed on forefoot, hindfoot and ankle joint motion. *Clinical Biomechanics*, *25*(8), 796–801. https://doi.org/10.1016/j.clinbiomech.2010.06.007

Egger, A. C., & Berkowitz, M. J. (2017). Achilles tendon injuries. *Current Reviews in Musculoskeletal Medicine*. https://doi.org/10.1007/s12178-017-9386-7

Esquenazi, A. (2014). Gait analysis in lower-limb amputation and prosthetic rehabilitation. *Physical Medicine and Rehabilitation Clinics of North America*. https://doi.org/10.1016/j.pmr.2013.09.006

Farris, D. J., Trewartha, G., & Polly McGuigan, M. (2011). Could intra-tendinous hyperthermia during running explain chronic injury of the human Achilles tendon? *Journal of Biomechanics*, *44*(5), 822–826. https://doi.org/10.1016/j.jbiomech.2010.12.015

Farrokhi, S., Keyak, J. H., & Powers, C. M. (2011). Individuals with patellofemoral pain exhibit greater patellofemoral joint stress: A finite element analysis study. *Osteoarthritis and Cartilage*. https://doi.org/10.1016/j.joca.2010.12.001

Farrokhi, Shawn, Jayabalan, P., Gustafson, J. A., Klatt, B. A., Sowa, G. A., & Piva, S. R. (2017). The influence of continuous versus interval walking exercise on knee joint loading and pain in patients with knee osteoarthritis. *Gait and Posture*. https://doi.org/10.1016/j.gaitpost.2017.05.015

Fletcher, J. R., Esau, S. P., & MacIntosh, B. R. (2010). Changes in tendon stiffness and running economy in highly trained distance runners. *European Journal of Applied Physiology*. https://doi.org/10.1007/s00421-010-1582-8

Fukuchi, C. A., Fukuchi, R. K., & Duarte, M. (2018). A public dataset of overground and treadmill walking kinematics and kinetics in healthy individuals. *PeerJ*. https://doi.org/10.7717/peerj.4640

Gaffney, B. M., Harris, M. D., Davidson, B. S., Stevens-Lapsley, J. E., Christiansen, C. L., & Shelburne, K. B. (2016). Multi-Joint Compensatory Effects of Unilateral Total Knee Arthroplasty During High-Demand Tasks. *Annals of Biomedical Engineering*. https://doi.org/10.1007/s10439-015-1524-z

Ganestam, A., Barfod, K., Klit, J., & Troelsen, A. (2013). Validity and Reliability of the Achilles Tendon Total Rupture Score. *Journal of Foot and Ankle Surgery*. https://doi.org/10.1053/j.jfas.2013.07.004

Ganestam, A., Kallemose, T., Troelsen, A., & Barfod, K. W. (2016). Increasing incidence of acute Achilles tendon rupture and a noticeable decline in surgical treatment from 1994 to 2013. A nationwide registry study of 33,160 patients. *Knee Surgery, Sports Traumatology, Arthroscopy*. https://doi.org/10.1007/s00167-015-3544-5

Garrido, I. M., Deval, J. C., Bosch, M. N., Mediavilla, D. H., Garcia, V. P., & González, M. S. (2010). Treatment of acute Achilles tendon ruptures with Achillon device: Clinical outcomes and kinetic gait analysis. *Foot and Ankle Surgery*. https://doi.org/10.1016/j.fas.2009.10.014

Geremia, J. M., Bobbert, M. F., Casa Nova, M., Ott, R. D., De Aguiar Lemos, F., De Oliveira Lupion, R., … Vaz, M. A. (2015). The structural and mechanical properties of the Achilles tendon 2 years after surgical repair. *Clinical Biomechanics*, *30*(5), 485–492. https://doi.org/10.1016/j.clinbiomech.2015.03.005

Goren, D., Ayalon, M., & Nyska, M. (2005). Isokinetic strength and endurance after percutaneous and open surgical repair of achilles tendon ruptures. *Foot and Ankle International*. https://doi.org/10.1177/107110070502600404

Grävare Silbernagel, K., Willy, R., & Davis, I. (2012). Preinjury and Postinjury Running Analysis Along With Measurements of Strength and Tendon Length in a Patient With a Surgically Repaired Achilles Tendon Rupture. *Journal of Orthopaedic & Sports Physical Therapy*, *42*(6), 521–529. https://doi.org/10.2519/jospt.2012.3913

Gwynne-Jones, D. P., & Sims, M. (2011). Epidemiology and Outcomes of Acute Achilles Tendon Rupture with Operative or Nonoperative Treatment Using an Identical Functional Bracing Protocol. *Foot & Ankle International*. https://doi.org/10.3113/fai.2011.0337

Hackney, J. M., Clay, R. L., & James, M. (2016). Force-displacement differences in the lower extremities of young healthy adults between drop jumps and drop landings. *Human Movement Science*. https://doi.org/10.1016/j.humov.2016.06.008

Halonen, K. S., Dzialo, C. M., Mannisi, M., Venäläinen, M. S., De Zee, M., & Andersen, M. S. (2017). Workflow assessing the effect of gait alterations on stresses in the medial tibial cartilage - Combined musculoskeletal modelling and finite element analysis. *Scientific Reports*. https://doi.org/10.1038/s41598-017-17228-x

Hamner, S. R., & Delp, S. L. (2013). Muscle contributions to fore-aft and vertical body mass center accelerations over a range of running speeds. *Journal of Biomechanics*. https://doi.org/10.1016/j.jbiomech.2012.11.024

Hamner, S. R., Seth, A., & Delp, S. L. (2010). Muscle contributions to propulsion and support during running. *Journal of Biomechanics*. https://doi.org/10.1016/j.jbiomech.2010.06.025

Hansen, P., Kovanen, V., Hölmich, P., Krogsgaard, M., Hansson, P., Dahl, M., … Magnusson, S. P. (2013). Micromechanical properties and collagen composition of ruptured human achilles tendon. *American Journal of Sports Medicine*. https://doi.org/10.1177/0363546512470617

Harris, M. D., MacWilliams, B. A., Bo Foreman, K., Peters, C. L., Weiss, J. A., & Anderson, A. E. (2017). Higher medially-directed joint reaction forces are a characteristic of dysplastic hips: A comparative study using subject-specific musculoskeletal models. *Journal of Biomechanics*. https://doi.org/10.1016/j.jbiomech.2017.01.040

Hebenstreit, F., Leibold, A., Krinner, S., Welsch, G., Lochmann, M., & Eskofier, B. M. (2015). Effect of walking speed on gait sub phase durations. *Human Movement Science*. https://doi.org/10.1016/j.humov.2015.07.009

Heikkinen, J., Lantto, I., Flinkkila, T., Ohtonen, P., Niinimaki, J., Siira, P., … Leppilahti, J. (2017). Soleus Atrophy Is Common after the Nonsurgical Treatment of Acute Achilles Tendon Ruptures: A Randomized Clinical Trial Comparing Surgical and Nonsurgical Functional Treatments. *American Journal of Sports Medicine*. https://doi.org/10.1177/0363546517694610

Hess, G. W. (2010). Achilles Tendon Rupture: A Review of Etiology, Population, Anatomy, Risk Factors, and Injury Prevention. *Foot & Ankle Specialist*. https://doi.org/10.1177/1938640009355191

Hunter, G. R., Katsoulis, K., Mccarthy, J. P., Ogard, W. K., Bamman, M. M., Wood, D. S., … Newcomer, B. R. (2011). Tendon length and joint flexibility are related to running economy. *Medicine and Science in Sports and Exercise*. https://doi.org/10.1249/MSS.0b013e318210464a

Ismadi Ismail, S. (2018). The Influence of Additional Surface on Force Platform's Ground Reaction Force Data During Walking and Running. *American Journal of Sports Science*. https://doi.org/10.11648/j.ajss.20180603.12

Jandacka, D., Plesek, J., Skypala, J., Uchytil, J., Silvernail, J. F., & Hamill, J. (2018). Knee Joint Kinematics and Kinetics During Walking and Running After Surgical Achilles Tendon Repair. *Orthopaedic Journal of Sports Medicine*. https://doi.org/10.1177/2325967118779862

Jandacka, D., Zahradnik, D., Foldyna, K., & Hamill, J. (2013). Running biomechanics in a long-term monitored recreational athlete with a history of achilles tendon rupture. *BMJ Case Reports*. https://doi.org/10.1136/bcr-2012-007370

John, C. T., Seth, A., Schwartz, M. H., & Delp, S. L. (2012). Contributions of muscles to mediolateral ground reaction force over a range of walking speeds. *Journal of Biomechanics*. https://doi.org/10.1016/j.jbiomech.2012.06.037

Kainz, H., Graham, D., Edwards, J., Walsh, H. P. J., Maine, S., Boyd, R. N., … Carty, C. P. (2017). Reliability of four models for clinical gait analysis. *Gait and Posture*. https://doi.org/10.1016/j.gaitpost.2017.04.001

Karimi, M. T., Salami, F., Esrafilian, A., Heitzmann, D. W. W., Alimusaj, M., Putz, C., & Wolf, S. I. (2017). Sound side joint contact forces in below knee amputee gait with an ESAR prosthetic foot. *Gait and Posture*. https://doi.org/10.1016/j.gaitpost.2017.08.007

Kean, C. O., Bennell, K. L., Wrigley, T. V., & Hinman, R. S. (2015). Relationship between hip abductor strength and external hip and knee adduction moments in medial knee osteoarthritis. *Clinical Biomechanics*, *30*(3), 226–230. https://doi.org/10.1016/j.clinbiomech.2015.01.008

Khan, K. M., Cook, J. L., Kannus, P., Maffulli, N., & Bonar, S. F. (2002). Time to abandon the tendinitis myth: Painful, overuse tendon conditions have a non-inflammatory pathology. *BMJ (Clinical Research Ed.)*. https://doi.org/10.1136/bmj.324.7338.626

Khan, K. M., Forster, B. B., Robinson, J., Cheong, Y., Louis, L., Maclean, L., & Taunton, J. E. (2003). Are ultrasound and magnetic resonance imaging of value in assessment of Achilles tendon disorders? A two year prospective study. *British Journal of Sports Medicine*. https://doi.org/10.1136/bjsm.37.2.149

Kharb, A., Saini, V., Jain, Y., & Dhiman, S. (2011). A review of gait cycle and its parameters. *IJCEM Int J Comput Eng Manag*.

Knapik, J. J., Bauman, C. L., Jones, B. H., Harris, J. M., & Vaughan, L. (1991). Preseason strength and flexibility imbalances associated with athletic injuries in female collegiate athletes. *The American Journal of Sports Medicine*, *19*(1), 76–81. https://doi.org/10.1177/036354659101900113

Knarr, B. A., & Higginson, J. S. (2015). Practical approach to subject-specific estimation of knee joint contact force. *Journal of Biomechanics*. https://doi.org/10.1016/j.jbiomech.2015.04.020

Knarr, B. A., Reisman, D. S., Binder-Macleod, S. A., & Higginson, J. S. (2013). Understanding compensatory strategies for muscle weakness during gait by simulating activation deficits seen post-stroke. *Gait and Posture*. https://doi.org/10.1016/j.gaitpost.2012.11.027

Kondo, H., & Someya, F. (2016). Changes in ground reaction force during a rebound-jump task after hip strength training for single-sided ankle dorsiflexion restriction. *Journal of Physical Therapy Science*, *28*(2), 319–325. https://doi.org/10.1589/jpts.28.319

Konradsen, L. (2002). Sensori-motor control of the uninjured and injured human ankle. In *Journal of Electromyography and Kinesiology* (Vol. 12, pp. 199–203). https://doi.org/10.1016/S1050-6411(02)00021-4

Kristianslund, E., Krosshaug, T., & Van den Bogert, A. J. (2012). Effect of low pass filtering on joint moments from inverse dynamics: Implications for injury prevention. *Journal of Biomechanics*, *45*(4), 666–671. https://doi.org/10.1016/j.jbiomech.2011.12.011

Kubo, K., Tabata, T., Ikebukuro, T., Igarashi, K., & Tsunoda, N. (2010). Alongitudinal assessment of running economy and tendon properties in long-distance runners. *Journal of Strength and Conditioning Research*. https://doi.org/10.1519/JSC.0b013e3181ddf847

Kujala, U. M., Sarna, S., & Kaprio, J. (2005). Cumulative incidence of achilles tendon rupture and tendinopathy in male former elite athletes. *Clinical Journal of Sport Medicine*, *15*(3), 133–135. https://doi.org/10.1097/01.jsm.0000165347.55638.23

Kunimasa, Y., Sano, K., Oda, T., Nicol, C., Komi, P. V., Locatelli, E., … Ishikawa, M. (2014). Specific muscle-tendon architecture in elite Kenyan distance runners. *Scandinavian Journal of Medicine and Science in Sports*. https://doi.org/10.1111/sms.12161

Kutzner, I., Trepczynski, A., Heller, M. O., & Bergmann, G. (2013). Knee adduction moment and medial contact force-facts about their correlation during gait. *PLoS ONE*, *8*(12). https://doi.org/10.1371/journal.pone.0081036

Lathrop-Lambach, R. L., Asay, J. L., Jamison, S. T., Pan, X., Schmitt, L. C., Blazek, K., … Chaudhari, A. M. W. (2014). Evidence for joint moment asymmetry in healthy populations during gait. *Gait and Posture*, *40*(4), 526–531. https://doi.org/10.1016/j.gaitpost.2014.06.010

Leardini, A., Lullini, G., Giannini, S., Berti, L., Ortolani, M., & Caravaggi, P. (2014). Validation of the angular measurements of a new inertial-measurement-unit based rehabilitation system: Comparison with state-of-the-art gait analysis. *Journal of NeuroEngineering and Rehabilitation*. https://doi.org/10.1186/1743-0003-11-136

Leppilahti, J., Puranen, J., & Orava, S. (1996). Incidence of Achilles tendon rupture. *Acta Orthopaedica Scandinavica*. https://doi.org/10.3109/17453679608994688

Lerner, Z. F., Board, W. J., & Browning, R. C. (2016). Pediatric obesity and walking duration increase medial tibiofemoral compartment contact forces. *Journal of Orthopaedic Research*. https://doi.org/10.1002/jor.23028

Lerner, Z. F., Haight, D. J., DeMers, M. S., Board, W. J., & Browning, R. C. (2014). The effects of walking speed on tibiofemoral loading estimated via musculoskeletal modeling. *Journal of Applied Biomechanics*. https://doi.org/10.1123/jab.2012-0206

Li, L., & Zhang, Y. (2013). Biomechanical simulation of achilles tendon strains during hurdling. In *Advanced Materials Research*. https://doi.org/10.4028/www.scientific.net/AMR.647.462

Lienhard, K., Schneider, D., & Maffiuletti, N. A. (2013). Validity of the Optogait photoelectric system for the assessment of spatiotemporal gait parameters. *Medical Engineering and Physics*. https://doi.org/10.1016/j.medengphy.2012.06.015

Liu, M. Q., Anderson, F. C., Schwartz, M. H., & Delp, S. L. (2008). Muscle contributions to support and progression over a range of walking speeds. *Journal of Biomechanics*. https://doi.org/10.1016/j.jbiomech.2008.07.031

Lohman, E. B., Balan Sackiriyas, K. S., & Swen, R. W. (2011). A comparison of the spatiotemporal parameters, kinematics, and biomechanics between shod, unshod, and minimally supported running as compared to walking. *Physical Therapy in Sport*, *12*(4), 151–163. https://doi.org/10.1016/j.ptsp.2011.09.004

Lorimer, A. V., & Hume, P. A. (2014). Achilles Tendon Injury Risk Factors Associated with Running. *Sports Medicine*. https://doi.org/10.1007/s40279-014-0209-3

Lorimer, A. V., & Hume, P. A. (2016). Stiffness as a Risk Factor for Achilles Tendon Injury in Running Athletes. *Sports Medicine*. https://doi.org/10.1007/s40279-016-0526-9

Maffulli, N., Regine, R., Angelillo, M., Capasso, G., & Filice, S. (1987). Ultrasound diagnosis of Achilles tendon pathology in runners. *British Journal of Sports Medicine*. https://doi.org/10.1136/bjsm.21.4.158

Maffulli, N. (1998). The clinical diagnosis of subcutaneous tear of the Achilles tendon. A prospective study in 174 patients. *The American Journal of Sports Medicine*, *26*(2), 266–270. https://doi.org/10.1177/03635465980260021801

Maffulli, Nicola. (1999). Current Concepts Review - Rupture of the Achilles Tendon*. *The Journal of Bone & Joint Surgery*, *81*(7), 1019–1036. https://doi.org/10.1097/00013611-198710000-00003

Magnan, B., Bondi, M., Pierantoni, S., & Samaila, E. (2014). The pathogenesis of Achilles tendinopathy: A systematic review. *Foot and Ankle Surgery*. https://doi.org/10.1016/j.fas.2014.02.010

Maquirriain, J. (2011). Achilles tendon rupture: Avoiding tendon lengthening during surgical repair and rehabilitation. *Yale Journal of Biology and Medicine*. https://doi.org/10.1016/j.injury.2014.06.022

McGowan, C. P., Kram, R., & Neptune, R. R. (2009). Modulation of leg muscle function in response to altered demand for body support and forward propulsion during walking. *Journal of Biomechanics*. https://doi.org/10.1016/j.jbiomech.2009.01.025

McGrath, R. L., Ziegler, M. L., Pires-Fernandes, M., Knarr, B. A., Higginson, J. S., & Sergi, F. (2019). The effect of stride length on lower extremity joint kinetics at various gait speeds. *PLoS ONE*. https://doi.org/10.1371/journal.pone.0200862

Mclean, B. (2008). Biomechanics of Running. In *Handbook of Sports Medicine and Science, Running*. https://doi.org/10.1002/9780470757116.ch3

McNair, P., Nordez, A., Olds, M., Young, S. W., & Cornu, C. (2013). Biomechanical properties of the plantar flexor muscle-tendon complex 6 months post-rupture of the Achilles tendon. *Journal of Orthopaedic Research*. https://doi.org/10.1002/jor.22381

Mei, Q., Gu, Y., Sun, D., & Fernandez, J. (2018). How foot morphology changes influence shoe comfort and plantar pressure before and after long distance running? *Acta of Bioengineering and Biomechanics*. https://doi.org/10.5277/ABB-01112-2018-02

Mei, Q., Gu, Y., Xiang, L., Baker, J. S., & Fernandez, J. (2019). Foot Pronation Contributes to Altered Lower Extremity Loading After Long Distance Running. *Frontiers in Physiology*. https://doi.org/10.3389/fphys.2019.00573

MEI QC, FENG N, REN X, LAKE M, GU Y, Mei, Q., … Gu, Y. Y. D. (2015). Foot Loading Patterns With Different Unstable Soles Structure. *Journal of Mechanics in Medicine and Biology*, *15*(1), 1550014. https://doi.org/10.1142/S0219519415500141

Meireles, S., De Groote, F., Reeves, N. D., Verschueren, S., Maganaris, C., Luyten, F., & Jonkers, I. (2016). Knee contact forces are not altered in early knee osteoarthritis. *Gait and Posture*. https://doi.org/10.1016/j.gaitpost.2016.01.016

Meireles, S., De Groote, F., Van Rossom, S., Verschueren, S., & Jonkers, I. (2017). Differences in knee adduction moment between healthy subjects and patients with osteoarthritis depend on the knee axis definition. *Gait and Posture*. https://doi.org/10.1016/j.gaitpost.2017.01.013

Mezzarobba, S., Bortolato, S., Giacomazzi, A., Valentini, R., Marcovich, R., & Fancellu, G. (2013). Achilles tendon percutaneous repair with tenolig: Quantitative analysis of postural control and gait pattern. *Gait & Posture*. https://doi.org/10.1016/j.gaitpost.2012.12.024

Modenese, L., Montefiori, E., Wang, A., Wesarg, S., Viceconti, M., & Mazzà, C. (2018). Investigation of the dependence of joint contact forces on musculotendon parameters using a codified workflow for image-based modelling. *Journal of Biomechanics*. https://doi.org/10.1016/j.jbiomech.2018.03.039

Moissenet, F., Bélaise, C., Piche, E., Michaud, B., & Begon, M. (2019). An Optimization Method Tracking EMG, Ground Reactions Forces, and Marker Trajectories for Musculo-Tendon Forces Estimation in Equinus Gait. *Frontiers in Neurorobotics*. https://doi.org/10.3389/fnbot.2019.00048

Mokhtarzadeh, H., Yeow, C. H., Hong Goh, J. C., Oetomo, D., Malekipour, F., & Lee, P. V. S. (2013). Contributions of the Soleus and Gastrocnemius muscles to the anterior cruciate ligament loading during single-leg landing. *Journal of Biomechanics*. https://doi.org/10.1016/j.jbiomech.2013.04.010

Montero-Odasso, M., Verghese, J., Beauchet, O., & Hausdorff, J. M. (2012). Gait and cognition: A complementary approach to understanding brain function and the risk of falling. *Journal of the American Geriatrics Society*. https://doi.org/10.1111/j.1532-5415.2012.04209.x

Morgan, K. D., Donnelly, C. J., & Reinbolt, J. A. (2014). Elevated gastrocnemius forces compensate for decreased hamstrings forces during the weight-acceptance phase of single-leg jump landing: Implications for anterior cruciate ligament injury risk. *Journal of Biomechanics*. https://doi.org/10.1016/j.jbiomech.2014.08.016

Mueller, M. J., Minor, S. D., Schaaf, J. A., Strube, M. J., & Sahrmann, S. A. (1995). Relationship of plantar-flexor peak torque and dorsiflexion range of motion to kinetic variables during walking. *Physical Therapy*, *75*(8), 684–693. https://doi.org/10.1093/ptj/75.8.684

Mullaney, M. J., McHugh, M. P., Tyler, T. F., Nicholas, S. J., & Lee, S. J. (2006). Weakness in end-range plantar flexion after achilles tendon repair. *American Journal of Sports Medicine*. https://doi.org/10.1177/0363546505284186

Müller, R., Siebert, T., & Blickhan, R. (2012). Muscle preactivation control: Simulation of ankle joint adjustments at touchdown during running on uneven ground. *Journal of Applied Biomechanics*. https://doi.org/10.1123/jab.28.6.718

Mummolo, C., Mangialardi, L., & Kim, J. H. (2013). Quantifying Dynamic Characteristics of Human Walking for Comprehensive Gait Cycle. *Journal of Biomechanical Engineering*. https://doi.org/10.1115/1.4024755

Munteanu, S. E., & Barton, C. J. (2011). Lower limb biomechanics during running in individuals with achilles tendinopathy: A systematic review. *Journal of Foot and Ankle Research*. https://doi.org/10.1186/1757-1146-4-15

Muro-de-la-Herran, A., García-Zapirain, B., & Méndez-Zorrilla, A. (2014). Gait analysis methods: An overview of wearable and non-wearable systems, highlighting clinical applications. *Sensors (Switzerland)*. https://doi.org/10.3390/s140203362

Nadeau, S., Betschart, M., & Bethoux, F. (2013). Gait analysis for poststroke rehabilitation: The relevance of biomechanical analysis and the impact of gait speed. *Physical Medicine and Rehabilitation Clinics of North America*. https://doi.org/10.1016/j.pmr.2012.11.007

Naim, F., Simşek, A., Sipahioğlu, S., Esen, E., & Cakmak, G. (2005). Evaluation of the surgical results of Achilles tendon ruptures by gait analysis and isokinetic muscle strength measurements. *Acta Orthopaedica et Traumatologica Turcica*, *39*(October 2003), 1–6.

Neptune, R. R., Kautz, S. A., & Zajac, F. E. (2001). Contributions of the individual ankle plantar flexors to support, forward progression and swing initiation during walking. *Journal of Biomechanics*, *34*(11), 1387–1398. https://doi.org/10.1016/S0021-9290(01)00105-1

Nigg, B. M. (2001). The role of impact forces and foot pronation: A new paradigm. *Clinical Journal of Sport Medicine*, *11*(1), 2–9. https://doi.org/10.1097/00042752-200101000-00002

Nilsson-Helander, K., Grävare Silbernagel, K., Thomeé, R., Faxén, E., Olsson, N., Eriksson, B. I., & Karlsson, J. (2010). Acute achilles tendon rupture: A randomized, controlled study comparing surgical and nonsurgical treatments using validated outcome measures. *American Journal of Sports Medicine*. https://doi.org/10.1177/0363546510376052

Nilsson-Helander, K., Thomeé, R., Grävare-Silbernagel, K., Thomeé, P., Faxén, E., Eriksson, B. I., & Karlsson, J. (2007). The Achilles tendon Total Rupture Score (ATRS): Development and validation. *American Journal of Sports Medicine*. https://doi.org/10.1177/0363546506294856

O'Brien, M. (2005). The anatomy of the achilles tendon. *Foot and Ankle Clinics*. https://doi.org/10.1016/j.fcl.2005.01.011

O'Neill, S., Watson, P. J., & Barry, S. (2016). A DELPHI STUDY OF RISK FACTORS FOR ACHILLES TENDINOPATHY- OPINIONS OF WORLD TENDON EXPERTS. *International Journal of Sports Physical Therapy*.

Oda, H., Sano, K., Kunimasa, Y., Komi, P. V., & Ishikawa, M. (2017). Neuromechanical Modulation of the Achilles Tendon During Bilateral Hopping in Patients with Unilateral Achilles Tendon Rupture, Over 1 Year After Surgical Repair. *Sports Medicine*. https://doi.org/10.1007/s40279-016-0629-3

Olsson, N., Nilsson-Helander, K., Karlsson, J., Eriksson, B. I., Thomée, R., Faxén, E., & Silbernagel, K. G. (2011). Major functional deficits persist 2 years after acute Achilles tendon rupture. *Knee Surgery, Sports Traumatology, Arthroscopy*. https://doi.org/10.1007/s00167-011-1511-3

Ornetti, P., Maillefert, J. F., Laroche, D., Morisset, C., Dougados, M., & Gossec, L. (2010). Gait analysis as a quantifiable outcome measure in hip or knee osteoarthritis: A systematic review. *Joint Bone Spine*. https://doi.org/10.1016/j.jbspin.2009.12.009

Pandy, M. G., & Andriacchi, T. P. (2010). Muscle and Joint Function in Human Locomotion. *Annual Review of Biomedical Engineering*. https://doi.org/10.1146/annurev-bioeng-070909-105259

Pataky, T. C., Robinson, M. A., & Vanrenterghem, J. (2013). Vector field statistical analysis of kinematic and force trajectories. *Journal of Biomechanics*. https://doi.org/10.1016/j.jbiomech.2013.07.031

Peng, W. C., Chao, Y. H., Fu, A. S. N., Fong, S. S. M., Rolf, C., Chiang, H., … Wang, H. K. (2019). Muscular Morphomechanical Characteristics After an Achilles Repair. *Foot and Ankle International*. https://doi.org/10.1177/1071100718822537

Pistacchi, M., Gioulis, M., Sanson, F., de Giovannini, E., Filippi, G., Rossetto, F., & Marsala, S. Z. (2017). Gait analysis and clinical correlations in early Parkinson's disease. *Functional Neurology*. https://doi.org/10.11138/FNeur/2017.32.1.028

Plotnik, M., Bartsch, R. P., Zeev, A., Giladi, N., & Hausdorff, J. M. (2013). Effects of walking speed on asymmetry and bilateral coordination of gait. *Gait and Posture*, *38*(4), 864–869. https://doi.org/10.1016/j.gaitpost.2013.04.011

Polk, J. D., Stumpf, R. M., & Rosengren, K. S. (2017). Limb dominance, foot orientation and functional asymmetry during walking gait. *Gait and Posture*, *52*, 140–146. https://doi.org/10.1016/j.gaitpost.2016.11.028

Powell, H. C., Silbernagel, K. G., Brorsson, A., Tranberg, R., & Willy, R. W. (2018). Individuals post achilles tendon rupture exhibit asymmetrical knee and ankle kinetics and loading rates during a drop countermovement jump. *Journal of Orthopaedic and Sports Physical Therapy*. https://doi.org/10.2519/jospt.2018.7684

Prinold, J. A. I., Mazzà, C., Di Marco, R., Hannah, I., Malattia, C., Magni-Manzoni, S., … Viceconti, M. (2016). A Patient-Specific Foot Model for the Estimate of Ankle Joint Forces in Patients with Juvenile Idiopathic Arthritis. *Annals of Biomedical Engineering*. https://doi.org/10.1007/s10439-015-1451-z

Radzak, K. N., Putnam, A. M., Tamura, K., Hetzler, R. K., & Stickley, C. D. (2017). Asymmetry between lower limbs during rested and fatigued state running gait in healthy individuals. *Gait and Posture*, *51*, 268–274. https://doi.org/10.1016/j.gaitpost.2016.11.005

Raikin, S. M., Garras, D. N., & Krapchev, P. V. (2013). Achilles tendon injuries in a United States population. *Foot and Ankle International*. https://doi.org/10.1177/1071100713477621

Rajagopal, A., Dembia, C. L., DeMers, M. S., Delp, D. D., Hicks, J. L., & Delp, S. L. (2016). Full-Body Musculoskeletal Model for Muscle-Driven Simulation of Human Gait. *IEEE Transactions on Biomedical Engineering*. https://doi.org/10.1109/TBME.2016.2586891

Richards, C., & Higginson, J. S. (2010). Knee contact force in subjects with symmetrical OA grades: Differences between OA severities. *Journal of Biomechanics*. https://doi.org/10.1016/j.jbiomech.2010.05.006

Rigney, S. M., Simmons, A., & Kark, L. (2016). A prosthesis-specific multi-link segment model of lower-limb amputee sprinting. *Journal of Biomechanics*. https://doi.org/10.1016/j.jbiomech.2016.07.039

Riley, P. O., Franz, J., Dicharry, J., & Kerrigan, D. C. (2010). Changes in hip joint muscle-tendon lengths with mode of locomotion. *Gait and Posture*. https://doi.org/10.1016/j.gaitpost.2009.11.005

Rosso, C., Buckland, D. M., Polzer, C., Sadoghi, P., Schuh, R., Weisskopf, L., … Valderrabano, V. (2015). Long-term biomechanical outcomes after Achilles tendon ruptures. *Knee Surgery, Sports Traumatology, Arthroscopy*. https://doi.org/10.1007/s00167-013-2726-2

Rosso, C., Vavken, P., Polzer, C., Buckland, D. M., Studler, U., Weisskopf, L., … Valderrabano, V. (2013). Long-term outcomes of muscle volume and Achilles tendon length after Achilles tendon ruptures. *Knee Surgery, Sports Traumatology, Arthroscopy*. https://doi.org/10.1007/s00167-013-2407-1

Sadeghi, H. (2003). Local or global asymmetry in gait of people without impairments. *Gait and Posture*, *17*(3), 197–204. https://doi.org/10.1016/S0966-6362(02)00089-9

Sadeghi, H., Allard, P., & Duhaime, M. (1997). Functional gait asymmetry in able-bodied subjects. *Human Movement Science*, *16*(2–3), 243–258. https://doi.org/10.1016/S0167-9457(96)00054-1

Salami, F., Niklasch, M., Krautwurst, B. K., Dreher, T., & Wolf, S. I. (2017). What is the price for the Duchenne gait pattern in patients with cerebral palsy? *Gait and Posture*. https://doi.org/10.1016/j.gaitpost.2017.09.006

Scarton, A., Guiotto, A., Malaquias, T., Spolaor, F., Sinigaglia, G., Cobelli, C., … Sawacha, Z. (2018). A methodological framework for detecting ulcers' risk in diabetic foot subjects by combining gait analysis, a new musculoskeletal foot model and a foot finite element model. *Gait and Posture*. https://doi.org/10.1016/j.gaitpost.2017.08.036

Schepsis, A. A., Jones, H., & Haas, A. L. (2002). Achilles tendon disorders in athletes. *American Journal of Sports Medicine*. https://doi.org/10.1177/03635465020300022501

Seth, A., Hicks, J. L., Uchida, T. K., Habib, A., Dembia, C. L., Dunne, J. J., … Delp, S. L. (2018). OpenSim: Simulating musculoskeletal dynamics and neuromuscular control to study human and animal movement. *PLoS Computational Biology*. https://doi.org/10.1371/journal.pcbi.1006223

Shapiro, D. C., Zernicke, R. F., Gregor, R. J., & Diestel, J. D. (1981). Evidence for generalized motor programs using gait pattern analysis. *Journal of Motor Behavior*. https://doi.org/10.1080/00222895.1981.10735235

Shim, V. B., Hansen, W., Newsham-West, R., Nuri, L., Obst, S., Pizzolato, C., … Barrett, R. S. (2019). Influence of altered geometry and material properties on tissue stress distribution under load in tendinopathic Achilles tendons – A subject-specific finite element analysis. *Journal of Biomechanics*. https://doi.org/10.1016/j.jbiomech.2018.10.027

Shin, C. S., Chaudhari, A. M., & Andriacchi, T. P. (2009). The effect of isolated valgus moments on ACL strain during single-leg landing: A simulation study. *Journal of Biomechanics*, *42*(3), 280–285. https://doi.org/10.1016/j.jbiomech.2008.10.031

Silbernagel, K. G., Steele, R., & Manal, K. (2012). Deficits in heel-rise height and Achilles tendon elongation occur in patients recovering from an Achilles tendon rupture. *American Journal of Sports Medicine*. https://doi.org/10.1177/0363546512447926

Simon, S. R. (1993). Gait Analysis, Normal and Pathological Function. *The Journal of Bone & Joint Surgery*. https://doi.org/10.2106/00004623-199303000-00027

Singh, D. (2017). Acute Achilles tendon rupture. *British Journal of Sports Medicine*. https://doi.org/10.1136/bjsports-2016-h4722rep

Smale, K. B., Conconi, M., Sancisi, N., Krogsgaard, M., Alkjaer, T., Parenti-Castelli, V., & Benoit, D. L. (2019). Effect of implementing magnetic resonance imaging for patient-specific OpenSim models on lower-body kinematics and knee ligament lengths. *Journal of Biomechanics*. https://doi.org/10.1016/j.jbiomech.2018.11.016

Speedtsberg, M. B., Kastoft, R., Barfod, K. W., Penny, J., & Bencke, J. (2019). Gait Function and Postural Control 4.5 Years After Nonoperative Dynamic Treatment of Acute Achilles Tendon Ruptures. *Orthopaedic Journal of Sports Medicine*. https://doi.org/10.1177/2325967119854324

Steele, K. M., DeMers, M. S., Schwartz, M. H., & Delp, S. L. (2012). Compressive tibiofemoral force during crouch gait. *Gait and Posture*. https://doi.org/10.1016/j.gaitpost.2011.11.023

Stenroth, L., Peltonen, J., Cronin, N. J., Sipila, S., & Finni, T. (2012). Age-related differences in Achilles tendon properties and triceps surae muscle architecture in vivo. *Journal of Applied Physiology*, *113*(10), 1537–1544. https://doi.org/10.1152/japplphysiol.00782.2012

Stolwijk, N. M., Koenraadt, K. L. M., Louwerens, J. W. K., Grim, D., Duysens, J., & Keijsers, N. L. W. (2014). Foot lengthening and shortening during gait: A parameter to investigate foot function? *Gait and Posture*. https://doi.org/10.1016/j.gaitpost.2013.10.014

Sun, D., Fekete, G., Baker, J. S., & Gu, Y. (2019). Foot Motion Character During Forward and Backward Walking With Shoes and Barefoot. *Journal of Motor Behavior*. https://doi.org/10.1080/00222895.2019.1605972

Sun, D., Fekete, G., Mei, Q., & Gu, Y. (2018). The effect of walking speed on the foot inter-segment kinematics, ground reaction forces and lower limb joint moments, 1–18. https://doi.org/10.7717/peerj.5517

Sun, D., Fekete, G., Mei, Q., & Gu, Y. (2019). Gait Abnormality and Asymmetry Analysis After 18–24 Months Surgical Repair of Unilateral Achilles Tendon Rupture. *Journal of Medical Imaging and Health Informatics*. https://doi.org/10.1166/jmihi.2019.2630

Suydam, S. M., Buchanan, T. S., Manal, K., & Silbernagel, K. G. (2015). Compensatory muscle activation caused by tendon lengthening post-Achilles tendon rupture. *Knee Surgery, Sports Traumatology, Arthroscopy*. https://doi.org/10.1007/s00167-013-2512-1

Ueno, H., Suga, T., Takao, K., Tanaka, T., Misaki, J., Miyake, Y., … Isaka, T. (2018). Relationship between Achilles tendon length and running performance in well-trained male endurance runners. *Scandinavian Journal of Medicine and Science in Sports*. https://doi.org/10.1111/sms.12940

Van Den Bogert, A. J., Geijtenbeek, T., Even-Zohar, O., Steenbrink, F., & Hardin, E. C. (2013). A real-time system for biomechanical analysis of human movement and muscle function. *Medical and Biological Engineering and Computing*. https://doi.org/10.1007/s11517-013-1076-z

Vint, P. F., & Hinrichs, R. N. (1996). Differences between one-foot and two-foot vertical jump performances. *Journal of Applied Biomechanics*. https://doi.org/10.1123/jab.12.3.338

Voleti, P. B., Buckley, M. R., & Soslowsky, L. J. (2012). Tendon Healing: Repair and Regeneration. *Annual Review of Biomedical Engineering*. https://doi.org/10.1146/annurev-bioeng-071811-150122

Wang, H. K., Chiang, H., Chen, W. S., Shih, T. T., Huang, Y. C., & Jiang, C. C. (2013). Early neuromechanical outcomes of the triceps surae muscle-tendon after an Achilles' tendon repair. *Archives of Physical Medicine and Rehabilitation*. https://doi.org/10.1016/j.apmr.2013.01.015

Whittle, M. W. (2007). *An Introduction to Gait Analysis*. *Library*.

Willy, R. W., Brorsson, A., Powell, H. C., Willson, J. D., Tranberg, R., & Grävare Silbernagel, K. (2017). Elevated Knee Joint Kinetics and Reduced Ankle Kinetics Are Present during Jogging and Hopping after Achilles Tendon Ruptures. *American Journal of Sports Medicine*. https://doi.org/10.1177/0363546516685055

Wren, T. A. L., Gorton, G. E., Õunpuu, S., & Tucker, C. A. (2011). Efficacy of clinical gait analysis: A systematic review. *Gait and Posture*. https://doi.org/10.1016/j.gaitpost.2011.03.027

Zellers, J. A., Marmon, A. R., Ebrahimi, A., & Grävare Silbernagel, K. (2019). Lower extremity work along with triceps surae structure and activation is altered with jumping after Achilles tendon repair. *Journal of Orthopaedic Research*. https://doi.org/10.1002/jor.24260

Zifchock, R. A., Davis, I., Higginson, J., McCaw, S., & Royer, T. (2008). Side-to-side differences in overuse running injury susceptibility: A retrospective study. *Human Movement Science*, *27*(6), 888–902. https://doi.org/10.1016/j.humov.2008.03.007

Zifchock, R. A., Davis, I., Higginson, J., & Royer, T. (2008). The symmetry angle: A novel, robust method of quantifying asymmetry. *Gait and Posture*, *27*(4), 622–627. https://doi.org/10.1016/j.gaitpost.2007.08.006